

**Towards Biocontrol of Tree Root Rot Pathogens from the
Genus *Armillaria***

PhD dissertation

Liqiong Chen

Supervisors:

Dr. László Kredics

Prof. Dr. Csaba Vágódy

Doctoral School of Biology



Department of Microbiology

Faculty of Science and Informatics

University of Szeged

2021

Szeged

TABLE OF CONTENTS

LIST OF ABBREVIATIONS.....	4
1 INTRODUCTION.....	5
1.1 Devastating forest pathogens from the Armillarioid clade cause root rot disease	5
1.1.1 Host preference.....	5
1.1.2 Distribution characteristics	6
1.1.3 Pathogenicity variation	7
1.1.4 Damages caused by <i>Armillaria</i>	8
1.1.5 The spread of <i>Armillaria</i> root disease.....	12
1.1.6 The potential <i>Armillaria</i> inoculum.....	13
1.2 Chemical and silvicultural means of <i>Armillaria</i> control	14
1.3 Biological control of <i>Armillaria</i>	15
1.3.1 Potential biocontrol of <i>Armillaria</i> by bacteria and saprobic basidiomycetes.....	15
1.3.2 Potential biocontrol of <i>Armillaria</i> by <i>Trichoderma</i> species	16
1.4 <i>Trichoderma</i> species as powerful biocontrol agents	19
1.4.1 Mycoparasitic activity of <i>Trichoderma</i> species	19
1.4.2 Extracellular enzymes of <i>Trichoderma</i> species	20
1.4.3 Metabolites produced by <i>Trichoderma</i> against fungal plant pathogens.....	22
1.4.4 Effects of <i>Trichoderma</i> species on plants	24
1.5 High-throughput sequencing technologies for studying <i>Armillaria</i> and <i>Trichoderma</i>	26
1.5.1 Genome sequencing of <i>Armillaria</i> species	26
1.5.2 Transcriptome profiling of various <i>Armillaria</i> activities	27
1.5.3 Genome expansion in biocontrol <i>Trichoderma</i> species.....	28
1.5.4 Transcriptional reprogramming in <i>Trichoderma</i> species induced by plant pathogens	29
2 AIMS OF THE STUDY	30
3 MATERIALS AND METHODS.....	32
3.1 Screening for biocontrol candidates from <i>Trichoderma</i> strains.....	32
3.1.1 Isolation of <i>Armillaria</i> and <i>Trichoderma</i> strains.....	32
3.1.2 Identification of <i>Armillaria</i> and <i>Trichoderma</i> isolates.....	32
3.1.3 Antagonistic activity assessment <i>in vitro</i> by dual culture assay	33
3.1.4 Extracellular enzyme activity measurements	33
3.1.5 Quantitative analysis of indole-3-acetic acid production.....	34

3.1.6 Siderophore production.....	34
3.2 Transcriptome analysis of the interaction mechanisms between <i>Armillaria ostoyae</i> and <i>Trichoderma atroviride</i>	35
3.2.1 Strains and culture conditions.....	35
3.2.2 Transcriptome analysis of <i>Trichoderma atroviride</i> – <i>Armillaria ostoyae</i> dual cultures	35
3.2.2.1 Experimental design, sample collection and total RNA extraction	35
3.2.2.2 cDNA library preparation, sequencing and data analysis	36
3.2.2.3 Quantitative real-time reverse transcription PCR (qRT-PCR)	37
3.3 Field study in the Keszthely Hills.....	38
4 RESULTS.....	40
4.1 Screening for biocontrol candidates from <i>Trichoderma</i> strains against <i>Armillaria</i> species	40
4.1.1 Diversity of the genera <i>Armillaria</i> and <i>Trichoderma</i> in healthy and <i>Armillaria</i> -damaged forests	40
4.1.2 <i>In vitro</i> antagonism of the isolated <i>Trichoderma</i> strains towards <i>Armillaria</i> species	41
4.1.3 Extracellular enzyme production of the <i>Trichoderma</i> isolates	42
4.1.4 Potential plant growth-promoting traits of the isolated <i>Trichoderma</i> strains	42
4.2 Molecular dynamics of the biocontrol interaction between <i>T. atroviride</i> and <i>A. ostoyae</i>	45
4.2.1 Antagonistic effect of <i>T. atroviride</i> SZMC 24276 against <i>A. ostoyae</i> strains	45
4.2.2 Time course analysis to understand the interaction dynamics between <i>T. atroviride</i> (TA) and <i>A. ostoyae</i> (AO).....	46
4.2.3 Validation of differentially expressed genes using qRT-PCR	48
4.2.4 Gene expression profiling of the major trends	50
4.2.4.1 Downtrend genes in <i>T. atroviride</i> (TA) and <i>A. ostoyae</i> (AO).....	50
4.2.4.2 The Metabolite and Mycoparasite interaction stages	52
4.3 Field experiment in a heavily <i>Armillaria</i> -damaged forest in the Keszthely Hills	65
5 DISCUSSION	66
5.1 Different diversity pattern of <i>Armillaria</i> and <i>Trichoderma</i> species were discovered between the healthy spruce forest in Rosalia and the severely infected oak stand in Keszthely	66
5.2 Several <i>Trichoderma</i> species showed strong antagonistic abilities against <i>Armillaria</i> species	67
5.3 Extracellular enzyme secretion, siderophore production and IAA production are important parameters during the screening for biocontrol agents among <i>Trichoderma</i> strains	68

5.4 Growth regression of <i>A. ostoyae</i> (AO) was reflected by its transcriptome patterns and defence reactions were induced in <i>A. ostoyae</i> by <i>T. atroviride</i> (TA)	70
5.5 Metabolite interactions were significantly induced	72
5.6 CAZymes play an important role in the biocontrol process	73
5.7 Peptidase dynamics is a crucial defence response of <i>A. ostoyae</i> (AO)	74
5.8 Two selected biocontrol candidates showed promising biocontrol effect in a field experiment	75
SUMMARY	77
ÖSSZEFOGLALÁS	80
FINANCIAL SUPPORT	84
ACKNOWLEDGEMENT	85
LIST OF REFERENCES	88
LIST OF PUBLICATIONS	106
SUPPLEMENTARY MATERIAL	110

LIST OF ABBREVIATIONS

Auxiliary activities (AAs)
Armillaria ostoyae SZMC 23093 (AO)
ATP binding cassette (ABC) transporters
Biocontrol Index (BCI)
Biocontrol agents (BCAs)
Biomass index (BMI)
Carbohydrate active enzymes (CAZymes)
Chrome azurol S (CAS)
Cell wall-degrading enzymes (CWDEs)
Dimethylallyltryptophan synthase (DMATS)
Glycoside Hydrolases (GHs)
Gene ontology (GO)
Internal Transcribed Spacer (ITS)
Indole-3-acetic acid (IAA)
Non-ribosomal peptide synthetase (NRPS)
Potato dextrose agar (PDA)
Polyketide synthase (PKS)
Quinolinic acid (QA)
Small secretory proteins (SSPs)
Short-chain dehydrogenase/reductase (SDR)
Szeged Microbiology Collection (SZMC)
Translation elongation factor 1-alpha gene (*tef1 α*)
Trichoderma atroviride SZMC 24276 (TA)

1 INTRODUCTION

1.1 Devastating forest pathogens from the Armillarioid clade cause root rot disease

Armillaria and *Desarmillaria* species (*Physalacriaceae*, *Basidiomycota*), representing two separate genera within the Armillarioid clade (Kedves *et al.*, 2021) are globally fungal plant pathogens varying in host range and pathogenicity (Baumgartner *et al.*, 2011; Chen *et al.*, 2019). They cause white rot, a severe destructive disease (also known as *Armillaria* root rot) on a wide range of woody hosts growing in managed plantations, natural forests, orchards and amenity plantings in urban areas, and their impacts often lead to devastating forest damages and immense economic losses (Sipos *et al.*, 2018). *Armillaria* colonies are spread in the soil by root-like rhizomorphs which can attack host trees through root contacts, and then the penetrating hyphae colonize heartwood and invade the cambium as mycelial fans (Sipos *et al.*, 2017; Chen *et al.*, 2019). In general, *Armillaria* root disease results in reduced forest productivity due to direct mortality or permanent non-lethal infections affecting the health and growth of the trees (Ross-Davis *et al.*, 2013; Chen *et al.*, 2019).

There has been a long history of great interest in exploring the ecology of *Armillarioid* species throughout the Northern Hemisphere (Shaw and Roth, 1976). The distribution of *Armillaria* and *Desarmillaria* (*tabescens*) species varies generally based on the tree species as well as on their stumps or dead substrates. Here, we focus on five common *Armillarioid* species, *D. tabescens*, *A. ostoyae*, *A. cepistipes*, *A. mellea* and *A. gallica*, which differ in virulence, geographical distribution and host range (Kedves *et al.*, 2021).

1.1.1 Host preference

It is well-known that most *Armillaria* species exhibit preference towards either coniferous or broadleaf environment and hosts (Lushaj *et al.*, 2010). Although native coniferous forests in the Northern Hemisphere are predominantly inhabited by *A. ostoyae* and *A. cepistipes*, various oak and other broadleaf species are mostly exposed to *A. mellea*, *A. gallica* and *D. tabescens* (Keča *et al.*, 2009). Investigation of the host preference in the case of *Armillaria* species revealed that *A. ostoyae* exhibited more virulence towards coniferous species than deciduous hosts, while *A. mellea* showed higher pathogenicity towards broadleaf species than conifer hosts (Omdal, 1995; Sicoli *et al.*, 2003). It was confirmed that the deciduous flowering plant aspen (*Populus tremuloides*) was significantly more tolerant to *A. ostoyae* infection than the tested conifers including ponderosa pine (*Pinus ponderosa*), white

pine (*Pinus strobiformis*), lodgepole pine (*Pinus contorta*), white fir (*Abies concolor*), blue spruce (*Picea pungens*), Douglas-fir (*Pseudotsuga menziesii*) and western larch (*Larix occidentalis*) (Omdal, 1995). Another convincing evidence came from pathogenicity tests for *A. ostoyae*, *A. mellea* and *A. gallica* on different oak trees (Sicoli *et al.*, 2003). The result indicated that *A. mellea* and *A. gallica* were significantly more virulent on seedlings and young trees of five tested *Quercus* species than *A. ostoyae*. It was also inferred that the coniferous species were more resistant to *A. mellea* infection than *A. ostoyae*, based on the comparative observation that *A. ostoyae* penetrated faster to cell layers in depth of unwound root bark of sitka spruce (*Picea sitchensis*) (Solla *et al.*, 2002). One more vital clue came from plant polyphenols, the secondary metabolites acting as the primary chemical defense to inhibit the parasitic fungal growth by restricting the production of cell wall degrading enzymes (Brazee *et al.*, 2011). Hydrolyzable tannins as one type of plant polyphenols are most abundant in the wood, bark and leaves of *Quercus* species. In contrast to *A. ostoyae*, *A. gallica* proved to be good at oxidizing and metabolizing polyphenols (Brazee *et al.*, 2011).

1.1.2 Distribution characteristics

Species of *Armillaria* are widely distributed in a variety of forest types. Interestingly, pathogenic species of *Armillaria* frequently co-exist with less pathogenic but more saprotrophic *Armillaria* species in the same forest stands. *A. mellea* was reported to share many forest types in common with *A. gallica*. For example, it was observed that *A. mellea* and *A. gallica* had overlapping geographic ranges in central North America, the main reason of which probably was that both of the two species favor similar hosts, especially various oak and broadleaf plant species (Baumgartner and Rizzo, 2001a; Mihail *et al.*, 2002). There are evidential phenomena from previous reports that sympatric genets of *A. mellea* and *A. gallica* were found to form mosaics within the forest floor in the field (Luisi and Lerario, 1996; Bruhn *et al.*, 2008). Species of *A. ostoyae* and *A. cepistipes* are also efficient colonizers and frequently occur in the same forest types. It was reported in Serbia, that the two cohabitating species were observed in the cold tolerant conifer forest type dominated with plant species of silver fir (*Abies alba*) and Norway spruce (*Picea abies*) (Keča *et al.*, 2009).

During a long co-evolution history, different *Armillaria* species probably have achieved a neutralistic or even harmonious coexistence by exploiting different strategies to compete for survival resources. As illustrated by an experimental study conducted in a managed Norway spruce forest, *A. ostoyae* and *A. cepistipes* were found to co-occur at the same site as efficient stump colonizers, but due to a mutual effect by interspecific competition, *A. ostoyae*

rhizomorphs were relatively more frequent on spruce stumps than in soil, while *A. cepistipes* rhizomorphs were relatively less frequent on stumps than in soil (Prospero *et al.*, 2006).

Sophisticated developmental changes especially regarding the morphology and function of rhizomorph systems may give a good explanation for their cohabitation (Smith *et al.*, 1992). More parasitic *Armillaria* species such as *A. ostoyae* and *A. mellea* equipped with dichotomously branched rhizomorphs proved to be more aggressive in killing seedlings than monopodially branched species such as *A. cepistipes* and *A. gallica* (Morrison, 2004). Moreover, rhizomorphs of facultative parasitic species reinforce their foraging efficiency by developing significantly more growth tips to increase their competitiveness in soil when confronted with the larger rhizomorph systems of saprotrophic species (Mihail and Bruhn, 2005). However, rather than causing lethal diseases, the more saprotrophic species prefer to derive nutrition from rotten wood or humus in the soil; their rhizomorphs, through non-invasive physical contacts, may also share nutrient resources with potential symbiotic plant partners (Guo *et al.*, 2016). The interspecific interactions of *Armillaria* species as well as their impacts on hosts give better understanding of their co-occurrence and provide important information about the disease spread.

1.1.3 Pathogenicity variation

A. ostoyae and *A. mellea* are generally considered to be primary necrotrophic parasites, whereas *A. cepistipes* and *A. gallica* are weakly secondary pathogenic on tree species (Baumgartner and Rizzo, 2001b; Bendel *et al.*, 2006; Metaliaj *et al.*, 2006; Heinzlmann *et al.*, 2017). In a field study, *A. ostoyae* showed more virulence on spruce seedlings half year after cutting, the stumps colonized by *A. ostoyae* reached to a higher level than by *A. cepistipes* (Heinzlmann *et al.*, 2017). The attached rhizomorphs of *A. ostoyae* on the root surface caused significantly more lesions (Prospero *et al.*, 2004). *A. mellea* was found more aggressive and pathogenic than *A. gallica*. Mycelial fans of *A. mellea* were frequently found on living roots. *A. gallica* also had the ability to attack live host, but more frequently occurred on living roots as epiphytic rhizomorphs (Baumgartner and Rizzo, 2001b). During the long history of cohabitation, *Armillaria* species somehow coevolve to reach a mutually beneficial relationship, in which less pathogenic species preferentially attack the weakened plants after primary infections caused by the more pathogenic species such as *A. ostoyae* (Bendel *et al.*, 2006). However, past observations have suggested that not only the species *A. mellea* but also *A. gallica* can be highly aggressive and pathogenic, and become a major threat resulting in the decline and loss of native tree species (Kim *et al.*, 2010). Under increasing stress such as

drought and climate change, the isolates of *A. gallica* from declining stands were found highly pathogenic, and turned out to be a contributing factor to forest decline in some areas on the island of Hawaii (Kim *et al.*, 2010). Similar observation was made in the declining oak trees in Southern Italy: due to the remarkable weakness of the oak woods under drought condition, instead of *A. mellea*, *A. gallica* dominated in the oak stand and became the primary mortality factor (Luisi and Lerario, 1996).

Pathogenic *Armillaria* species induce different patterns of structural and biochemical responses such as cambial damage and xylem compartmentalization in susceptible hosts (Cleary *et al.*, 2012b). The fate of individuals of various host species upon *Armillaria* infection is probably determined by the tolerance and resistance patterns expressed at lower stem or root. Structural responses to *A. ostoyae* in the roots of three different conifer species including western hemlock (*Tsuga heterophylla*), Douglas-fir and western redcedar (*Thuja plicata*) indicated that *A. ostoyae* could induce greater resistance response in western redcedar (Cleary *et al.*, 2012a). Lesions bounded by necrophyllactic periderms with multiple phellem bands were more frequently observed on roots of western larch (*Larix occidentalis*) infected by *A. ostoyae* than on Douglas-fir roots (Robinson and Morrison, 2001). On the other hand, there was a trend of infection occurrence inversely related to stand age class among coniferous species, such as slash pine (*Pinus elliottii*), Khasi pine (*P. kesiya*), Caribbean pine (*P. caribaea*) and patula pine (*P. patula*); a higher frequency of roots decayed and killed by *A. ostoyae* was observed in juvenile plantations (Lundquist, 1993). Mortality rate declining with increasing plantation age was supposed to be associated with increasing host resistance. In the conifer stand of Douglas-fir, a decline in mortality caused by *A. ostoyae* usually began after 15-18 years (Morrison, 2009).

1.1.4 Damages caused by *Armillaria*

Armillaria species frequently observed in disease centers causing gradual, multiyear reduction of growth and yield of healthy trees (Baumgartner and Rizzo, 2001b; Bendel *et al.*, 2006; Metaliaj *et al.*, 2006; Heinzelmann *et al.*, 2017). Original forests usually establish a more adaptive or even harmonious relationship between plants and plant pathogens. Plant species in natural forests were generally considered to be less susceptible to *Armillaria* infection (Rizzo *et al.*, 1995; Chapman *et al.*, 2011). However, they still can be compromised by various kinds of impact factors such as natural hazards and animal attacks and cannot escape *Armillaria* infection, not even to mention the less stable managed forests. Plantation forestry is of growing economical importance world-wide. With the plantation increasing, the

threat of *Armillaria* root disease to these new timber resources is also increasing. Tree mortality caused by *Armillaria* frequently occurs in discrete disease centers and forest land occupied by *Armillaria* pathogens is usually unavailable for fiber production (Labbé *et al.*, 2015).

As plants die, the *Armillaria* inocula incubate on their root systems, then spread and kill surrounding trees resulting in large scale tree mortality and formation of canopy gaps (Bendel *et al.*, 2006). Disease centers sometimes may not only limit to a few trees but encompass several hectares. Gaps associated with root disease can enlarge triggered by coalescence of multiple smaller gaps (Rizzo and Slaughter, 2001). Among all the factors predicted to directly affect canopy gap size in a pristine ponderosa pine stand in the Black Hills of South Dakota, *Armillaria* root disease seems to have the most considerable overall impact, followed by other small-scale disturbances (bark beetles, weak pathogens, ice/snow damage, lightning and wildfires) (Lundquist, 2000). In the Swiss National Park, *A. ostoyae*, *A. cepistipes* and *A. borealis* were identified from recently dead or dying mountain pine (*Pinus mugo*) from 42 canopy gaps; among them, *A. ostoyae* proved to be the dominant *Armillaria* pathogen accounting for 72% of all *Armillaria* isolates (Bendel *et al.*, 2006). In south-western Australia it was estimated that a total of 125 susceptible plant species collected from the disease centers were killed by the infection of *A. luteobubalina* in coastal dune vegetation (Shearer *et al.*, 1998). In Yosemite valley, California, canopy gaps caused by *A. mellea* occupied a total area of 4.1 ha (Rizzo and Slaughter, 2001). *A. mellea* also caused chronic root disease on grapevines. The expansion of dying and dead grapevines caused by *A. mellea* was the contributing factor to the formation of disease centers in the commercial vineyards of California (Baumgartner and Rizzo, 2002).

Loss of tree growth and the presence of dead trees are common inside a disease center (Mallett and Volney, 1998). Above-ground symptoms that are suggestive of an already impacted root and vascular system associated with *Armillaria* infection are wilting, premature defoliation, dwarfed or downward-hanging foliage, foliage yellowing, dwarfed fruit, resinosis, stunted shoots, stand-structural changes, lower-stem deformations, down-wood accumulations, crown thinning, branch dieback and premature death in the case of conifers as well as nut and fruit crops (Gutter *et al.*, 2004; Baumgartner and Rizzo, 2006; Skovsgaard *et al.*, 2009; Lehtijärvi *et al.*, 2012; Chandelier *et al.*, 2016). Diseased trees infected with *Armillaria* are generally smaller than healthy trees for all measured variables, in respect of diameter, height, sapwood area at the base of live crown, crown width and length (Cruickshank and Filipescu, 2012). As compared to uninfected trees, symptomatic trees were tested to experience a

sustained 5 to 15 years decline in basal area before death in upland black spruce (*Picea mariana*) forests (Westwood *et al.*, 2012). A research trial (Kimberley *et al.*, 2002) indicated that a significant wood volume yield reduction occurred in first rotation stands of Monterey pine (*Pinus radiata*) in many parts of New Zealand because of the widespread of root rot disease caused by *A. novae-zelandiae* and *A. limonea*.

Symptoms and signs related to *Armillaria* root disease were observed, as shown in some vivid pictures from previous studies (Figure 1). In the partially decayed woods, *Armillaria* was discovered to produce thick, white mats of mycelial fans beneath the bark of infected basal stems and roots or intercalated within multiple bark layers, which was a diagnostic feature of *Armillaria* root rot disease (Klopfenstein *et al.*, 2009). They also formed rhizomorphs attached to the infected roots and further extended to the surface of uninfected roots (Tsykun *et al.*, 2012). However, sometimes rhizomorph is considered a poor indicator of *A. mellea* or *A. ostoyae* infection (Redfern, 1973), because the rhizomorphs formed by more saprotrophic species such as *A. cepistipes* and *A. gallica* were generally more extensive and common than those of *A. mellea* or *A. ostoyae* in natural environments (Guillaumin *et al.*, 1993), whereas the mycelial fans of more pathogenic species such as *A. mellea* or *A. ostoyae* are usually more frequent in roots than mycelial fans of *A. gallica* or *A. cepistipes* (Baumgartner and Rizzo, 2001b; Lygis *et al.*, 2005; Marçais and Bréda, 2006; Bendel and Rigling, 2008; Ford *et al.*, 2017).

The presence of characteristic mycelial fans under the bark of the basal trunk indicated that *A. ostoyae* already occupied the root systems (Roth *et al.*, 1980). Invasion by mycelial growth along stems was observed from the indigenous stands of rimu (*Dacrydium cupressinum*, *Podocarpaceae*) by *A. novae-zelandiae* in the southern Westland of New Zealand (Hood, 2012). They can expand into the inner bark of both the roots and trunk and subsequently cause root lesions and basal canker at trunk bases known as collar rots or foot rots (Shaw, 1980). The decayed wood is often stringy or spongy and sometimes wet (Aguñ-Casal *et al.*, 2004). Internal decays including spongy rot and heart rot in black alder (*Alnus glutinosa*) stands of central-eastern Latvia were primarily caused by *Armillaria* species and *Inonotus radiatus* (Arhipova *et al.*, 2012). Basal resinosis and dead cambium caused by *A. ostoyae* were frequently observed in resinous species such as ponderosa pine, mountain pine (*P. mugo* ssp. *uncinata*), Norway spruce and Douglas-fir (Sicoli *et al.*, 2003; Bendel and Rigling, 2008).

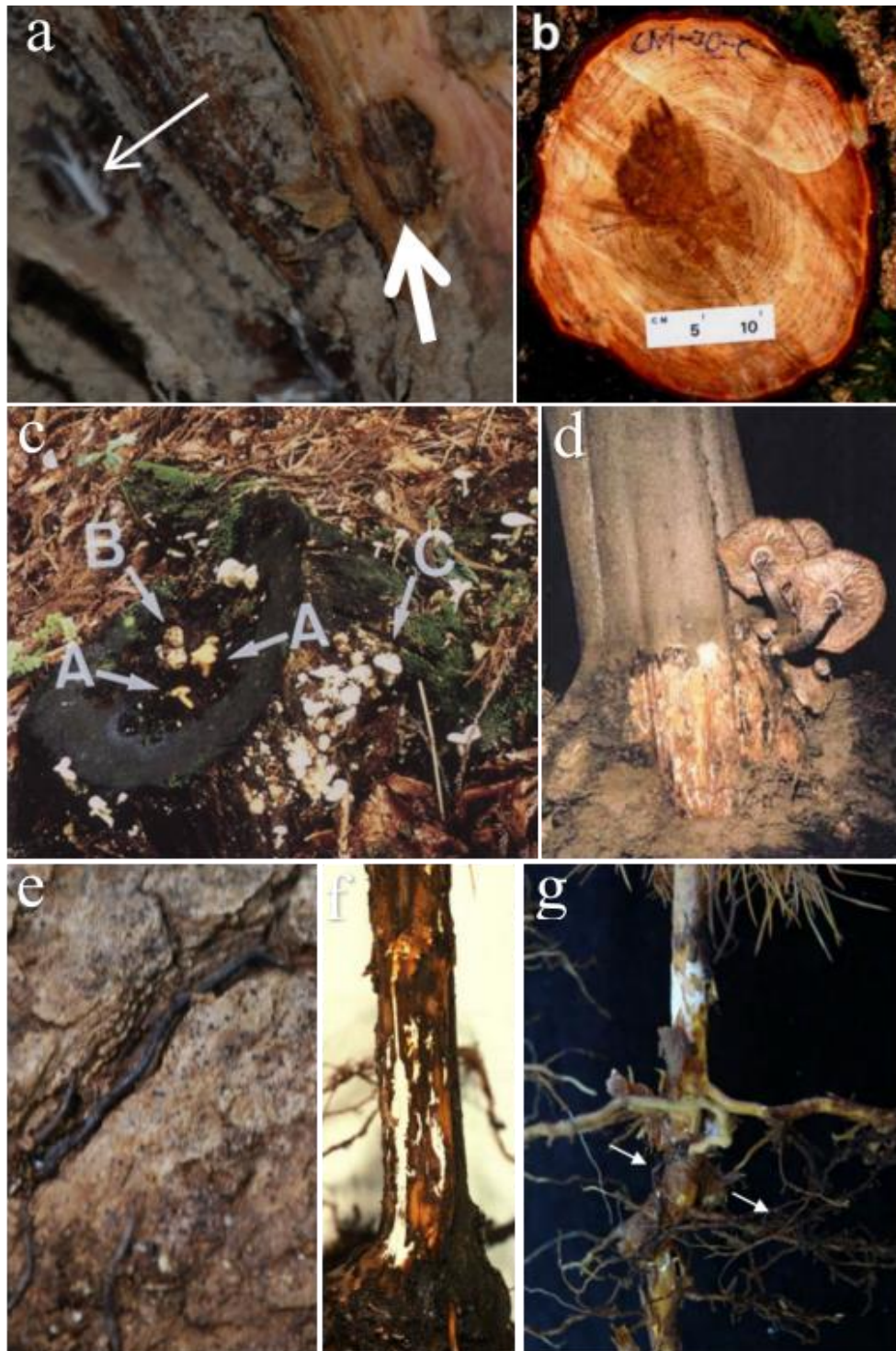


Figure 1. Symptoms and signs of *Armillaria* root rot disease: (a) Lesion (thick arrow) on decayed oak root in association with *Armillaria* mycelium (thin arrow) (Lee *et al.*, 2016a); (b) Heart-rot in black alder stem caused by *Armillaria* sp. (Arhipova *et al.*, 2012); (c) Basidiome formation of *A. gallica* (A) and *Rhodophyllus abortivus* (B and C) on a decaying stump (Cha and Igarashi, 1996; Coetzee *et al.*, 2001); (d) Mushroom gills of *A. mellea* on citrus tree horizontally lying on the ground (Munnecke *et al.*, 1981); (e) Example of *Armillaria* rhizomorph (root-like structure) following bark fissure observed on oak stumps in Missouri clearcuts (Lee *et al.*, 2016a); (f) Mycelial fans of *A. mellea* (white and thick fungal tissue) underneath the bark of affected vine root (*Vitis vinifera*) (Baumgartner and Rizzo, 2006); (g) 2.5-year-old maritime pine (*Pinus pinaster*) tree colonized by *A. ostoyae* with white mycelia and rhizomorphs indicated by arrows underneath the stem (Solla *et al.*, 2011).

1.1.5 The spread of *Armillaria* root disease

Short distance infection caused by physical root contact plays an important role in the spread of *Armillaria* species, since some virulent species form much less rhizomorphs in soil, whereas others such as *A. cepistipes* and *A. gallica* easily spread by the explorative rhizomorphs (Prospero *et al.*, 2006). The infection caused by the elaborate mycelial structures including mycelial fans and rhizomorphs penetrating the host tissue and contaminating the surrounding soil are supposed to be the predominant mode for the clonal local spread of *Armillaria* root rot disease (Solla *et al.*, 2002; Marcais and Cađ, 2006). In northern Turkey, as multilocus genotyping indicated, a single genet of *A. ostoyae* at least 0.2 ha in size was identified from the disease center associated with the dying 60-year-old Scots pines (*Pinus sylvestris*) in a naturally regenerated forest (Lehtijärvi *et al.*, 2012).

Rhizomorphs appear on the infected host tissues and further extend into soil to travel between host plants (Solla *et al.*, 2002). They breach mechanical obstacles and may function as an organ system where absorption and transportation occur and facilitate underground spread (Cairney *et al.*, 1988; Pareek *et al.*, 2001; Yafetto *et al.*, 2009). Air pores developed in *Armillaria* mycelium associated with a complex system of gas channels conduct oxygen into rhizomorphs. This complicated aerating system facilitates efficient oxygen diffusion and aeration for *Armillaria*, probably contributing to a broader and deeper spread of the inoculum into low oxygen environments such as a depth of more than 16 cm in soil (Pareek *et al.*, 2006). These beneficial features of rhizomorphs have resulted in the devastating expansion of *Armillaria* species such as *A. ostoyae*, *A. mellea*, *A. gallica* and *A. cepistipes* over vast territories (Smith *et al.*, 1994; Mar çais and Bréda, 2006; Chandelier *et al.*, 2016).

At the larger regional scale, *Armillaria* species probably spread by the way of dispersion of basidiospores (Dutech *et al.*, 2017). Although the fruiting bodies of *Armillaria* release huge quantities of basidiospores, usually leaving dense local spore prints behind or occasionally dispersing at regional scale by wind, haploid mycelia germinating from the spores and causing plant infection appear fairly unobservable in nature (Hood *et al.*, 2002; Hood *et al.*, 2008). As a possible explanation, the haploid mycelia and germinating basidiospores could either become dormant or be short-lived, and also their infectious ability are largely relied on the opportunities to mate with another compatible propagule (basidiospore or haploid mycelium) and generate a new diploid mycelium (Heinzelmann *et al.*, 2018). Actually, in an outdoor inoculation experiment, the isolates of haploid *A. ostoyae* could form mycelial fans on dead woods, but failed to invade seedlings and saplings of Norway spruce, and only diploid mycelia could be recovered from the infected plants (Heinzelmann and Rigling, 2016).

New genotypes from basidiospores would favor colonization on clear-cutting or the planting of new conifer stands (Legrand *et al.*, 1996). Sexual spore dispersal may be more efficient at fine spatial – for example, a few kilometers – in contrast to larger spatial scales (Travadon *et al.*, 2012; Dutech *et al.*, 2017).

1.1.6 The potential *Armillaria* inoculum

Root fragments, woody debris and small woody plants provide nutrition for the survival of *Armillaria*; these survival substrates serve as potential sources of root disease inoculum (Reaves *et al.*, 1993). Thus, pre-existing forests are supposed to act as sources of pathogen inoculum leading to the colonization of *Armillaria* on newly planted stands and spreading around the vicinity of afforested areas (Lung-Escarmant and Guyon, 2004). For example, pre-existing *A. ostoyae* inoculum in the maritime pine forest of the Landes de Gascogne (France) caused heavy infection and tree mortality: the tree mortality increased after planting, and from the third year on, newly dead pines served as secondary inoculum and played an increasing role along with time, not even to mention that the contribution of the primary inoculum was still essential (Lung-Escarmant and Guyon, 2004). White root rot in vineyards was primarily caused by *A. mellea*, and the low frequency of the disease incidence caused by *A. cepistipes* and *A. gallica* was probably just due to the fact that the vineyards were located on cleared forestry sites (Aguñ-Casal *et al.*, 2004). The mortality rate increased as the distance between the colonized stumps and the healthy trees decreased.

An expanding list of non-woody plants susceptible to *A. mellea* suggested more widespread infection of herbaceous species than currently acknowledged (Ford *et al.*, 2017). Some non-woody plants may also serve as a potential inoculum (Klein-Gebbinck *et al.*, 1993; West *et al.*, 2000). The lodgepole pine seedlings inoculated with root segments of fireweed (*Epilobium angustifolium*) colonized by *A. mellea* were infected and killed. Hence it was suggested that fireweed may serve as a potential inoculum reservoir for the spread of *A. mellea* in the pine forest (Klein-Gebbinck *et al.*, 1993). *A. ostoyae* artificially inoculated to herbaceous plants under field condition resulted in infection, therefore *A. ostoyae* was also supposed to have the potential ability to infect herbaceous plants (West *et al.*, 2000). However, there were no infection symptoms on lodgepole pine seedlings inoculated with fireweed colonized by *A. ostoyae* (Klein-Gebbinck *et al.*, 1993).

1.2 Chemical and silvicultural means of *Armillaria* control

The serious economical and ecological damages triggered by pathogenic *Armillaria* species require robust control strategies. *Armillaria* species as wood decay fungi usually hide beneath the infected root bark to decompose wood and cause damages in plant tissues (Figure 1). Besides, even after hosts die, they still survive in soil saprotrophically for decades. Therefore, control of *Armillaria* becomes even more challenging than we expected (Smith *et al.*, 1992). What, if anything, could or should be done with the productive growing sites for various coniferous or broadleaf species that are progressively dying from root rot disease caused by *Armillaria* pathogens?

Chemical fungicides, such as paclobutrazol, fenpropidin, flutriafol, hexaconazole, cyproconazole, methyl bromide, vapam, carbon disulfide, chloropicrin and vorlex showed their efficacy in fungal growth inhibition and some of them proved to be effective for reducing the progress of *Armillaria* root disease (Filip and Roth, 1977; Turner and Fox, 1977; Adaskaveg *et al.*, 1999; Jacobs and Berg, 2000; Aguin *et al.*, 2006; Thomidis and Exadaktylou, 2012; Chen *et al.*, 2021). However, several problems appeared during the application of chemicals. Eradicating *Armillaria* pathogens from a living host can be of lower efficiency due to failing to deliver a fungicide directly to the infected roots. Chemicals like fumigants do not penetrate the soil deeply enough to kill all *Armillaria* inocula in soil or from the infected roots, thus can not guarantee long-term control (Munnecke *et al.*, 1981; Appel and Kurdyla, 1992; Adaskaveg *et al.*, 1999; West and Fox, 2002; Amiri *et al.*, 2008). Moreover, the use of chemicals caused a lot of environmental concerns and faced several safety and health issues for worker and farmer, and it is also very costly and labour intensive (Robinson and Smith, 2001).

On the other hand, it remains unclear what roles the silvicultural treatments are playing in disease development in the forested landscapes, since *Armillaria* infection seems unlikely to be reduced by some silvicultural managements such as clearcutting and replantation or thinning, which provide new stumps, roots and wood debris suitable for vegetative colonization or basidiospore dispersal (Morrison *et al.*, 2001; Oliva *et al.*, 2008; Chapman *et al.*, 2011; Lee *et al.*, 2016a). Although the inoculum removal measures such as stump or root removal reduced the level of *Armillaria* root rot disease (Sturrock, 2000; Baumgartner, 2004; Vasaitis *et al.*, 2008; Schnabel *et al.*, 2012), it reoccurred over a period of time (Cleary *et al.*, 2013). Thus, silvicultural practices do not seem to guarantee a long-term controlling effect and these approaches are also time consuming and costly.

1.3 Biological control of *Armillaria*

Concerning the environmental threats posed by chemical fungicides as well as the unstable and undurable control efficacy of silvicultural practices, biological control strategies are considered as alternatives (Kedves *et al.*, 2021). The emergence of potential biocontrol microorganisms can serve plant protection purposes or even do better (Moraes Bazioli *et al.*, 2019). It is full of benefits to our environment with no pesticide residue or pollution and is conducive to the safety of animals and humans. It can promote plant growth and effectively protect plants from various pathogen-induced diseases, resulting in increased harvest and production (Syed Ab Rahman *et al.*, 2018). Biological control emphasizes on environment protection and ecological sustainability usually by the exploitation and employment of beneficial microorganisms, especially some free-living soil fungi (Knudsen and Dandurand, 2014). The use of naturally occurring antagonistic fungi (*e.g.*, certain *Trichoderma* species) and bacteria (*e.g.*, *Bacillus* and *Pseudomonas* species) has uncovered great potential to successfully reduce the pathogenic activities of *Armillaria*. Particularly, native microorganisms isolated from soil, rhizosphere or directly from plant roots usually have a better adaptation to that specific soil and plant environment, and thus can display more efficient control of diseases than introduced exotic microorganisms (Weller, 1988).

1.3.1 Potential biocontrol of *Armillaria* by bacteria and saprobic basidiomycetes

Potential biocontrol bacteria showed their efficacy to control some fungal pathogens of agronomic crops (Olanrewaju *et al.*, 2017); however, their applications in *Armillaria* control are still waiting for investigation. Antagonistic bacteria isolated from native soil environments such as *Pseudomonas* spp. (*e.g.*, *Pseudomonas fluorescens*), *Bacillus* spp. (*e.g.*, *Bacillus simplex*), *Serratia* spp., *Enterobacter* spp., *Rhizobium radiobacter* (formerly *Agrobacterium radiobacter*), *Erwinia billingiae*, actinobacteria as well as *Streptomyces* spp. (*e.g.*, *Streptomyces aurantiacogriseus*, *S. jumonjinensis*, *S. kasugaensis* and *S. setonensis*) proved to show antagonistic interactions with several *Armillaria* spp. (*e.g.*, *A. ostoyae*) along with the reduction of their pathogenic effects (Dumas, 1992; Vasconcellos and Cardoso, 2009; DeLong *et al.*, 2011; Zagryadskaya *et al.*, 2015; Mesanza *et al.*, 2016; Kedves *et al.*, 2021).

Some saprobic basidiomycete fungi (*e.g.*, *Hypholoma fasciculare*) as effective competitors of pathogenic *Armillaria* species were proven effective to restrict colonization of dead or dying trees by *Armillaria* and reduce *Armillaria* viability and growth through competitive spatial exclusion of *Armillaria* from stumps and roots (Chapman and Xiao, 2000). The wood decay saprophytic fungi including *Rigidoporus conrescens*, *Hypholoma acutum*,

Hypholoma australe, *Sistotrema brinkmannii*, *Phlebiopsis gigantea*, *Phanerochaete filamentosa*, *Stereum sanguinolentum*, *Resinicium concrescens* and *Resinicium bicolor* showed their biocontrol potential against *Armillaria novae-zelandiae* and *A. luteobubalina* (Pearce and Malajczuk, 1990; Pearce *et al.*, 1995; Hood *et al.*, 2015). The investigation of the biocontrol potential of eight common saprophytic fungi on newly cut stem segments of Monterey pine revealed that *Ganoderma mastoporum* and *Rigidoporus catervatus* evidently reduced colonization by *Armillaria* pathogens, but comparing to those competitive basidiomycete antagonists, species of *Trichoderma* displayed markedly more antagonism to *A. limonea* and *A. novae-zelandiae* (Li and Hood, 1992).

1.3.2 Potential biocontrol of *Armillaria* by *Trichoderma* species

Species of the soilborne genus *Trichoderma* have been explored as biocontrol agents (BCAs) against *Armillaria* (Kedves *et al.*, 2021). Examples of *Trichoderma* BCAs for controlling *Armillaria* pathogens are shown in Table 1. Soil isolates of *T. atroviride* and *T. harzianum* were frequently under investigation for their biocontrol potential against *A. mellea* and other *Armillaria* species. The high efficacy of using *Trichoderma* BCAs to overcome the *Armillaria* challenge has resulted in increased investigations and explorations for unveiling their antagonistic strategies and interaction mechanisms. Several studies indicated that the antagonistic *Trichoderma* species affected *Armillaria* species through antibiosis reflected by growth inhibition of *Armillaria*, by competition for nutrients and space, and most importantly through direct mycoparasitic action (Table 1).

Antibiotic metabolites of *Trichoderma* inhibited the mycelial growth as well as rhizomorph formation of *Armillaria* (Reaves *et al.*, 1990; Tarus *et al.*, 2003). For instance, diffusible compounds from *T. citrinoviride* were proven responsible for the strong inhibition effect on colony growth and rhizomorphs production of *A. solidipes* (Reaves *et al.*, 1990). These antifungal compounds were metabolites but not enzymes, as they still had inhibitory effect on *Armillaria* after the denaturation of all proteins in the *Trichoderma* filtrates by autoclaving (Reaves *et al.*, 1990). The metabolite 6-n-pentyl- α -pyrone isolated from the fermentation broth of *T. longibrachiatum* and *T. harzianum* showed significant activity on several tested bacteria and fungi, and also showed complete growth inhibition of *A. mellea* colonies at a concentration of 200 ppm (Tarus *et al.*, 2003). However, not all the antibacterial and antifungal metabolites from *Trichoderma* showed activity on *Armillaria*. For example, sorbicillin had antifungal activity on the fungi *Paecilomyces variotii* and *Penicillium notatum* but showed no activity on *A. mellea* (Tarus *et al.*, 2003).

The mycoparasitic process of biocontrol against *Armillaria* was observed and investigated under light and scanning electron microscopy; this process included colonization and penetration of rhizomorphs by *Trichoderma* hyphae, sporulation of *Trichoderma* on the surface of rhizomorphs, as well as lysis and degeneration of rhizomorph tissue along with discharge of rhizomorph content (Asef *et al.*, 2008). The mycoparasitic interaction process was further investigated by monitoring active degradation and metabolic assimilation through isotope ratio mass spectrometry during physical contact by dual-culture tests (Pellegrini *et al.*, 2012). During the direct physical interaction with ^{13}C -labeled *A. mellea*, the ^{13}C content in *T. atroviride* mycelia increased substantially by absorbing some leaching exudates and metabolites secreted by the labeled pathogen, mostly assimilating through proactively parasitizing the pathogen (Pellegrini *et al.*, 2012). A similar experiment using the same method was also carried out on a strain of *T. harzianum*, since it suppressed *A. mellea* development with a growth inhibition rate of $80 \pm 0.19\%$ (Pellegrini *et al.*, 2013). During mycelial contact with ^{13}C -labelled *A. mellea*, ^{13}C values detected in *T. harzianum* mycelia significantly increased to a higher level than the absorption of ^{13}C values in two tested antagonistic bacteria *Rhodospiridium babjevae* and *Pseudomonas fluorescens*, and the mycoparasitic activity of *T. harzianum* on the labeled *A. mellea* maintained for one month in dual culture (Pellegrini *et al.*, 2013).

The introduced *Trichoderma* establishes to survive and disperse in a new environment adapting as an integrant part of the native microbial community. The exotic *T. atroviride* SC1 was able to survive and colonize the rhizosphere and also dispersed to the leaves of grapevine, even one year after soil treatments it could still persist and be recovered from the inoculation sites (Longa *et al.*, 2009). Long-term maintenance of the biocontrol effects on pathogenic *Armillaria* species in field largely rely on the environmental adaptation of *Trichoderma* species. Therefore, the investigation of the environmental impacts resulting from long persistence and rapid spread of *Trichoderma* was required. As suggested, the introduction of *T. atroviride* SC1 posed a risk but a lot lower than other abiotic environmental factors to non-target native communities of fungi and bacteria in the soil of a vineyard; the strain SC1 had only slight influence on the biodiversity and composition of local soil microbiota (Savazzini *et al.*, 2009). Further investigation into the influences of *T. atroviride* SC1 introduction on local microorganisms was conducted at the transcriptional level. It was found that *T. atroviride* SC1 was recognized specifically; resistance mechanisms and defence reaction processes were activated in a simplified soil microcosm from a combination of 11 soil microorganisms. In response, biocontrol mechanisms of *T. atroviride* SC1 were already

activated by the soil microcosm even before *A. mellea* introduction, probably in order to competitively occupy niches (Perazzolli *et al.*, 2016).

Table 1. *Trichoderma* species used as biocontrol agents against pathogenic *Armillaria* species

<i>Trichoderma</i> strains	Pathogenic <i>Armillaria</i>	Biocontrol efficacy	References
<i>T. citrinoviride</i> <i>T. harzianum</i>	<i>A. ostoyae</i>	Reduction of <i>Armillaria</i> mycelial growth and rhizomorph formation on solid media amended with <i>Trichoderma</i> filtrates	(Reaves <i>et al.</i> , 1990)
<i>T. koningii</i> <i>T. harzianum</i> <i>T. longibrachiatum</i>	<i>Armillaria</i> spp.	<i>Armillaria</i> growth inhibition	(Onsando and Waudou, 1994)
<i>Trichoderma</i> spp.	<i>A. luteobubalina</i>	Significant reduction of root colonization along with an adverse effect on the fruiting of <i>Armillaria</i> by inoculation of five combined isolates of <i>Trichoderma</i> spp. into stumps of karri (<i>Eucalyptus diversicolor</i>)	(Nelson <i>et al.</i> , 1995)
<i>T. harzianum</i>	<i>Armillaria</i> spp.	Significant reduction of the viability of <i>Armillaria</i> in the plant materials and failure to colonize and invade the stem sections that had already been occupied by <i>Trichoderma</i>	(Otieno <i>et al.</i> , 2003a; Otieno <i>et al.</i> , 2003b)
<i>T. harzianum</i> <i>T. longibrachiatum</i>	<i>A. mellea</i>	Complete growth inhibition of <i>A. mellea</i> by the antifungal metabolite 6-n-pentyl- α -pyrone from <i>Trichoderma</i> at a concentration of 200 ppm	(Tarus <i>et al.</i> , 2003)
<i>T. hamatum</i> Thaml <i>T. harzianum</i> Th23 <i>T. viride</i> Tv3	<i>A. mellea</i>	Protection from <i>Armillaria</i> infection resulting in increased survival rate of the potted strawberry plants and healthier plants developing more leaves when inoculated with <i>Trichoderma</i>	(Raziq and Fox, 2004; Raziq and Fox, 2005)
<i>T. virens</i> <i>T. harzianum</i>	<i>A. mellea</i>	Inhibition of mycelial growth and rhizomorph formation of <i>A. mellea</i> by the volatiles from <i>Trichoderma</i> and the lysis discharge and degeneration of rhizomorph tissue caused by penetration of <i>Trichoderma</i> hyphae	(Asef <i>et al.</i> , 2008)
<i>T. harzianum</i>	<i>A. mellea</i>	Root collar excavation by air-spading followed by <i>T. harzianum</i> inoculation as a joint cultural/biocontrol strategy to eradicate <i>A. mellea</i> from infected strawberry plants	(Percival <i>et al.</i> , 2011)
<i>T. atroviride</i> SC1 <i>T. harzianum</i>	<i>A. mellea</i>	Dissolution of <i>Armillaria</i> cell wall and membrane followed by metabolic assimilation by <i>Trichoderma</i> during aggressive mycoparasitic interaction	(Pellegrini <i>et al.</i> , 2012, 2013)
<i>T. atroviride</i> SC1	<i>A. gallica</i>	Long period protection of strawberry plants from <i>A. gallica</i> infection by a bark mixture pre-inoculated with <i>T. atroviride</i> SC1	(Pellegrini <i>et al.</i> , 2014)

1.4 *Trichoderma* species as powerful biocontrol agents

Biocontrol mechanisms of *Trichoderma* BCAs acting on pathogenic *Armillaria* species still remain unclear and need further exploration. However, there is no doubt about the great potential of *Trichoderma* to control *Armillaria*. The biocontrol abilities of *Trichoderma* strains are based on a wide arsenal of various antagonistic mechanisms (Sood *et al.*, 2020). Understanding the mode of action of *Trichoderma* BCAs is essential for plant disease control. Mycoparasitism appears to be the most outstanding strategy, which involves the production of a series of extracellular fungal cell wall hydrolytic enzymes. Antibiosis to inhibit pathogens by the release of antimicrobial volatile and nonvolatile secondary metabolites, competition for space and nutrients as rapid colonizers, plant growth promotion as well as inducing plant defence reactions as avirulent plant symbionts are also among the most excellent biocontrol strategies deployed by *Trichoderma* BCAs (Sood *et al.*, 2020).

1.4.1 Mycoparasitic activity of *Trichoderma* species

The outstanding mycoparasitic potential of *Trichoderma* species was proved to be a very complex process comprising the differentiation of mycelial structure and several successive steps ((Kubicek *et al.*, 2008; Inbar and Chet, 1996). Shortly, actively branching mycelia of *Trichoderma* parasitize or even kill plant pathogens through robust physical penetration and assimilation, thus reducing their inoculum size in the rhizosphere. The destructive parasitic process initiates with the recognition and attachment of *Trichoderma* to the cell wall of the plant pathogenic hosts (Kubicek *et al.*, 2008), followed by the degradation of host hyphae by a variety of lytic enzymes, finally, concluding with the uptake and assimilation of the host's cellular content (Inbar and Chet, 1996). In addition, the hyphae of *Trichoderma* form appressoria during their extension towards the host mycelia and grow on the surface of the host. Conidia of *Trichoderma* adhere to the hyphae of the host pathogens and germinate on them after attachment. The young germinated hyphae parasitize the host mycelia again (Lu *et al.*, 2004).

The specific mycoparasitic behavior shown by certain *Trichoderma* stains or isolates plays a role in their biocontrol performance. Significant strain-specificity in photoconidiation and mycoparasitism was reflected by two strains of *T. atroviride* during confrontation with the tested phytopathogen *Fusarium oxysporum*. *T. atroviride* isolate IMI 206040 failed to fully overgrow and lyse *F. oxysporum*, while *T. atroviride* P1 was more active and able to fully mycoparasitize the host fungus (Speckbacher and Ruzsanyi, 2020). The mycoparasitic behavior of *Trichoderma* was influenced during the interaction with different hosts. Taking

one strain of *T. atroviride* as an example, before contact with the pathogen *Rhizoctonia solani*, the *Trichoderma* mycelium formed a cluster of branches approaching towards the host hyphae; subsequently, they aligned with the hyphae of the pathogen and caused breakage. Whereas different mycelial performances were observed during parasitism on *Pythium ultimum*, the mycoparasite grew alongside the host hyphae, coiled around them, and at the same time, branched towards adjacent hyphae (Lu *et al.*, 2004). Different performances of parasitic hyphae were also observed in *T. citrinoviride* when confronted with several different ginseng pathogens. After the mycoparasite unrestrictedly grew along the host hyphae in the contact area, *T. citrinoviride* coiled around, but failed to penetrate *Rhizoctonia solani* and *Botrytis cinerea* hyphae. However, the hyphae of *Trichoderma* directly penetrated *Phytophthora cactorum* and *Alternaria panax* hyphae without coiling. In addition, appressorium formation of *T. citrinoviride* was observed without coiling or penetration on *Pythium* spp. and *Cylindrocarpon destructans* (Park *et al.*, 2019).

Mycoparasitic interactions and their efficiency in biocontrol can be easily monitored in dual cultures between *Trichoderma* and its hosts, or directly observed through light and scanning electron microscopy (Asef *et al.*, 2008), therefore it is one of the most important parameters for screening *Trichoderma* BCAs. For example, by observation in two dual culture bioassays, candidate biocontrol fungi were screened based on the ability to reduce apothecium production and degrade sclerotia of *Sclerotinia sclerotiorum*; therefore *T. hamatum* was selected as the best biocontrol agent to control carpogenic infection in cabbage caused by *S. sclerotiorum* (Jones *et al.*, 2014a).

1.4.2 Extracellular enzymes of *Trichoderma* species

The extracellular enzymes produced by *Trichoderma* species have exposed great biocontrol potential against phytopathogens (Sharma *et al.*, 2003). Host specific detection and penetration during the process of mycoparasitism stimulate biosynthesis and secretion of a set of extracellular enzymes and mycotoxic secondary metabolites. Transcriptional regulation of genes encoding extracellular enzymes was proven to be controlled by an array of transcriptional factors. Several transcriptional activators including ACE3, XYR1 (Zhang *et al.*, 2019a), RXE1 (Wang *et al.*, 2019a), ACEII (Aro *et al.*, 2001) and CLP1 (Wang *et al.*, 2019b) and fungal transcriptional repressors (Rce1 (Cao *et al.*, 2017) and ACEI (Aro *et al.*, 2003)) play important roles in controlling expression of cellulases, xylanases and other lytic enzymes. In *T. atroviride*, the repressor of cellulase expression I (ACE1) was responsible for the biocontrol potential during the antagonistic action on plant pathogens *R. solani* and *F.*

oxysporum through controlling the expression of polyketide synthase (PKS) and the activities of cell wall-degrading enzymes (CWDEs) including β -1,3-glucanase, chitinase, protease, cellulase, galacturonase and xylanase (Fang and Chen, 2018).

Direct mycoparasitism is closely associated with the production of CWDEs playing an important role in the degradation of the cell wall and the penetration into the host hyphae (Sharma *et al.*, 2003; Gajera and Vakharia, 2012). Such a strategy was common in *Trichoderma* species during antagonistic interaction with soil plant pathogens. As clearly observed through high-resolution scanning electron microscopy, *T. harzianum* actively attached to the mycotoxin-producing and plant-pathogenic *Aspergillus* species and caused substantial enzymatic lysis of host mycelial filaments (Braun *et al.*, 2018). Antifungal activity of hydrolytic enzymes from *Trichoderma* species can be strong and highly efficient. For example, 60 U/mL of chitinase obtained from *T. asperellum* PQ34 nearly completely suppressed the growth of *Sclerotium rolfisii* and *Colletotrichum* sp. and prevented anthracnose on chilli fruits and mango infected with *Colletotrichum* sp. Besides, chitinase at 20 U/mL significantly reduced the *S. rolfisii* infection incidence in peanut plants (Loc *et al.*, 2019). β -1,3-glucanase and β -1,4-N-acetylglucosaminidase (NAGase) activities showed a significant increase on *Trichoderma* biocontrol effectiveness in reducing apothecium density of *S. sclerotiorum* with a consequent reduction in disease severity on common beans (Geraldine *et al.*, 2013).

Trichoderma species are also excellent competitors for space and nutrients. Their extracellular polysaccharide-degrading enzyme systems including cellulases (*e.g.*, endocellulases, cellobiohydrolases and β -glucosidases) and xylanases (*e.g.*, endoxylanases and β -xylosidases) enable the efficient utilization of plant polysaccharides (Monfil and Casas-Flores, 2014). Polysaccharide-degrading enzymes in *Trichoderma* species contribute to their success as saprotrophic competitors of soil-borne plant pathogens. 119 *Trichoderma* isolates originating from decaying wood samples and belonging to 12 species or species complexes were examined and screened for their ability to produce xylanolytic and cellulolytic enzymes; all of the isolates were able to degrade birch wood xylan and cellulose, however, the levels of xylanase and cellulase activities were varying among different species and isolates (Błaszczuk *et al.*, 2016). Other extracellular enzymes involved in saprotrophism of *Trichoderma* were also considered to be responsible for biocontrol abilities, such as NAGase; its deficiency in *T. hamatum* GD12 significantly reduced the fitness of the strain as a biocontrol agent of *S. sclerotiorum* in soil and also impaired saprotrophic competitiveness when confronted with *R. solani* (Ryder *et al.*, 2012). In conclusion, *Trichoderma* species

originating from forest soil and equipped with a wide arsenal of extracellular polysaccharide-degrading enzyme systems are usually excellent saprotrophs on woody debris. Thus, detection and characterization of enzymes such as β -glucosidase, cellobiohydrolase, β -xylosidase as well as other enzymes such as phosphatase in *Trichoderma* species are also considered important in screening for good candidates of *Trichoderma* BCAs from native forest soils.

Acid phosphatases produced by *Trichoderma* play a specific role in acquisition, mobilization and scavenging of phosphate, therefore enhancing plant growth and soil fertility. The production of phosphatases can be induced by cell walls of plant pathogens (Qualhato *et al.*, 2013). *Trichoderma* strains isolated from the Amazon rainforest were screened for their ability of solubilizing phosphate. 19.5% of the *Trichoderma* strains were able to solubilize or mineralize soil phosphate with the efficiency of phosphorus uptake up to 141% and also showed significant promotion of soybean growth up to 41.1% (Bononi *et al.*, 2020).

Extracellular enzymes of *Trichoderma* have provided plenty of evidence not only for their biocontrol roles as mycoparasitic factors, but also as elicitors of plant defense responses against bacterial and fungal pathogens (Dean and Anderson, 1991). During interaction with plant roots, two endopolygalacturonase genes were expressed in *T. virens* I10; further experiments indicated that constitutive production of endopolygalacturonase in tomato (*Lycopersicon esculentum*) could induce systemic resistance to infection caused by *B. cinerea* (Sarrocco *et al.*, 2017). The xylanases secreted by *T. asperellum* also proved to be good candidates for plant resistance induction and improving plant immunity against pathogens (Wu *et al.*, 2017). When interacting with tobacco (*Nicotiana tabacum*) leaves, *T. viride* secreted xylanase proteins and caused tissue necrosis. Further studies suggested that xylanase induced systemic resistance in the plant by stimulating the ethylene biosynthesis pathway (Dean and Anderson, 1991).

1.4.3 Metabolites produced by *Trichoderma* against fungal plant pathogens

Biocontrol activities of *Trichoderma* by directly weakening and inhibiting pathogens through antifungal compounds were commonly observed (Nagamani *et al.*, 2017). For example, volatile metabolites from *T. viride* were effective in reducing sclerotium production and mycelial growth in the plant pathogens *S. sclerotiorum* and *S. rolfsii* (Amin *et al.*, 2010). *Trichoderma* isolates from chickpea rhizosphere soil, with highly efficient non-volatile and volatile compound production, were proved to have high growth inhibition efficacy against the pathogens *F. oxysporum*, *Rhizoctonia bataticola* and *S. rolfsii* (Nagamani *et al.*, 2017).

Volatile-mediated battle between plant pathogens and biocontrol agents was investigated. *Trichoderma* species significantly increased the activity or the amount of antifungal volatiles. In response to *Trichoderma* invasion, *F. oxysporum* also immediately sensed and recognized volatiles from *Trichoderma* by producing its own volatiles to inhibit *Trichoderma* growth (Li *et al.*, 2018). To better understand the characteristics of antimicrobial metabolites related to the biocontrol capability of *Trichoderma* antagonists, metabolite analyses were conducted using analytical techniques such as spectrophotometry, nuclear magnetic resonance spectroscopy, liquid chromatography, gas chromatography, mass spectrometry, etc. *Trichoderma* metabolite databases have been constructed (Khan *et al.*, 2020).

Antifungal secondary metabolites including pyrones, polyketides and non-ribosomal peptides play important roles in the antibiotic effects of *Trichoderma* strains against fungal plant pathogens (Monfil and Casas-Flores, 2014). In a recent review, 390 non-volatile metabolites from 20 known *Trichoderma* species included amides, cyclopentenones, lactones, pyranone derivatives, peptides, pyridines, polyketides, peptaibols, steroids, terpenes, and tetrone acid derivatives (Li *et al.*, 2019). Some compounds exhibited important biocontrol activities during the mycoparasitic process; those antifungal secondary metabolites included peptaibols, pyrones, epipolythiodioxopiperazines, butenolides, pyridones, azaphilones, koniginins, steroids, anthraquinones, lactones, trichothecenes, etc. (Khan *et al.*, 2020). The antifungal compounds obtained from *T. viride* and *T. harzianum* achieved high growth inhibition on *Alternaria alternata*; they were identified as 17-octadecynoic acid (36.23%) and 6-O- α -D-galactopyranosyl-D-glucose (38.45%) (Meena *et al.*, 2017). Some non-volatiles such as azaphilone and harzianopyridone obtained from fungal culture filtrates of *T. harzianum* inhibited the growth of *Phytophthora cinnamomi*, *Leptosphaeria maculans* and *B. cinerea* even at low dose (1-10 μg per plug); while some metabolites required higher dose (>100 μg per plug) for inhibition, such as butenolide and harzianolide (Vinale *et al.*, 2009). The organic extracts of *T. harzianum* P11, *T. afroharzianum* P8, *T. gamsii* IT-62 and *T. erinaceum* IT-58 contained high amounts of polyphenol and flavonoids and significantly suppressed the mycelial growth of *Pythium myriotylum* (Tchameni *et al.*, 2020). The minimal concentrations for pathogen inhibition were 10 $\mu\text{g}/\mu\text{L}$, 20 $\mu\text{g}/\mu\text{L}$, 40 $\mu\text{g}/\mu\text{L}$ and 80 $\mu\text{g}/\mu\text{L}$ for extracts obtained from P11, P8, IT-62 and IT-58 respectively. There was strong correlation between the antagonistic effects of the examined *Trichoderma* strains on the pathogen and the production of total amounts of polyphenolic compounds and flavonoids (Tchameni *et al.*, 2020).

Diverse volatiles secreted by *Trichoderma* BCAs showing antagonistic effects on a wide

range of plant pathogens were identified and assigned to the classes of acids, alkanes, alcohols, furanes, ketones, esters, mono- and sesquiterpenes and pyrenes (Stoppacher *et al.*, 2010). Most of the volatiles are species-specific. In the study from several *Trichoderma* species, the only alcohol emitted by *T. virens* was 3-methylcyclopentanol, while *T. harzianum* produced several alcohols, such as 1-octanol, 1-heptanol, 1-hexanol, 1-pentanol, 2-methyl-1-propanol, 2-phenylethyl alcohol and 3-methyl-1-butanol. It was also proved that *T. virens* emitted more sesquiterpenes than *T. harzianum*. The compounds secreted from both species are acetic acid, 1-octen-3-ol and 3-octanone (Li *et al.*, 2018). A strong correlation was found between the antagonistic ability of *Trichoderma* BCAs *in vitro* and the production of 6-pentyl- α -pyrone; results showed that this compound not only caused growth reduction of *R. solani* and *F. oxysporum*, but also completely inhibited the germination of *Fusarium* spores (Scarselletti and Faull, 1994). The production of volatiles with fungistatic activity such as 6-pentyl-2H-pyran-2-one and (E)-6-pent-1-enylpyran-2-one from *T. atroviride* was suspected to be regulated by the NADPH oxidase Nox2 (Cruz-Magalhães *et al.*, 2019). There seems to be a vast diversity of metabolites related to the biocontrol potential *Trichoderma*, the examples related with antifungal volatiles and nonvolatiles discussed above may just be the tip of the iceberg.

1.4.4 Effects of *Trichoderma* species on plants

Besides the direct mechanisms of antagonism on plant pathogens, the ability of *Trichoderma* to promote plant growth through phosphorous mobilization, extracellular phosphatases, the production of siderophore and indole-3-acetic acid (IAA) derivatives and induction of systemic resistance in the plant should also be considered when screening for biocontrol agents (Monfil and Casas-Flores, 2014; Kumar *et al.*, 2017). The antagonistic behavior of some *Trichoderma* species resulted from the interaction with plant roots, leading to promotion of plant growth and improvement of tolerance to abiotic stresses as well as resistance to diseases (Contreras-Cornejo *et al.*, 2014).

When *Trichoderma* species competitively colonized the plant rhizosphere, deposition of lignin and callose was enhanced in specialized plant cells in protecting the vascular system in shoots, roots and leaves against pathogen infection, which contributed to better hydration and nutrition of plants (Nawrocka *et al.*, 2018a). Protection of plant was mostly resulted from enhanced activity of defense enzymes. *T. tomentosum* reduced disease severity and activated protective antioxidant responses by promoting significant increase in catalase, superoxide dismutase as well as flavonoid and glutathione enzymes in wheat plants infected by *Bipolaris*

sorokiniana (Pittner *et al.*, 2019). Protection activities triggered by *Trichoderma* might also rely on accumulation of salicylic acid derivatives as well as volatiles in plants. These volatiles played an important role in the upregulation of the PR4 gene in induced systemic resistance as well as the PR1 and PR5 genes in systemic acquired resistance (Nawrocka *et al.*, 2018a). In the closed-chamber experiments with *Arabidopsis thaliana* seedlings, the plant experienced an increase in shoot and root biomass induced by a blend of several volatile organic compounds of *T. atroviride*. The plant growth promotion effects from these volatiles tended to be regulated by the membrane-bound NADPH oxidases NoxR and Nox1 (Cruz-Magalhães *et al.*, 2019). In previous studies, more than 141 unique volatiles including several unknown terpenes were identified from 20 strains of *Trichoderma* representing 11 species. The type and abundance of species- and strain-specific volatiles were also dependent on the age of the fungal cultures and the plant, as well as external environmental conditions such as temperature and nutrition (Lee *et al.*, 2015; Lee *et al.*, 2016b; Gonzalez *et al.*, 2018).

The production of the auxin phytohormone IAA in *Trichoderma* is strain specific and depends on diverse external stimuli. *Trichoderma* species such as *T. atroviride*, *T. asperellum* and *T. virens* that had the ability of IAA production functioned as root growth promoters (Nieto-Jacobo *et al.*, 2017). Auxins released by the biocontrol agent *T. harzianum* Th5cc to the rhizosphere was suggested to be involved in overcoming the nitrate-inhibition of soybean nodulation, which indicated that soybean plants coinoculated with N₂-fixing *Bradyrhizobium japonicum* E109 and *T. harzianum* Th5cc might benefit from biocontrol process against plant pathogens, as a result, contributing to nitrogen preservation in soil (Iturralde *et al.*, 2020). The IAA production and the increased 1-aminocyclopropane-1-carboxylate-deaminase (ACC-deaminase) activity in *T. longibrachiatum* strain TL-6 effectively enhanced wheat growth and improved plant tolerance to NaCl stress by regulating transcriptional expression of IAA and ethylene synthesis genes in roots of wheat seedling under salt stress (Zhang *et al.*, 2019b).

Production of siderophores by *Trichoderma* species is also one of the important contributors to plant growth promotion due to their high affinity to iron (Fe). *T. stilbohypoxylis* LBM 120 and *T. atroviride* LBM 112 were tested positive on phosphate solubilization as well as hydrolytic enzyme and siderophore production, thus they showed high biocontrol efficacy and plant growth promotion properties to improve yerba mate (*Ilex paraguariensis* St. Hil) yield (López *et al.*, 2019). The siderophores produced by *T. asperellum* Q1 were suggested to stimulate the conversion of insoluble iron, thereby contributing to the accumulation of IAA in roots and promotion of *A. thaliana* seedlings growth (Zhao and Wang, 2020). Besides, the

intracellular siderophore in *T. virens* was proven to be associated with growth, conidiation, the biosynthesis of gliotoxin and systemic resistance induction in maize against *Cochliobolus heterostrophus* (Mukherjee *et al.*, 2018).

1.5 High-throughput sequencing technologies for studying *Armillaria* and *Trichoderma*

The availability of whole-genome sequences for an increasing number of *Armillarioid* species (Sipos *et al.*, 2017) and the identification of species-specific pathogenicity factors will further contribute to the development of more efficient root rot control strategies. Comparative transcriptome analysis to identify biocontrol factors from plant beneficial fungi such as *Trichoderma* species will continue providing molecular insights into mechanisms that play a crucial role in fungal interaction and plant protection. So far, molecular repertoires, particularly those required for the function and regulation of antagonistic secondary metabolites and cell wall degrading enzymes, have been revealed by genomics and transcriptomics studies between *Trichoderma* and *R. solani* (Halifu *et al.*, 2020), whereas, the interaction between *Trichoderma* and *Armillaria* is yet to be explored. Therefore, extensive and comprehensive gene expression analyses are needed to examine the gene repertoires involved in their multilevel interactions.

1.5.1 Genome sequencing of *Armillaria* species

Our understanding of root rot fungal pathogens is improving with the increasing availability of genome sequence data for several *Armillaria* species. To date, the genomes of six *Armillaria* species, *A. ostoyae* (Sipos *et al.*, 2017), *A. solidipes* (Sipos *et al.*, 2017), *A. mellea* (Collins *et al.*, 2013), *A. gallica* (Zhan *et al.*, 2020), *A. cepistipes* (Sipos *et al.*, 2017) and *A. fuscipes* (Wingfield *et al.*, 2016) have been sequenced and released. As reported, the draft genome of *A. cepistipes* and *A. gallica* differed greatly from *A. solidipes*, *A. ostoyae*, *A. mellea* and *A. fuscipes* in terms of genome size (53-85Mb) and the number of predicted genes (14473-26261). The number of protein coding genes of *A. mellea* and *A. fuscipes* was at similar level but much less than that identified in *A. solidipes*, *A. ostoyae*, *A. gallica*, and *A. cepistipes*. However, comparison regarding intron length, exon length, number of exons per gene and average gene length revealed similar results for all sequenced *Armillaria* species (Collins *et al.*, 2013; Wingfield *et al.*, 2016; Sipos *et al.*, 2017). The diversified genomic structures and genetic diversity among the *Armillaria* species may explain their varying morphologies, differing pathogenic activities and host specificities.

Comparative genomics including 22 Agaricales genomes indicated the expansion of gene repertoires in the genomes of *A. ostoyae*, *A. solidipes*, *A. gallica* and *A. cepistipes*. The genome expansion in *Armillaria* species is mainly associated with lineage-specific genes for rhizomorph morphology and function, diverse extracellular functions such as lignocellulose-degrading enzymes and several pathogenicity-related genes (Sipos *et al.*, 2017). Interestingly, the genome of an *A. gallica* strain, isolated as a *Gastrodia elata* symbiont, showed contracted numbers of gene families associated with pathogenic activities, including various hydrophobins, AA3 carbohydrate-active enzymes and cytochrome P450 monooxygenases (Zhan *et al.*, 2020). Such alterations in the genome of a plant symbiont *Armillaria* isolate may prevent invasive interactions in the symbiotic relationship (Zhan *et al.*, 2020).

1.5.2 Transcriptome profiling of various *Armillaria* activities

The increasing number of available *Armillaria* genomes paves the way to genome level comparative transcriptome analyses. Up to now, several transcriptome analyses were carried out on some primary pathogenic species, *A. ostoyae* (also *A. solidipes*) (Ross-Davis *et al.*, 2013), *A. mellea* (Mesanza *et al.*, 2016), *A. sinapina* (Fradj *et al.*, 2020) and on the opportunistic pathogen *A. cepistipes* (Sipos *et al.*, 2017). The transcriptome of an *A. ostoyae* strain isolated from host-pathogen interface was analysed to screen candidate genes responsible for host substrate utilization and to investigate the specific transcriptome profile during plant infection and wood degradation (Ross-Davis *et al.*, 2013). A specific transcriptome reprogramming of *A. sinapina* was induced by betulin of white birch bark; enzyme transcripts associated with the redox reaction of betulin into betulinic acid, an anti-inflammatory and anticancer drug, were identified (Fradj *et al.*, 2020).

The expanded genomes of *Armillaria* species equipped with a full complement of cell wall degrading enzymes not only give them easy access to plant wood but also a strategy to out-compete other microbes (Sipos *et al.*, 2017). Only a few studies on the expression patterns of *Armillaria* triggered by other soil microorganisms were conducted for the investigation of antimicrobial activities. Thirty proteins identified in *A. mellea* including attack-type, redox-active and degradative proteins were suggested to be associated with the antifungal activity during co-culturing with *Candida albicans* (Collins *et al.*, 2013). By transcriptome analysis, *A. mellea* was proved to be a non-competitive intruder in the soil ecosystem. As compared with *T. atroviride* as a biocontrol agent and an aggressive intruder for other microbes, the expression of genes encoding toxic secondary metabolites and lytic enzymes

was underrepresented in *A. mellea*. Moreover, genes in *A. mellea* implicated in carbohydrate and energy metabolism as well as sugar transport were downregulated in the presence of *T. atroviride*, possibly caused by the inhibition of *A. mellea* growth in response to the biocontrol agent. Likewise, genes responsible for cell wall reinforcement and signal transduction (a Ras-related protein and a calmodulin) were downregulated in *A. mellea* in the presence of *T. atroviride* in the simplified soil microcosm (Perazzolli *et al.*, 2016).

1.5.3 Genome expansion in biocontrol *Trichoderma* species

Genome sequencing of *Trichoderma* species revealed an expansion of genes with possible relevance to mycoparasitism, which revealed the wealth of genes closely related to their biocontrol potential (Kubicek *et al.*, 2019). The carbohydrate active enzymes (CAZymes) of *Trichoderma* mycoparasites appear to be well adapted to degradation of fungal cell wall of plant pathogens (Kubicek *et al.*, 2011). As a prominent example, the glycosyl hydrolase (GH) family associated with the hydrolysis of β -1,3 glucan and chitin/chitosan are expanded in mycoparasitic *Trichoderma* species including *T. atroviride* and *T. virens* (Kubicek *et al.*, 2011). The GH family expanded in mycoparasitic *Trichoderma* species was associated with better capability of fungal cell wall degradation in comparison with *T. reesei* (Kubicek *et al.*, 2019). Likewise, proteases have also expanded in *T. atroviride* and *T. virens*, supporting the hypothesis that protein degradation is a significant trait of mycoparasites (Kubicek *et al.*, 2011).

The huge diversity of secondary metabolites expanded in mycoparasitic *Trichoderma* species such as *T. atroviride* and *T. virens* may contribute to their excellent biocontrol properties. The *T. atroviride* genome was predicted to contain genes for 14 terpenoid synthase domains, 18 PKSs, 14 NRPSs and a single NRPS-PKS hybrid (Schmoll *et al.*, 2016). Besides, *T. atroviride* has further enhanced its antibiotic arsenal with expanded arrays of cytochrome subfamilies and soluble epoxide hydrolases, genes for cytolytic peptides and a higher complexity of small secreted cysteine-rich proteins (SSCRPs) (Kubicek *et al.*, 2011). Some SSCRPs from *T. hamatum* expanding the SSCRPs repertoire are likely to function as potential effector molecules that are involved in plant growth promotion and biocontrol of pathogens (Shaw *et al.*, 2016). 186 and 158 predicted transporters were found in the mycoparasitic species *T. virens* and *T. atroviride*, respectively (Schmoll *et al.*, 2016). The strong expansion of genes encoding for fungal transporters is speculated to support the successful adaptation of *Trichoderma* to harsh environments and competition in natural habitats (Kubicek *et al.*, 2011).

1.5.4 Transcriptional reprogramming in *Trichoderma* species induced by plant pathogens

Different patterns of transcriptional reprogramming towards biocontrol were observed in *Trichoderma* species (Guo *et al.*, 2020). In a comparative transcriptomics study of *T. virens*, *T. atroviride* and *T. reesei* confronted with *R. solani*, the three *Trichoderma* species showed dramatically different transcriptomic responses already before hyphal contact with the pathogen; *T. virens* and *T. atroviride* changed gene expression towards an attack upon sensing the alien hyphae, whereas, *T. reesei* attempted to outcompete the invader by faster nutrient acquisition (Atanasova *et al.*, 2013). A large percentage of the predicted secretome that collaborated in biocontrol of *S. sclerotiorum* was found to be unique to *T. hamatum* strain GD12 (Ding *et al.*, 2020). Key lytic enzymes, enzymes for biosynthesis of antifungal metabolites and transporters involved in the production of antifungal molecules potentially implicated in biocontrol of *A. mellea* were already activated in *T. atroviride* by the simplified soil microcosm, but they were not further modulated or enhanced by the introduction of *A. mellea* (Perazzolli *et al.*, 2016). The above examples implied that the strongly mycoparasitic *Trichoderma* species differed in the strategies that were deployed for compromising, predated and killing their host fungal pathogens. It also indicated that not only the availability of specific mycoparasitic genes, but also the regulation of gene expression may contribute to a more refined transcription expression pattern for successful antagonism and mycoparasitism.

2 AIMS OF THE STUDY

The frequent emergence of *Armillaria* root rot disease in forests and its severe economic consequences often led to the use of environmentally harmful, polluting fungicides. Above and beyond their commercial values, woody plants are essential components of wildlife habitats worldwide. Although *Armillaria* species are regular, natural components of the forests, under extreme biotic and abiotic conditions leading to loss of resistance of their woody host plants, *Armillaria* may become a dominant factor in the forests and cause severe diseases leading to compromised trees and seedlings. Although *Trichoderma* formulas have been applied broadly as important biocontrol agents for controlling a variety of plant pathogens, the experimental investigation of the efficiency of *Trichoderma* species for the biological control of *Armillaria* species still has a long way to go.

Commercial products based on *Trichoderma* have been available on the market for plant protection. However, isolating and screening for antagonistic *Trichoderma* strains from diverse populations distributed at different geographic regions may be more helpful for developing efficient biocontrol agents against a broad range of pathogens from the genus *Armillaria*. Therefore, we focused on isolation and characterization of *Trichoderma* and *Armillaria* strains from forest soils, as well as on the examination of the biocontrol efficiency of various *Trichoderma* isolates. The best biocontrol agents could be applied for *Armillaria* biocontrol and further field applications.

The aims of this work were:

- 1) To isolate and identify *Trichoderma* as well as *Armillaria* strains from soil samples collected in both healthy and *Armillaria*-damaged forests
- 2) To screen for potential biocontrol candidates among the identified *Trichoderma* isolates using *in vitro* dual culture assays and assessing the antagonistic activities, as well as by detecting extracellular enzyme production and plant growth-promoting traits
- 3) To determine the biocontrol potential of a selected *Trichoderma* strain when confronted with both diploid and haploid isolates of *A. ostoyae*
- 4) To capture the relevant points of time for adequately assessing the characteristic interaction stages between *Trichoderma* and *Armillaria* mycelia and to investigate the dual RNA-Seq profiles, assess the molecular background of metabolite-level and mycoparasitic (physical) interactions, and dissect the molecular interaction dynamics by time-course transcriptome analyses.

- 5) To analyze the mycoparasitism-related genes in the examined *Trichoderma* strain for the identification of biocontrol factors
- 6) To analyze the possible defence mechanisms of *A. ostoyae* for the identification of defence factors
- 7) To determine the potential of selected biocontrol candidate *Trichoderma* strains to control *Armillaria* in the field

3 MATERIALS AND METHODS

3.1 Screening for biocontrol candidates from *Trichoderma* strains

3.1.1 Isolation of *Armillaria* and *Trichoderma* strains

Samples of bulk soil (soil outside the rhizosphere), upper rhizospheric soil, *Armillaria* rhizomorphs and their surrounding soil, as well as *Armillaria* fruiting bodies were collected from a heavily *Armillaria*-damaged oak stand (Keszthely Hills, Hungary) and healthy native spruce forests (Rosalia, Austria). The rhizomorph samples were taken as aliquots of the soil pools associated with the collected rhizomorphs. The Roth and Shaw medium (Shaw and Roth, 1976) supplemented with 15 mg/L benomyl and 250 mg/L streptomycin was applied for *Armillaria* isolation from the field samples. For *Trichoderma* isolation, 1 g of fresh soil per sample was suspended in sterile 0.9% NaCl solution, diluted serially (10^{-1} , 10^{-2} and 10^{-3} dilutions) and spread on *Trichoderma*-selective media. The composition of the media for selectively isolating *Trichoderma* strains was 10 g/L glucose, 5 g/L peptone, 1 g/L KH_2PO_4 , 0.5 g/L $\text{MgSO}_4 \times 7\text{H}_2\text{O}$, 20 g/L agar, amended with 0.25 mL/L 5% Rose-Bengal in water, 0.5 mL/L 0.2% dichloran in ethanol, 0.01% streptomycin, 0.01% oxytetracycline and 0.01% chloramphenicol (King *et al.*, 1979). After 3 days of incubation at 25 ± 0.5 °C, fungal colonies including *Trichoderma* were detected and transferred onto potato dextrose agar (PDA).

3.1.2 Identification of *Armillaria* and *Trichoderma* isolates

One hundred mg of fresh mycelia from each fungal isolate was collected for DNA extraction following the manufacturer's instructions of the E.Z.N.A.® Fungal DNA Mini Kit (Omega Bio-tek, USA). The Internal Transcribed Spacer (ITS) region of the nuclear ribosomal RNA gene cluster was amplified using the ITS4 and ITS5 universal primers for fungi (Supplementary Table 3) (White *et al.*, 1990). The PCR reactions were carried out in a final volume of 25 µL consisting of 2.5 µL 10× DreamTaq Buffer with 20 mM MgCl_2 , 2.5 µL of 2 mM dNTP mix, 0.1 µL of 5 U/µl DreamTaq DNA Polymerase (Thermo Scientific), 0.5 µL of each primer (10 µM), 18 µL bidistilled water and 1 µL template DNA. Amplifications were performed in a Doppio Thermal Cycler (VWR, Hungary). Thermal cycling parameters were as follows: initial denaturation at 94 °C for 5 min; 35 cycles of DNA denaturation at 94 °C for 30 s, primer annealing at 50 °C for 30 s, elongation at 72 °C for 50 s; and a final elongation step at 72 °C for 7 min. For amplification of a translation elongation factor 1-alpha gene (*tefla*) fragment, reaction mixtures were the same as described above, but with universal primers TEF-LLErev and EF1-728F (Supplementary Table 3) (Oskiera *et al.*, 2015) and the

thermal cycling program with an initial denaturation at 94 °C for 5 min; 40 cycles of DNA denaturation at 94 °C for 45 s, primer annealing at 57 °C for 30 s, elongation at 72 °C for 90s ; and a final elongation step at 72 °C for 7 min. The amplicon quality was detected by 1% agarose gel electrophoresis of 4 µl samples from the reaction mixtures. Direct sequencing of the unpurified PCR products was performed by the sequencing platform of the Biological Research Centre, Szeged. The resulting sequences were analyzed by *TrichOkey* 2.0 (Druzhinina *et al.*, 2005), *TrichoBLAST* (Kopchinskiy *et al.*, 2005) and NCBI Nucleotide BLAST. The isolated and identified *Armillaria* and *Trichoderma* strains were deposited in the Szeged Microbiology Collection (SZMC, www.szmc.hu), Szeged, Hungary, whereas the sequences were submitted to the GenBank Nucleotide database (ncbi.nlm.nih.gov) under the accession numbers listed in Supplementary Table 1.

3.1.3 Antagonistic activity assessment *in vitro* by dual culture assay

Trichoderma isolates were screened for their antagonistic abilities against *Armillaria* isolates *in vitro* using dual-culture confrontation test. During the experiments, *Armillaria* isolates were confronted with *Trichoderma* isolates on PDA plates. *Armillaria* strains were inoculated with agar plugs (5 mm in diameter, cut from the edge of 14-days-old colonies) 1.5 cm from the center of PDA plates. After 14 days, the *Trichoderma* isolates were inoculated in a similar way, 1.5 cm from the center of PDA plates in the opposite direction, resulting in a distance of 3 cm between the two inoculation positions. After a further 5 days of incubation, image analysis of plate photographs was performed by ImageJ. Biocontrol Index (BCI) values were calculated with Microsoft Excel 2010 according to the formula: $BCI = (\text{area of } Trichoderma \text{ colony} / \text{total area occupied by the colonies of both } Trichoderma \text{ and the plant pathogenic fungus}) \times 100$ (Szekeres *et al.*, 2006). All confrontation tests were repeated three times under the same experimental conditions. Values were recorded as the means with standard deviations for triplicate experiments.

3.1.4 Extracellular enzyme activity measurements

Conidiospores (2×10^5 / plate) of *Trichoderma* strains were transferred into Petri-plates (9 cm in diameter), each containing 3 g spelt bran and 10 mL distilled water. After 9 days of incubation at room temperature, the enzyme extraction was carried out in 25 mL distilled water at 5 °C for 3 hours, followed by filtering through gauze to remove fungal hyphae and spelt bran, and centrifugation of the crude extract in a Heraeus Multifuge 3SR (Thermo Fisher Scientific, Hungary) at 4300 g for 10 min. One mg/mL stock solutions were prepared from

chromogenic substrates in distilled water. β -glucosidase, cellobiohydrolase, β -xylosidase and phosphatase enzyme activities were measured with p-nitrophenyl- β -D-glucopyranoside, p-nitrophenyl- β -D-cellobioside, p-nitrophenyl- β -D-xylopyranoside (all from Sigma-Aldrich, Hungary) and p-nitrophenyl-phosphate, respectively. One-hundred microliters of substrate solution, 25 μ L 10-fold diluted culture supernatant and 75 μ L distilled water were mixed in the wells of a microtiter plate. After 1 h of incubation at room temperature, 50 μ L 10% Na_2CO_3 was added to stop the reaction. The optical densities were measured with a Spectrostar Nano microplate reader (BMG Biotech) at 405 nm. Background values of the crude extract and the value resulting from the self-degradation of the substrate were subtracted from the optical density of the enzymatic reactions. The U/ml values were calculated according to the formula $((A / \epsilon \times l) \times 10^6) / 60$, where "A" is the absorbance of the solution at 405 nm, " ϵ " is the molar extinction coefficient (for p-nitrophenol: $1.75 \times 10^4 \text{ M}^{-1} \text{ cm}^{-1}$) and "l" is the pathlength of the light in the solution. All measurements were carried out in three biological replicates.

3.1.5 Quantitative analysis of indole-3-acetic acid production

IAA production of *Trichoderma* isolates was analyzed by colorimetric analysis using Salkowsky's reagent (Gordon and Weber, 1951) with some modifications. The isolates were inoculated into 20 mL tryptone-soy broth (TSB) (15 g/L tryptone, 5 g/L peptone from soy, 5 g/L NaCl, 1 mg/mL tryptophan) and incubated for 7 days at 25 $^{\circ}\text{C}$ with shaking at 150 rpm. After the incubation period, 2 mL of each culture was centrifuged in a Heraeus Fresco 17 Microcentrifuge (Thermo Fisher Scientific, Hungary) at 5000 g for 15 min. The supernatant was preserved and 100 μ L was mixed with 200 μ L of Salkowski's reagent (300 mL H_2SO_4 (98%), 15 mL FeCl_3 (0.5 M), 500 mL distilled water) and incubated at room temperature in the dark for 1 h. The optical density (OD) was measured at 530 nm with a Spectrostar Nano microplate reader (BMG Labtech, Germany) after 30 min. The IAA concentration was determined using a calibration curve of standard IAA solutions. All measurements were carried out in three biological replicates.

3.1.6 Siderophore production

Siderophore production of *Trichoderma* isolates was determined by using a modified chrome azurol S (CAS) agar test (Milagres *et al.*, 1999). One half was CAS blue agar and the other half was an iron-free medium in 9-cm-diameter Petri plates. The CAS agar was prepared according to Schwyn and Neilands (Schwyn and Neilands, 1987). The iron-free medium was

MEA agar medium (10 g/L glucose, 12.5 g/L yeast extract, 5 g/L malt extract, and 20 g/L agar). A fungal mycelial disc (4 mm) of active culture was transferred to the plates with iron-free medium. Orange and purple halos around the colonies on the blue medium were indicative of siderophore production. All measurements were carried out in three biological replicates.

3.2 Transcriptome analysis of the interaction mechanisms between *Armillaria ostoyae* and *Trichoderma atroviride*

3.2.1 Strains and culture conditions

Trichoderma atroviride SZMC 24276 was isolated from a soil sample collected in a native spruce forest located in Rosalia, Austria (Supplementary Table 1). The diploid strains of *A. ostoyae* SZMC 24128, SZMC 24129 and SZMC 24130 were isolated from collected samples of *Armillaria* fruiting bodies or rhizomorphs obtained from the Rosalia forest (Supplementary Table 1). The diploid strain C18 of *A. ostoyae* is a field isolate from Switzerland (Prospero *et al.*, 2004), while the haploid derivatives of *A. ostoyae* (C18/9, C18/2, C18/3 and C18/4) were derived from C18 as single spore isolates. Strains of *Trichoderma* and *Armillaria* were all deposited in the Szeged Microbiology Collection (SZMC, www.szmc.hu), Szeged, Hungary. For *A. ostoyae* strains C18, C18/9, C18/2, C18/3 and C18/4, their corresponding SZMC numbers are SZMC 23083, SZMC 23093, SZMC 27047, SZMC 27048 and SZMC 27049 respectively. All those fungal strains were cultured on PDA medium (VWR, Hungary).

3.2.2 Transcriptome analysis of *Trichoderma atroviride* – *Armillaria ostoyae* dual cultures

3.2.2.1 Experimental design, sample collection and total RNA extraction

For the time-course analysis of the *Armillaria-Trichoderma* interaction, PDA plates were first inoculated with the haploid derivative *A. ostoyae* SZMC 23093 and grown for 21 days at 26°C. Then, on the 22nd day, plates in parallel were co-inoculated with the *T. atroviride* SZMC 24276 biocontrol isolate pregrown on two-day-old PDA plates. Inoculations were always carried out using agar plugs (5 mm in diameter) with fungal mycelia. *Armillaria* colonies were inoculated to a position about 2 cm near the Petri plates' edge, and then, after 21 days, the *Trichoderma* colonies were inoculated 3.5 cm from the edge of the *Armillaria* colonies, and the co-inoculated plates were incubated further at 26°C. The interactive fungal mycelia from both sides were harvested 53, 62 and 105 hours after *Trichoderma* inoculation,

representing non-physical (or metabolite-level), physical (or mycoparasitic) and post-mycotrophic (or post-necrotrophic) interaction stages, respectively (Supplementary Figure 1). While *Trichoderma* and *Armillaria* mycelia were separately harvested at the metabolite stage (53 hours), the physically interacting mycelia were co-scraped from the mycoparasitic (62 hours) and post-mycoparasitic settings (105 hours) (Supplementary Figure 1). Three biological replicates were considered for each time point, including individually growing, non-interactive cultures (the 21-day-old *Armillaria* and two-day-old *Trichoderma* colonies) as the controls (Supplementary Figure 1). All collected mycelial samples were immediately frozen in liquid nitrogen and stored at -80°C.

Four conditions were established and analysed: 0th hour/Control samples (*Armillaria* and *Trichoderma* grew separately on PDA media); 53rd hour/Metabolite Interaction stage samples (considering the impact of various metabolites between *Trichoderma* and *Armillaria* before physical contact); 62nd hour/Mycoparasitic Interaction stage samples (mycoparasitic stage once *Armillaria* and *Trichoderma* started to contact); 5th day post interactive stage (when the *Armillaria* colony was entirely covered with mycelia and conidia of *Trichoderma*). Details about the culturing of fungi for the collection of mycelia are provided in Supplementary Figure 1.

Total RNA extraction from the mycelial samples was carried out with the E.Z.N.A.® Plant RNA kit (Omega Bio-tek) according to the manufacturer's extraction protocol with minor modifications. Briefly, mycelia were transferred into an autoclaved mortar and frozen under liquid nitrogen, and then immediately grinded with an autoclaved pestle before samples thawed. Degrading RNA content was first estimated using 2% agarose gel electrophoresis. RNA concentration and quality were monitored using the TapeStation 2200 analyzer (Agilent Technologies, Santa Clara, CA, USA).

3.2.2.2 cDNA library preparation, sequencing and data analysis

Sequencing libraries were prepared for the transcriptome samples using the TruSeq RNA Library Prep Kit v2 (Illumina). Paired-end fragment reads were generated on an Illumina NextSeq sequencer using TG NextSeq® 500/550 High Output Kit v2 (300 cycles). Primary data analysis (base-calling) was carried out with the “bcl2fastq” software (v2.17.1.14, Illumina). The quality of the raw reads obtained from the sequencing company were analyzed using FastQC (Andrews S, 2010) and low quality bases (Q score < 20) were trimmed using Trimmomatic v0.39 (Bolger *et al.*, 2014). Salmon v1.1.0 (Patro *et al.*, 2017) was used to quantify the transcripts and generate count matrix. Time course analysis was performed using

TCSeq (Wu M, 2020) R-package in Rv3.5.1 environment with generalized linear model (GLM) +and clustered using the Fuzzy cmeans clustering method (K=3 for *A. oostoyae* and *T. atroviride*) based on log2FC compared to first timepoint ($\log_2FC > |0.5|$ & $\text{adj.pvalue} < 0.05$). From the clusters, we filtered and grouped the genes according to their expression trends (upregulation/downregulation) at different stages. Downtrend genes included those set of genes from Cluster 1 which specifically showed continuous downregulation in either AO or TA whereas Metabolite and Mycoparasite cluster genes are those genes from clusters 2 and 3 which showed the highest upregulation in the Metabolite (53 hours) or the Mycoparasite stage (62 hours).

Amino acid sequences from *Armillaria oostoyae* (https://ftp.ncbi.nlm.nih.gov/genomes/all/GCA/900/157/425/GCA_900157425.1_version_2/GCA_900157425.1_version_2_protein.faa.gz) and *Trichoderma atroviride* (https://ftp.ncbi.nlm.nih.gov/genomes/all/GCF/000/171/015/GCF_000171015.1_TRIAT_v2.0/GCF_000171015.1_TRIAT_v2.0_protein.faa.gz) were used for secretory protein prediction. The pipeline used for predicting classically secreted proteins, i.e., proteins having signal peptides and cleavage site at the N-terminal is shown in Supplementary Figure 2A and the other group of secretory proteins which do not contain signal peptide and are generally referred to as proteins secreted using unconventional pathway (UPS proteins) were predicted using the pipeline shown in Supplementary Figure 2B.

We used the Pannzer2 (Törönen *et al.*, 2018) server for the gene ontology (GO) annotation and InterproScan v5.38 (Jones *et al.*, 2014b) for functional characterization of proteins. CAZy annotation was performed using dbCAN2 (Zhang *et al.*, 2018) and proteases were identified using Diamond Blast against the MEROPS database (Rawlings *et al.*, 2014). The NetGPI (Lawn, 2005) online server was used for GPI anchor prediction. Secondary metabolite gene/protein prediction was performed using SMIPS (Wolf *et al.*, 2016). KEGG annotation was performed using KofamKoala (Aramaki *et al.*, 2020) and transporter proteins were predicted using the TCDB database (Saier *et al.*, 2021). GO enrichment analysis was performed in Cytoscape v3.7.2. (Shannon *et al.*, 2003) using BiNGO (Maere *et al.*, 2005) v3.0.3 and enrichmentMap v3.3.1 (Merico *et al.*, 2010) plugins (adjusted p value < 0.05). We used ClusterProfiler R-package (Yu *et al.*, 2012) for KEGG and Interpro enrichment analysis. All images were generated using the ggplot2 (Wickham, 2016) R package.

3.2.2.3 Quantitative real-time reverse transcription PCR (qRT-PCR)

For qRT-PCR analysis, total RNA samples were extracted using the E.Z.N.A.® Plant

RNA kit (Omega Bio-tek) according to the manufacturer's extraction protocol. The quality of each RNA samples was checked in 2% agarose gel. cDNA synthesis was performed by using Maxima H Minus First Strand cDNA Synthesis Kit (Thermo Scientific). Oligo (dT)18 and random hexamer primers were used in the reaction mixture according to manufacturer's instructions.

The qRT-PCR experiments were performed in a CFX96 real-time PCR detection system (Bio-Rad) using the Maxima SYBR Green qPCR Master Mix (Thermo Scientific) and the primers presented in Supplementary Table 3. The reaction was carried out using the following conditions: denaturation at 95 °C for 3 min, followed by 40 cycles of amplification (95 °C for 5 s, 60 °C for 30 s and 72 °C for 30s). The relative quantification of gene expression was carried out by the 2- $\Delta\Delta$ Ct method (Livak and Schmittgen, 2001) using the housekeeping gene glyceraldehyde-3-phosphate dehydrogenase (*gpd*, ARMOST_14637) or actin (ARMOST_03733) for *A. ostoyae* and the *tef1 α* gene for *T. atroviride*. For each sample, two technical replicates of the qRT-PCR assay were used with a minimum of three biological replicates (except for samples for the Mycoparasite stages which only contained two biological replicates). Data analysis and graph plotting were performed using Excel 2017 and GraphPad Prism 8.

3.3 Field study in the Keszthely Hills

A field study was set up on the 13th of April 2017 in the Keszthely Hills, in a forest clearing surrounded by a 2-meter-high fence, located in the central part of a heavily *Armillaria*-damaged Turkey oak (*Quercus cerris*) stand. A total of 235 two-year-old, bare rooted seedlings of *Q. cerris* from the nursery of the Bakonyerdő Ltd. forestry company with a stem length of 10-52 cm, a main root length of minimum 25 cm and a stem base diameter of minimum 6 mm, were planted. Before planting, 10 L plastic buckets were used to soak the roots of 115 seedlings for at least 2 h in tap water (control group), whereas the roots of the other 120 seedlings were soaked in tap water containing conidia of *T. virens* SZMC 24205 and *T. atrobrunneum* SZMC 24206, both at a concentration of 10⁶ conidia per mL (treated group) for at least 2 h. The seedlings were planted in groups of 40 into parcels of 6.4 × 6.3 m resulting in a density of 1 seedling per m². The allocation of the parcels was random in a block design of 3 × 4 parcels, with 3 parcels treated, 3 parcels untreated (control), and 6 parcels left empty, to cover a larger area for balancing the eventual differences in soil quality and distribution of potential *Armillaria* inoculum in the soil. Seedlings were planted into 20 cm deep holes made with 10 cm wide drain spades. Seedling stem height (in mm) and stem

base diameter (in mm with one decimal precision) were recorded individually for each tree with measuring tape and slide calipers, respectively. From the recorded values a biomass index (BMI) was calculated for each seedling according to the following formula: $(BD / 2)^2 \times \pi \times L$, where BD is the stem base diameter and L is the stem length. The area received no further treatment. Half a year later, on the 17th of October 2017, the seedlings were evaluated for survival, their L and BD values recorded again, and the BMI values calculated. A seedling was recorded as “dead” if it was degraded or showed a dry brown appearance without any leaves, and it was not possible to excoriate the surface around the stem base with the orifice of a 1 ml plastic pipette tip. Stem height extensions (dL), stem base diameter extensions (dBD) and BMI changes (dBMI) were calculated. Seedlings with green leaves and an increase in biomass production were taken as “growing” live plants. All other seedlings without a significant biomass extension but with stems still green under the bark and slightly damp to the touch were considered “surviving” ones. In the end, after the second round of the measurements, size values lower than the ones measured directly after planting were considered as the result of measurement error and were removed from the total pools. The percentage of dead and surviving seedlings was calculated for each parcel, and their total numbers were compared between the control and treated groups by testing “independence” with the aid of the χ^2 test with Yates’s correction.

4 RESULTS

4.1 Screening for biocontrol candidates from *Trichoderma* strains against *Armillaria* species

4.1.1 Diversity of the genera *Armillaria* and *Trichoderma* in healthy and *Armillaria*-damaged forests

Armillaria and *Trichoderma* strains were isolated from different locations of healthy and *Armillaria*-infested forests. The sampling sites were two different regions, one in Northwest Hungary (Keszthely-hills) and one in Northeast Austria (Rosalia Mountains) (Supplementary Table 1). Four *Armillaria* species could be identified by the sequence analysis of a fragment of the *tefla* gene: the conifer-specific species *A. cepistipes* (2 isolates) and *A. ostoyae* (3 isolates) were abundant in the neighboring Rosalia spruce forest stands, whereas the presence of *A. mellea* (18 isolates) and *A. gallica* (4 isolates) was revealed in the Keszthely oak stand (Supplementary Table 1).

A total of 64 strains showing typical morphology of *Trichoderma* were also isolated from soil, rhizosphere or *Armillaria* rhizomorph-associated samples collected in the two examined forest areas (Supplementary Table 1). Forty-two and 22 isolates were collected from the oak stand near Keszthely (Hungary) and the spruce forest at Rosalia (Austria), respectively. As the ITS sequences did not enable an exact, species-level identification in the case of many *Trichoderma* isolates, the species identification was set up based on the sequence of a *tefla* gene fragment. The isolates proved to represent 14 *Trichoderma* species: *T. simmonsii* (17), *T. koningii* (11), *T. virens* (8), *T. atroviride* (8), *T. atrobrunneum* (7), *T. asperellum* (3), *T. hamatum* (2), *T. citrinoviride* (2), *T. tomentosum* (1), *T. paratroviride* (1), *T. crassum* (1), *T. guizhouense* (1), *T. paraviridescens* (1) and *T. longipile* (1) (Supplementary Table 1). The diversity of *Trichoderma* species showed a difference between the two forests. Only two species – *T. atroviride* and *T. simmonsii*–were isolated from both locations. The species *T. virens*, *T. atrobrunneum*, *T. citrinoviride*, *T. hamatum*, *T. tomentosum*, *T. paratroviride* and *T. crassum* were only isolated from the oak stand near Keszthely (Hungary), whereas *T. koningii*, *T. asperellum*, *T. guizhouense*, *T. paraviridescens* and *T. longipile* were only found in the spruce forest at Rosalia (Austria) (Supplementary Table 1). Eleven samples revealed isolates from a single species. A frequent species pair detected in Rosalia samples was *T. koningii* – *T. asperellum*, whereas in the Keszthely samples, the co-occurrence of *T. simmonsii* – *T. virens* and *T. virens* – *T. atrobrunneum*. Communities consisting of more than 2 species in the same sample were *T. guizhouense* – *T. paraviridescens* – *T. simmonsii* (Rosalia), *T. paratroviride* –

T. citrinoviride – *T. simmonsii* (Keszthely) and *T. atrobrunneum* – *T. simmonsii* – *T. crassum* – *T. virens* (Keszthely).

4.1.2 *In vitro* antagonism of the isolated *Trichoderma* strains towards *Armillaria* species

All 8 isolates of *T. virens*, and some isolates of *T. simmonsii*, *T. atrobrunneum*, *T. guizhouense*, *T. atroviride*, *T. citrinoviride*, *T. paratroviride*, *T. hamatum*, and *T. tomentosum* proved to be highly effective against the 25 examined *Armillaria* isolates. A representative set of plate photographs was taken during the *in vitro* antagonism experiments (Figure 2). Supplementary Figure 3 reflects all species combinations of *Trichoderma* and *Armillaria*. In many cases, antagonistic *Trichoderma* isolates were able to overgrow *Armillaria* colonies and intensely produce conidia on their surface, thereby potentially restricting *Armillaria* growth. Isolates of *T. virens*, such as SZMC 24205, SZMC 24294, SZMC 24303, SZMC 24293 and SZMC 26774, proved to be the best *in vitro* antagonists with BCI values above 80 for more than 17 out of 25 *Armillaria* strains (Supplementary Table 2). Isolates of *T. simmonsii* showed high *in vitro* antagonistic activities with BCI values above 80 for more than 15 out of the 25 tested *Armillaria* isolates, whereas the *T. koningii*, *T. asperellum*, *T. paraviridescens* and *T. longipile* isolates had the lowest BCI values against almost all of the tested *Armillaria* isolates. The distribution of antagonistic *Trichoderma* species with higher BCI values showed a geographical pattern. Except for the two species - *T. simmonsii* and *T. atroviride*, isolated from both the oak stand in Keszthely - and the spruce forest in Rosalia, having relatively high antagonistic activities, species that were only isolated from the Keszthely Hills, including *T. virens*, *T. atrobrunneum*, *T. hamatum*, *T. citrinoviride*, *T. paratroviride* and *T. tomentosum*, exhibited good *in vitro* antagonistic abilities against most of the tested *Armillaria* isolates. All isolates of *T. koningii*, *T. asperellum*, *T. paraviridescens* and *T. longipile*, which seem to dominate in the soil of the Rosalia forest, showed lower BCI values against most *Armillaria* isolates.

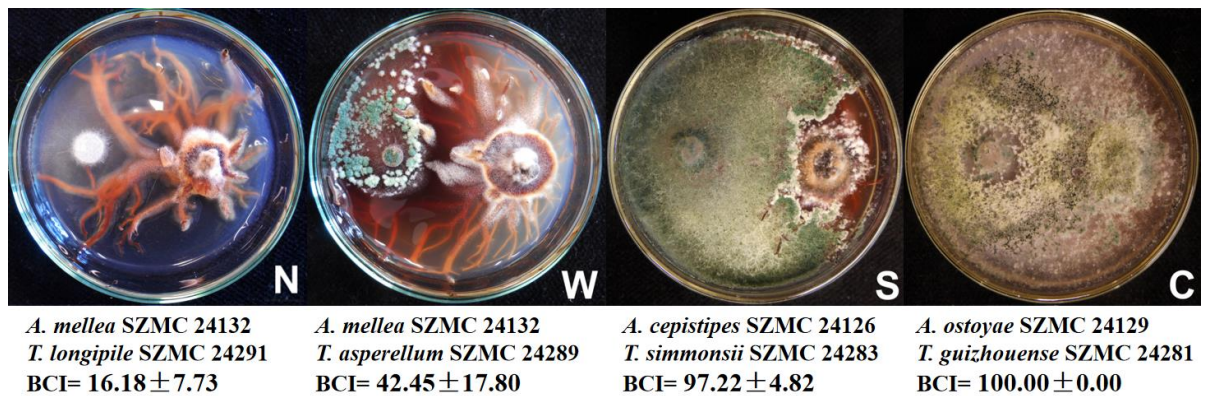


Figure 2. Example plate photographs of *in vitro* antagonism of *Trichoderma* strains against *Armillaria* strains. The plates are marked with N: no inhibition; W: weak inhibition; S: strong inhibition; C: complete overgrowth of *Armillaria* by *Trichoderma*. BCI values were recorded as the means with standard deviations for triplicate experiments.

4.1.3 Extracellular enzyme production of the *Trichoderma* isolates

The extracellular enzyme measurements revealed that isolates of the same *Trichoderma* species have similar enzyme activity values (Supplementary Figure 4). Altogether, most of the isolates could be characterized with high β -glucosidase (Supplementary Figure 4a) and phosphatase (Supplementary Figure 4d), but lower cellobiohydrolase (Supplementary Figure 4b) and β -xylosidase (Supplementary Figure 4c) activities. The 11 *T. koningii* isolates along with *T. asperellum* SZMC 24288, SZMC 24280 and *T. paraviridescens* SZMC 24282, showed high β -glucosidase and β -xylosidase activities. Among them, *T. paraviridescens* SZMC 24282 had high phosphatase, whereas *T. koningii* SZMC 24286 and SZMC 24270 showed high cellobiohydrolase activities as well. The examined *T. virens*, *T. atrobrunneum*, *T. simmonsii* and *T. atroviride* isolates showed lower activity levels for all enzymes tested, except for *T. atroviride* SZMC 26780 which had a very high β -xylosidase activity.

4.1.4 Potential plant growth-promoting traits of the isolated *Trichoderma* strains

All of the examined isolates from *T. atrobrunneum*, *T. simmonsii*, *T. hamatum* and *T. citrinoviride*, along with the single isolates of *T. tomentosum*, *T. longipile*, *T. paratroviride* and *T. guizhouense* proved to be IAA producers, whereas the *T. atroviride* isolates, as well as the examined single isolates of *T. paraviridescens* and *T. crassum* were unable to produce this metabolite (Figure 3). Both producers and non-producers were found among the examined isolates of *T. virens*, *T. koningii* and *T. asperellum*. The highest amounts of IAA were detected in the case of the isolates of *T. tomentosum*, *T. citrinoviride*, *T. hamatum* as well as certain isolates of *T. atrobrunneum*, *T. simmonsii* and *T. koningii*.

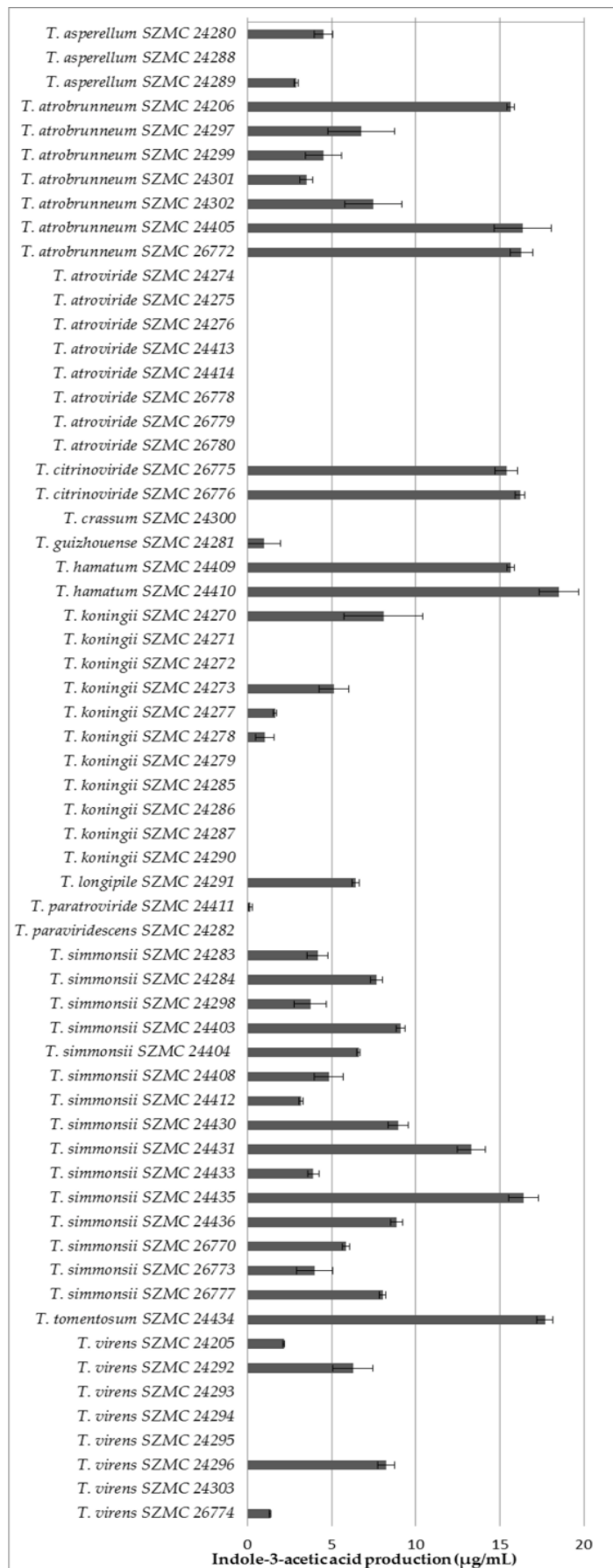


Figure 3. Indole-3-acetic acid production of *Trichoderma* isolates derived from forest soil samples.

All the *Trichoderma* isolates tested were able to produce siderophores, which was indicated by the change of the colour of blue to orange or purple (Figure 4). The different colors of the medium suggested that the produced siderophores were structurally different. There are two major groups of siderophores, known as catechol-type and hydroxamate-type (Milagres *et al.*, 1999). In the case of catechol-type siderophores the medium turns to purple, which was detected in the case of the *T. atroviride*, *T. paraviridescens* and *T. koningii* isolates, whereas the hydroxamate-type siderophores result in an orange color, as it was the case for all other examined species (Figure 4). The isolates of the species *T. asperellum* seemed to produce both types of siderophores (see plate 8 on Figure 4).

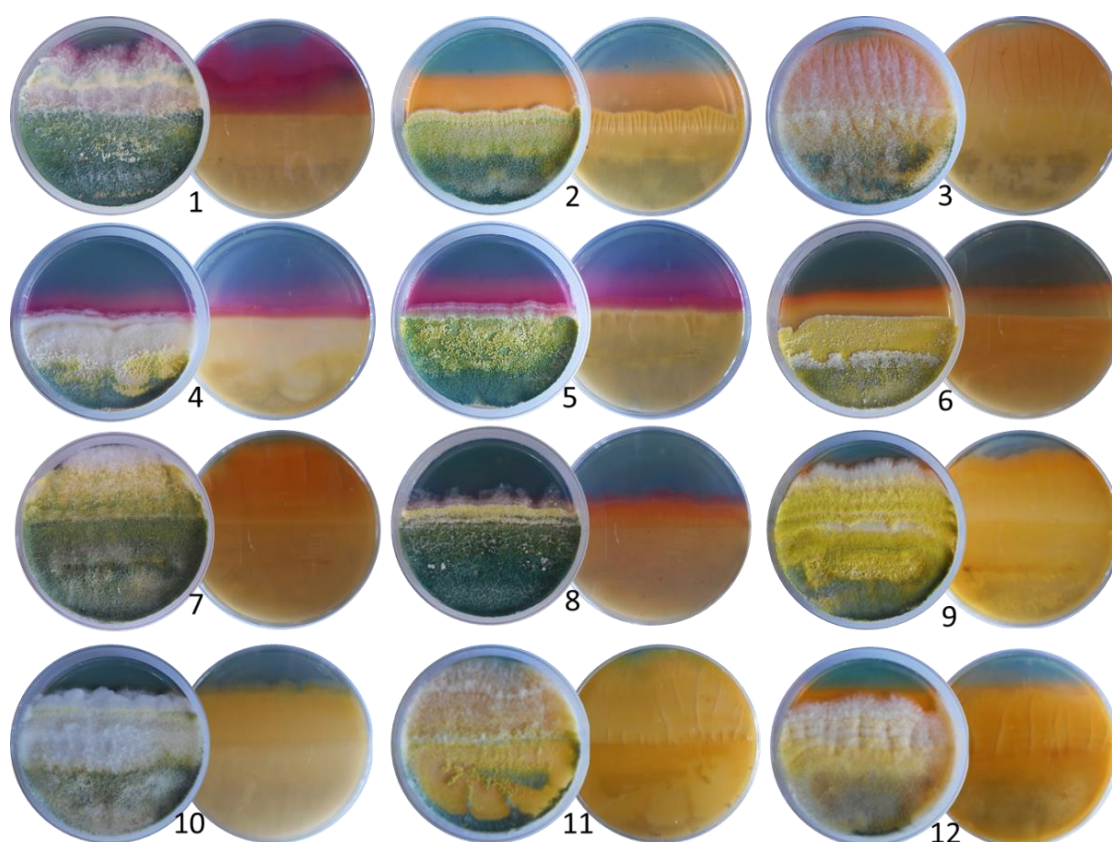


Figure 4. Production of siderophores on modified CAS agar medium by forest-derived *Trichoderma* isolates belonging to different species. (1) *T. atroviride* SZMC 24275, (2) *T. virens* SZMC 24205, (3) *T. hamatum* SZMC 24410, (4) *T. paraviridescens* SZMC 24282, (5) *T. koningii* SZMC 24287, (6) *T. citrinoviride* SZMC 26776, (7) *T. simmonsii* SZMC 24431, (8) *T. asperellum* SZMC 24280, (9) *T. atrobrunneum* SZMC 24206, (10) *T. guizhouense* SZMC 24281, (11) *T. tomentosum* SZMC 24434, and (12) *T. crassum* SZMC 24300.

4.2 Molecular dynamics of the biocontrol interaction between *T. atroviride* and *A. ostoyae*

4.2.1 Antagonistic effect of *T. atroviride* SZMC 24276 against *A. ostoyae* strains

The *T. atroviride* SZMC 24276 was selected as a biocontrol agent for our transcriptomic study. After three weeks incubation at 26°C, all the diploid strains of *A. ostoyae* displayed typical *Armillaria* morphology with rhizomorph formation and mycelial growth on PDA. Aerial hyphae of diploid strains were significantly differentiated based on their morphological attributes which seemed to get darken, flatten and become crustaceous. By comparison, the mycelia of the haploid derivatives of *A. ostoyae* remained white and fluffy producing abundant aerial mycelia and did not turn crustose. During the 105 hours coincubation of dual cultures, *T. atroviride* SZMC 24276 showed a significant antagonistic effect against diverse diploid or haploid *A. ostoyae* strains (Figure 5, Table 2). *T. atroviride* grew fast toward the colony of *A. ostoyae* and gradually invaded the growth area of *A. ostoyae* strains. Obviously, on the 5th day, haploid *A. ostoyae* derivatives were easier overgrown by *T. atroviride* and *T. atroviride* produced abundant green conidia and mycelia on the surface of the haploid *A. ostoyae* colony. For these reasons, one of the haploid derivatives of *A. ostoyae* (AO) SZMC 23093 was selected for transcriptome analysis, together with *T. atroviride* (TA) SZMC 24276.

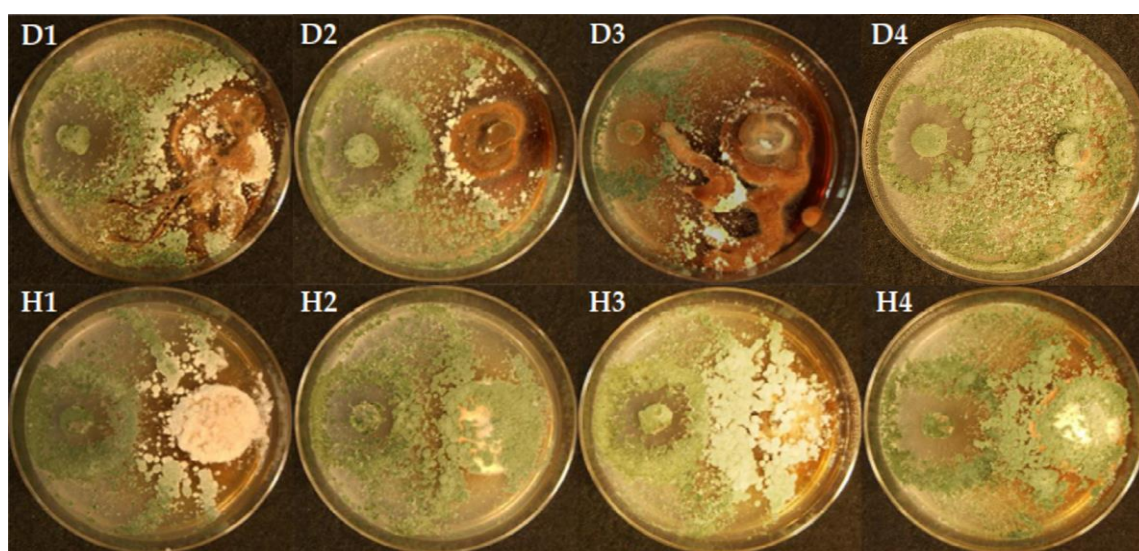


Figure 5. Antagonistic effect of *T. atroviride* (TA) on various diploid (D1-D4) strains and haploid (H1-H4) derivatives of *A. ostoyae*

Table 2. BCI values of the dual interaction tests with various diploid and haploid *A. ostoyae*

Diploid	SZMC 23083 (D1)	SZMC 24128(D2)	SZMC 24129 (D3)	SZMC 24130 (D4)
BCI	88.13±0.56	93.29±2.99	85.49±8.03	100.00±0.00
Haploid	SZMC 27047 (H1)	SZMC 27048 (H2)	SZMC27049 (H3)	SZMC23093 (H4)
BCI	99.40±1.04	99.55±0.77	99.37±1.09	98.46±1.83

4.2.2 Time course analysis to understand the interaction dynamics between *T. atroviride* (TA) and *A. ostoyae* (AO)

The dual co-culture method was employed to study the interaction between TA and AO at 3 different time points: 53, 62 and 105 hours after the inoculation of TA (Figure 6). The dual RNA-seq analysis of co-scraped TA-AO samples at 105 hours did not show any transcripts for AO (0.3 % reads could be mapped) (Supplementary Figure 5) and since our main interest focused on understanding the metabolite-level and mycoparasitic interaction, we did not consider the 105 hour interaction sample in this study. On average, 17 million reads with mean read length of 150 bp were obtained for both TA and AO after quality trimming. We performed time course analysis of the transcriptome data and generated 3 significant clusters for TA and AO. From the clusters, we identified the genes which showed highest expression at the Metabolite and Mycoparasite stages (Figure 7, Table 3); and we also identified those genes showing continuous downtrend pattern in AO and TA (Figure 7, Table 3).

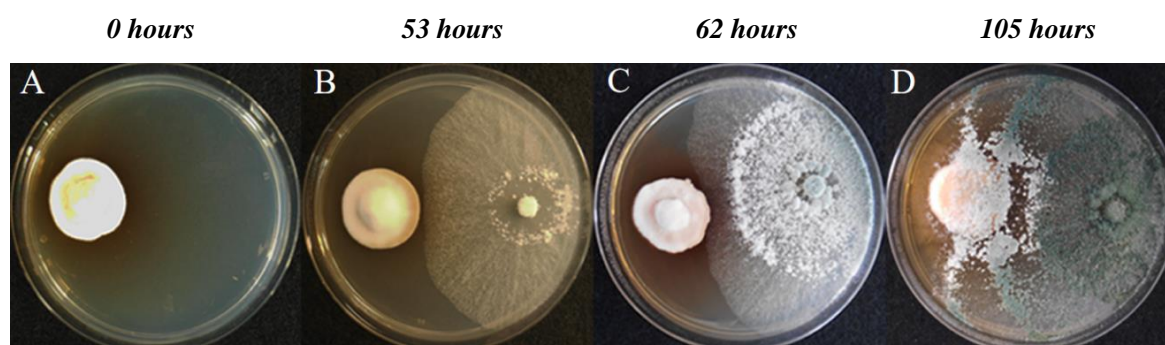


Figure 6. Time course interaction tests between *A. ostoyae* (AO) and *T. atroviride* (TA). (A) individually growing, non-interactive cultures; 53 hours (B), 62 hours (C) and 105 hours (D) after inoculation of TA.

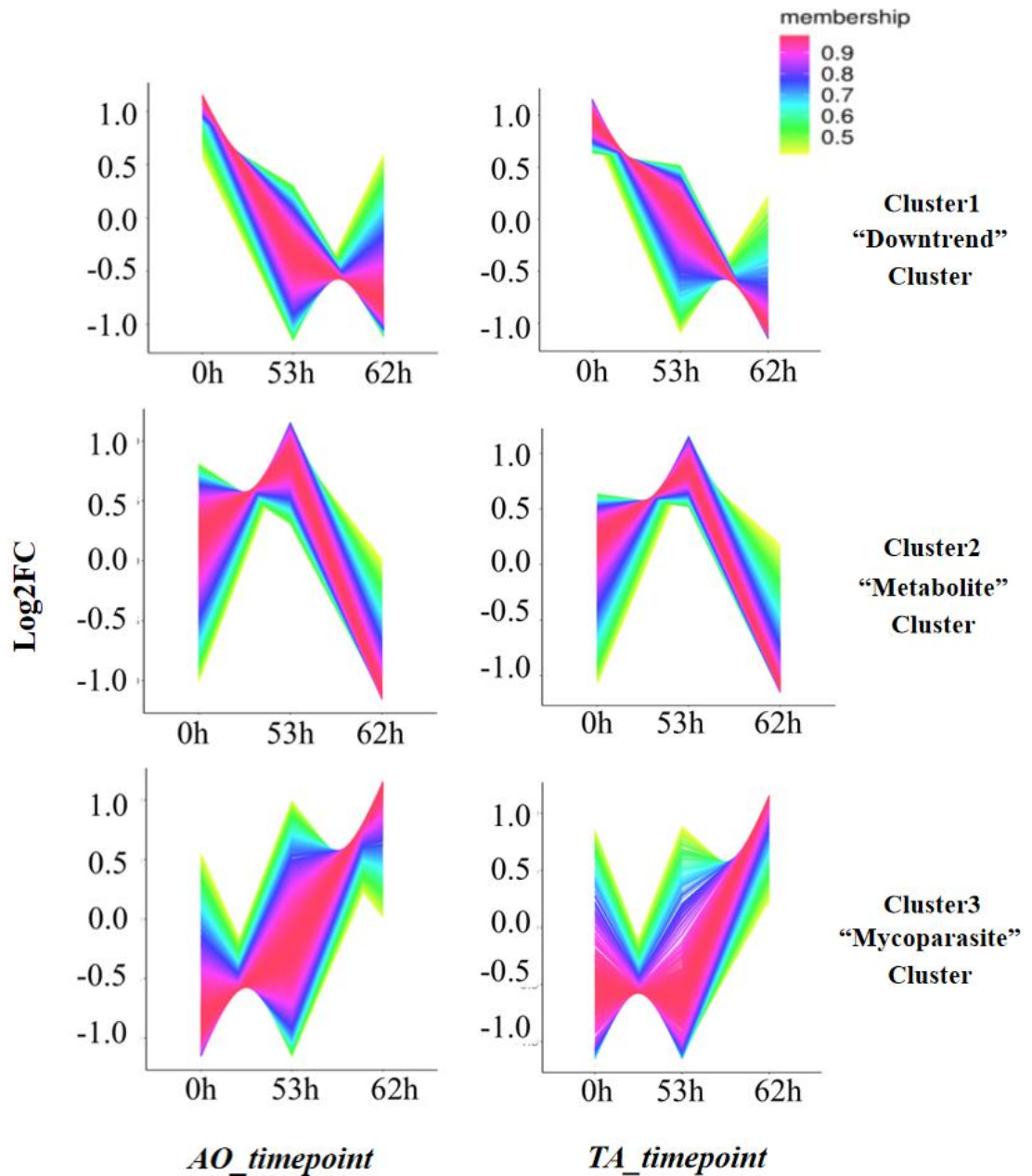


Figure 7. Identification of trends and gene clusters in gene regulation from the interaction transcriptome data of *A. ostoyae* (AO) and *T. atroviride* (TA) during TA invasion at 53h before mycelia contact with AO and 62 hours when the physical contact occurred.

Table 3. Total number of genes grouped from cluster according to the stages where they show differential regulation in *T. atroviride* (TA) and *A. ostoyae* (AO)

Organism	Metabolite stage cluster genes	Mycoparasite stage cluster genes	Downtrend genes
AO	250	1412	768
TA	1024	985	747

4.2.3 Validation of differentially expressed genes using qRT-PCR

To confirm the reliability of the RNA-Seq data, the transcriptional level of 10 unigenes was examined by qRT-PCR (Figure 8) including ARMOST_13362, ARMOST_03616, ARMOST_5857, ARMOST_18537, ARMOST_05856, ARMOST_05616, ARMOST_04226 and ARMOST_18535 for *A. ostoyae* (AO), as well as XM_014093434.1 and XM_014092940.1 for *T. atroviride* (TA). All the 10 genes exhibited higher expression at the Metabolite and Mycoparasite stages in response to the biocontrol interaction before physical contact and during physical contact, respectively. Taken together, all of these unigenes were upregulated in comparison with the control, consistent with the RNA-Seq data, indicating that our experimental results were valid.

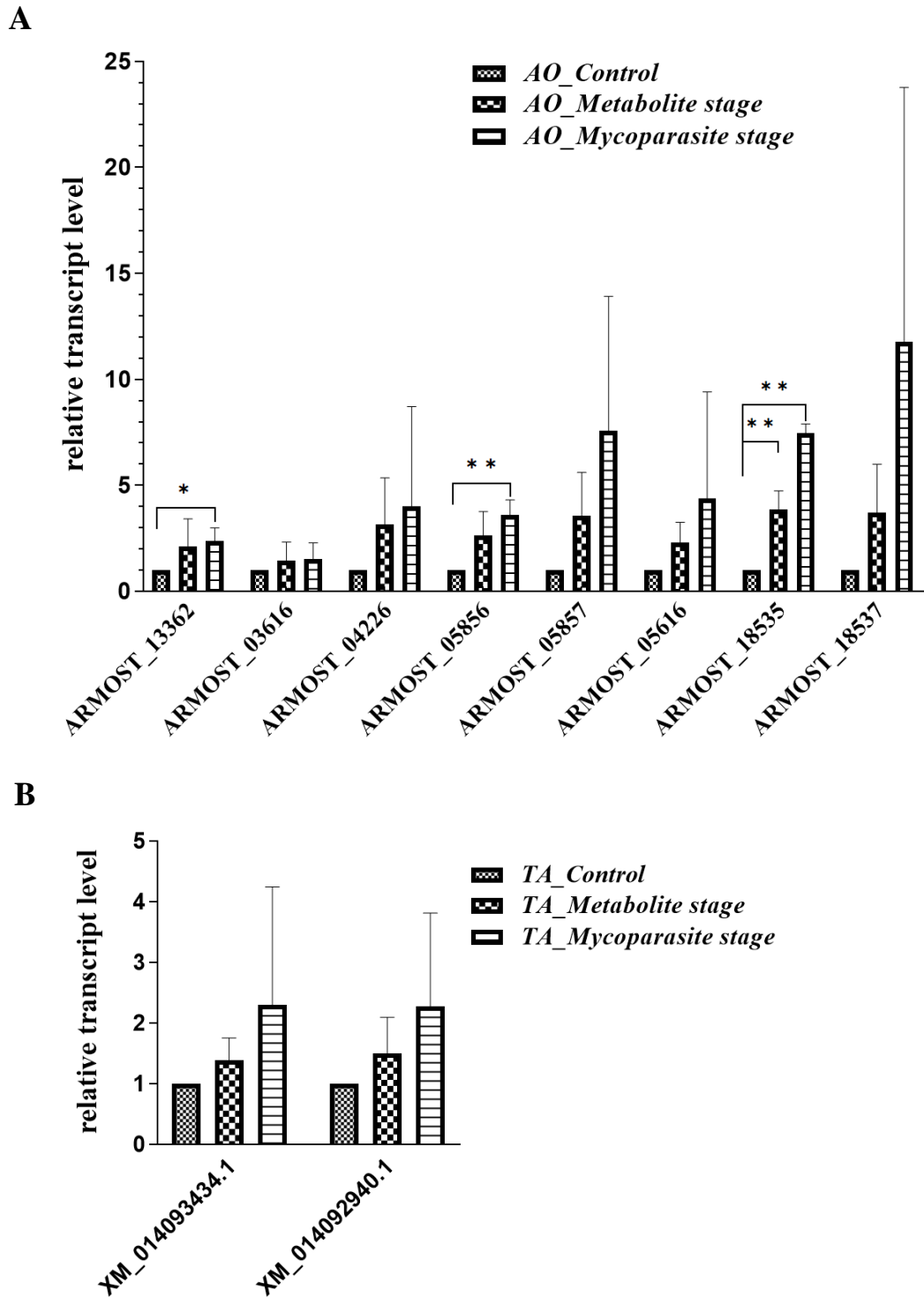


Figure 8. qRT-PCR validations of 10 genes that were differentially expressed in the *A. ostoyae* (AO) at the Metabolite stage and Mycoparasite stage respectively (A) and *T. atroviride* (TA) at the Metabolite stage and Mycoparasite stage respectively (B) during the biocontrol interaction process. For each qRT-PCR validation, the actin gene was used as internal control of ARMOST_13362, ARMOST_03616, ARMOST_5857, ARMOST_18537 and ARMOST_05856, the *gpd* gene was used as internal control of ARMOST_05616, ARMOST_04226 and ARMOST_18535, while the *tefla* gene was used as the internal control of XM_014093434.1 and XM_014092940.1. Asterisks represent statistical significance (** $p < 0.01$ and * $p < 0.05$).

4.2.4 Gene expression profiling of the major trends

To analyze major gene expression trends, we considered TA-AO genes showing continuous downtrend patterns or genes exhibiting the highest upregulation at Metabolite or Mycoparasite stages (Figure 7, Table 3) for further analysis.

4.2.4.1 Downtrend genes in *T. atroviride* (TA) and *A. ostoyae* (AO)

We observed 768 and 747 downtrend genes in AO and TA respectively (Table 3). Gene ontology (GO) enrichment analysis of downtrend genes in AO showed enrichment of 14 biological processes, 3 molecular functions and 20 cellular components (Figure 9). In AO, biological processes such as cell cycle, DNA replication, DNA dependent RNA replication, DNA repair, mitotic cell cycle, sterol metabolic/biosynthetic processes and cellular response to stress/DNA damage stimulus (Figure 9) were enriched. However, TA showed enrichment of 13 biological processes, 2 molecular functions and 5 cellular components in the Downtrend gene cluster. Biological processes enriched in TA included oxidation reduction activity, amino acid metabolic process, organic acid metabolic process, cellular ketone metabolic process and sulfur metabolic processes (Supplementary Figure 6).

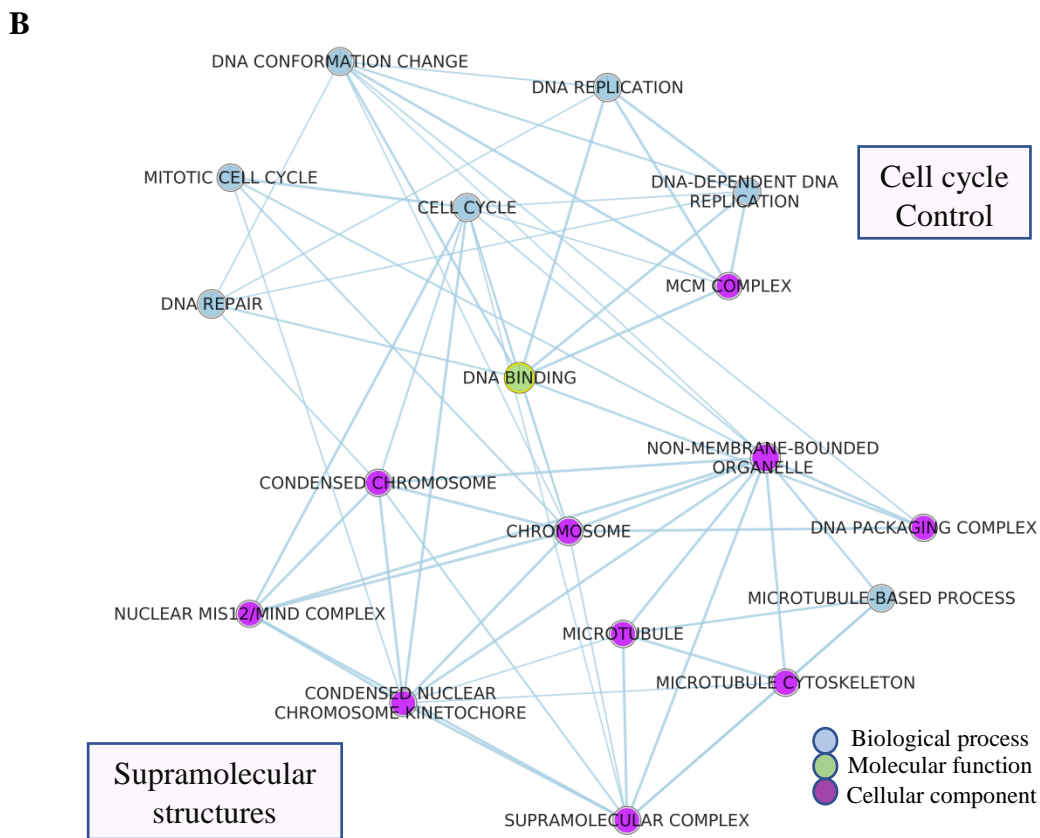
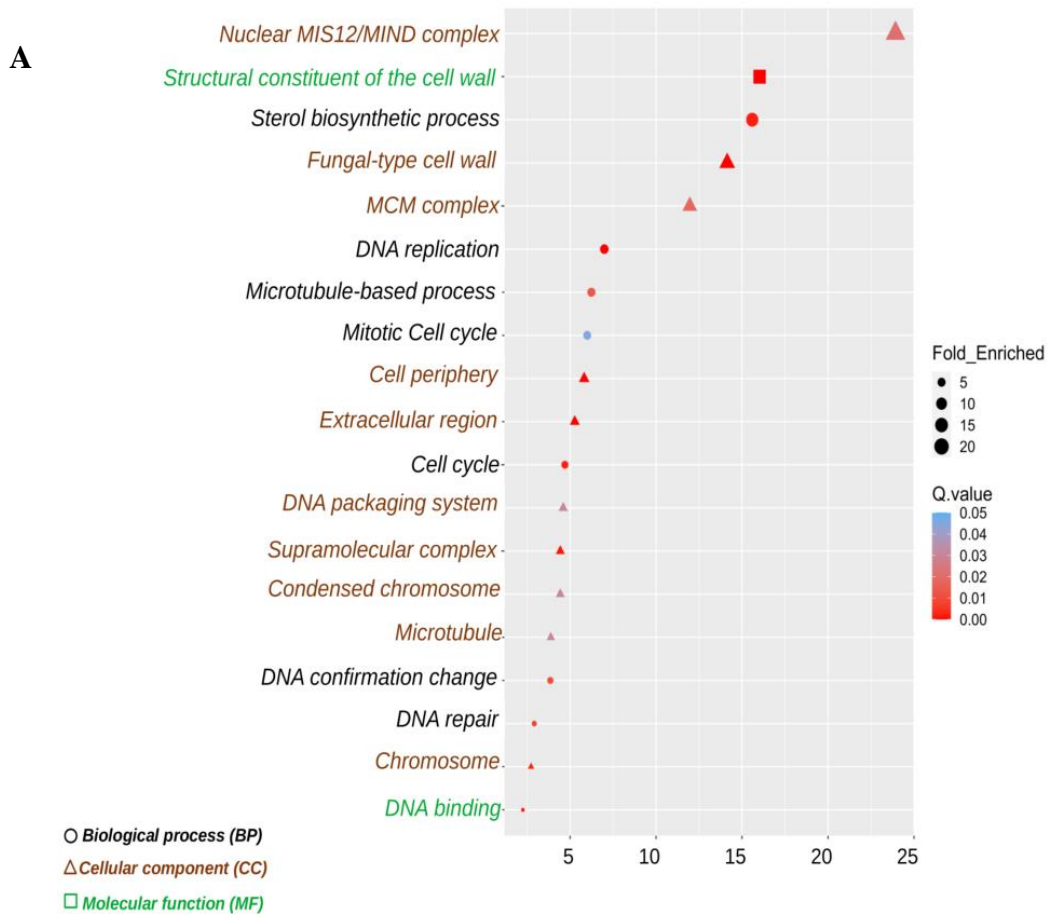


Figure 9. AO_Downtrend: Enriched GO terms (A) and GO enrichment map (B) from the Downtrend cluster genes in *A. ostoyae* (AO).

4.2.4.2 The Metabolite and Mycoparasite interaction stages

During the Metabolite stage, there were 1024 and 250 genes exclusively upregulated in TA and AO, respectively (Table 3). Functional analysis of those genes showed enrichment of interpro domains such as cerato-ulmin hydrophobin, chaperonin Cpn60/TCP-1, nucleoside phosphorylase, NWD NACHT-NTPase, glycoside hydrolase, condensation domain, NACHT nucleoside triphosphatase, heterokaryon incompatibility and ankyrin repeat in TA (Figure 10). Whereas, AO showed upregulation of cyanate lyase, glutathione peroxidase, indoleamine 2,3-dioxygenase, C-terminal dimerisation domain of phenol hydroxylase, condensation domain, flavin-dependent halogenase, Ctr copper transporter, DAHP synthetase I/KDSA, Class I-like SAM-dependent O-methyltransferase (Figure 10), as well as SnoaL, where the overexpression of the genes ARMOST_05856 and ARMOST_05857 could also be validated by qPCR (Figure 8).

In the Mycoparasite stage we identified 985 genes in TA and 1412 genes in AO that were specifically upregulated (Table 3). During that stage, gene families such as N-terminal of Pex, alpha crystallin/Hsp20 domain, CDR ATP binding cassette (ABC) transporter, thiolase, ABC-2 type transporter, NAD(P)-binding domain, cytochrome b5-like heme/steroid binding domain, NAD-dependent epimerase/dehydratase and short-chain dehydrogenase/reductase SDR were enriched in TA (Figure 10), whereas AO showed upregulation of domains like cellobiohydrolase, DSBA-like thioredoxin domain, C-terminal and N-domain of P-type ATPase, NmrA-like domain, malic acid transport protein, DJ-1/Pfpl, domain of unknown function DUF2235, N-domain of NADH:flavin oxidoreductase/NADH oxidase and voltage-dependent anion channel (Figure 10).

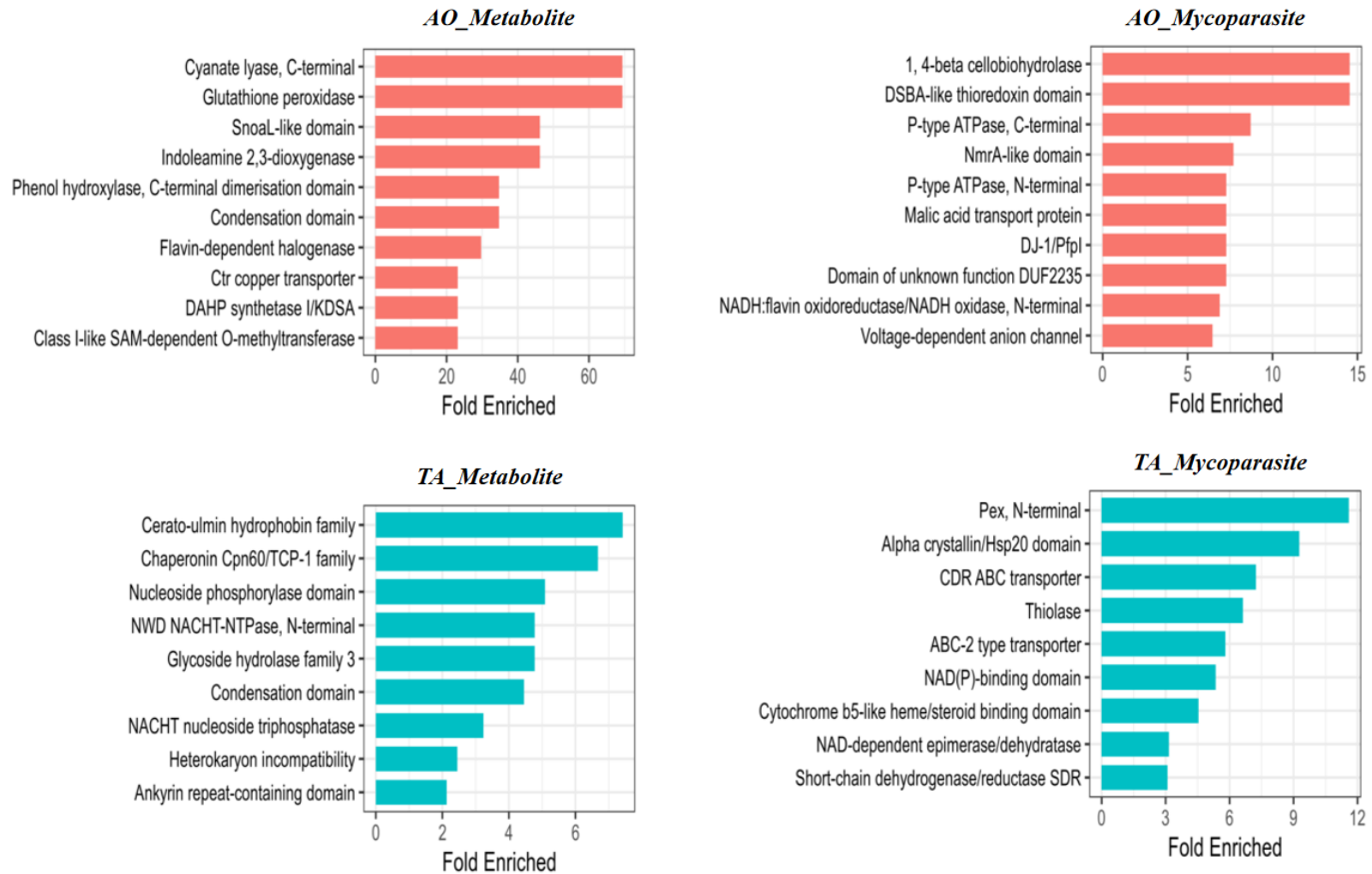


Figure 10. Top Interpro domains enriched in the Metabolite and Mycoparasite cluster genes of *A. ostoyae* (AO) and *T. atroviride* (TA)

We also examined the secondary metabolite potential in TA which could be a representative of its mycoparasitism-related arsenal and contrasted it against AO. In TA, GO enrichment analysis showed that nine biological processes including sterol biosynthetic process, cellular alcohol biosynthetic process, phytosteroid biosynthetic process, cellular alcohol metabolic process, phytosteroid metabolic process, ergosterol metabolic process, nucleoside metabolic process, nucleobase nucleoside and nucleotide metabolic process and carbohydrate metabolic process and four molecular functions including catalytic activity, phosphopantetheine binding, carbohydrate binding and ADP binding were enriched at the Metabolite stage (Figure 11).

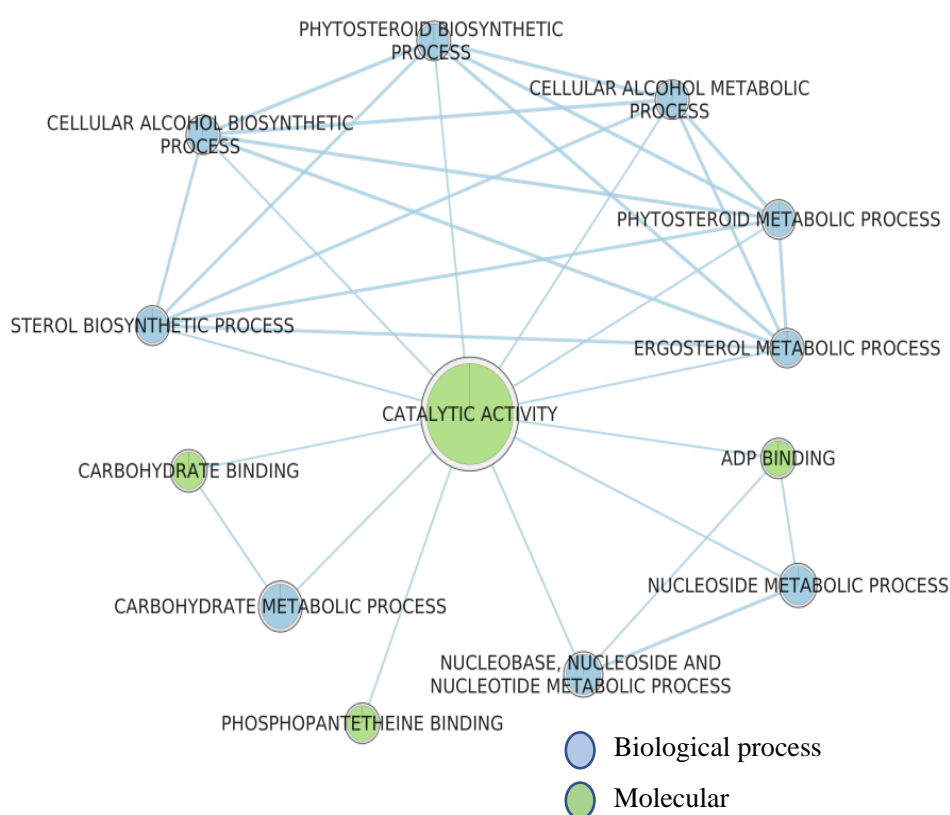


Figure 11. TA_ Metabolite: GO Enrichment map of the Metabolite stage cluster genes from *T. atroviride* (TA)

During the Metabolite stage, TA showed upregulation of 7 genes related to non-ribosomal peptide synthetase (NRPS), 2 genes related to PKS and PKS-like each, and 1 gene related to NRPS-like and NRPS-PKS hybrid. AO showed up-regulation of 2 genes related to PKS and 1 gene for each NRPS and NRPS-like proteins. During the Mycoparasite stage, TA showed 2 genes related to NRPS-like, 2 genes related to PKS, and 1 gene related to DMATS (dimethylallyltryptophan synthase). In AO, there were 2 genes related to DMATS and PKS, and 1 gene for NRPS-like (Figure 12).

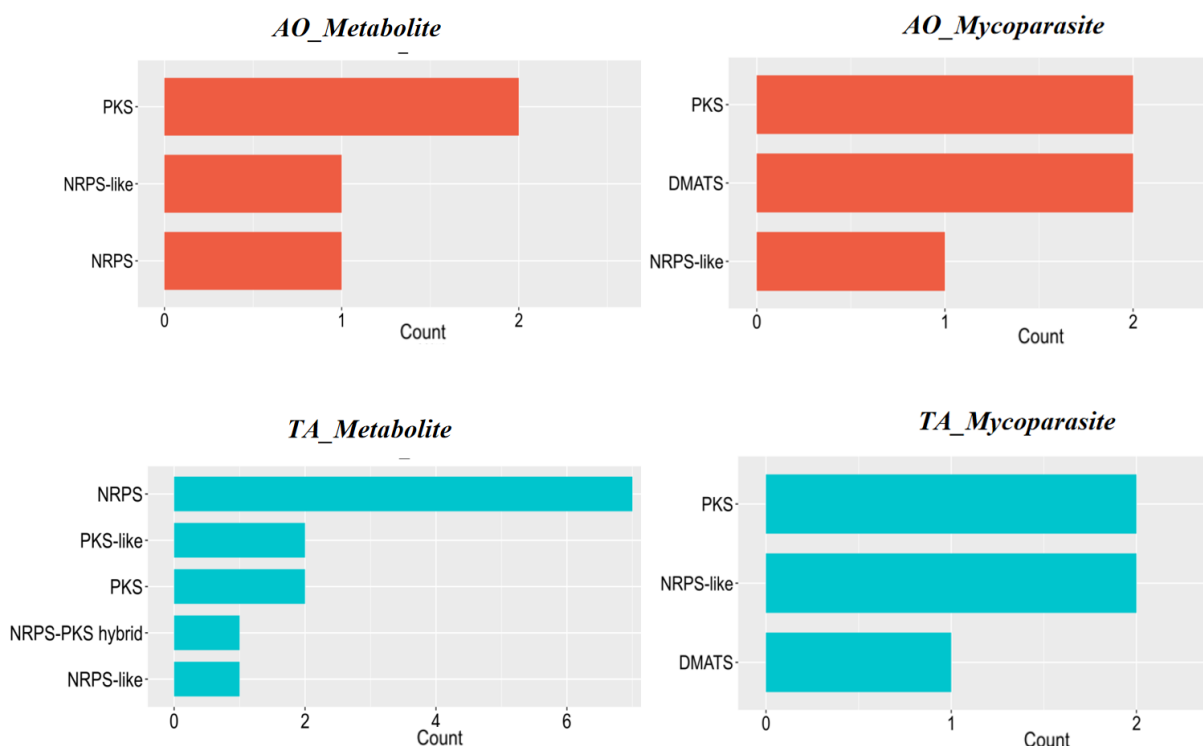


Figure 12. Secondary metabolite related gene count in *A. ostoyae* (AO) and *T. atroviride* (TA) in the Metabolite and Mycoparasite stages of the interaction process

GO enrichment analysis of genes during the Metabolite interaction stage showed that the enriched biological processes including cellular amino acid metabolic process, carboxylic acid catabolic process, organic acid metabolic process, cellular ketone metabolic process, small molecule metabolic process, tryptophan catabolic process to kynurenine, indolalkylamine metabolic process, alpha-amino acid metabolic process and aromatic amino acid family metabolic process in AO (Figure 13A), GO enrichment results hinted the possibility of quinolinic acid (QA) production in AO to counter TA. To test the possibility of QA production, we checked the genes that were necessary in stepwise conversion of tryptophan to quinolinic acid using BLAST analysis (Supplementary Figure 7). We identified the following genes homologous to the BNA genes of *Saccharomyces cerevisiae*: ARMOST_04226 (BNA2), ARMOST_13362 (BNA2), ARMOST_08419 (BNA7), ARMOST_03616 (BNA4), ARMOST_03615 (BNA5) and ARMOST_12859 (BNA1) (Supplementary Figure 7). All the BNA homologous genes in AO showed upregulation at the Metabolite stage (Figure 13B), which was also supported by the qPCR results for 3 genes tested (ARMOST_04226, ARMOST_13362 and ARMOST_03616, Figure 8).

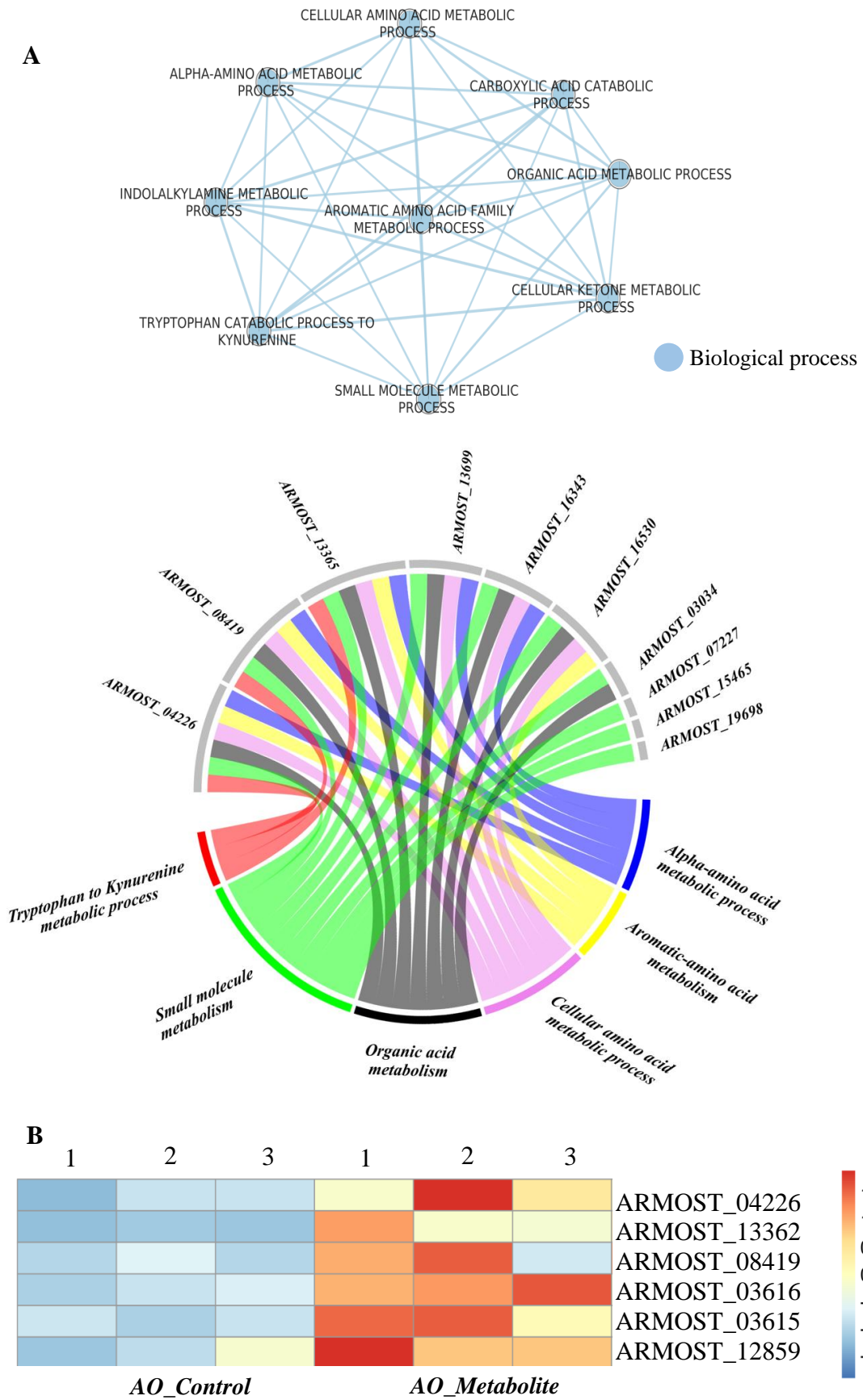


Figure 13. (A) AO_Metabolite: GO Enrichment map of the Metabolite stage cluster genes from *A. ostoyae* (AO); (B) Upregulation of the pathway leading to quinolinic acid (QA) production in *A. ostoyae* (AO) at the Metabolite stage (based on yeast homologs, pathway shown in Supplementary Figure 7)

GO enrichment analysis showed nine biological processes related to peroxisome including peroxisome organization, peroxisomal transport, transmembrane transport, protein transmembrane import into intracellular organelle, protein targeting to peroxisome, peroxisomal membrane transport, protein localization to peroxisome, protein import into peroxisome matrix and establishment of protein localization of peroxisome to be enriched in TA at the Mycoparasite stage. TA also showed GO enrichment of nine cellular components including peroxisome, microbody, microbody membrane, intrinsic component of membrane, integral component of membrane, membrane, peroxisomal membrane, intrinsic component of peroxisomal membrane and integral component of peroxisomal membrane (Figure 14).

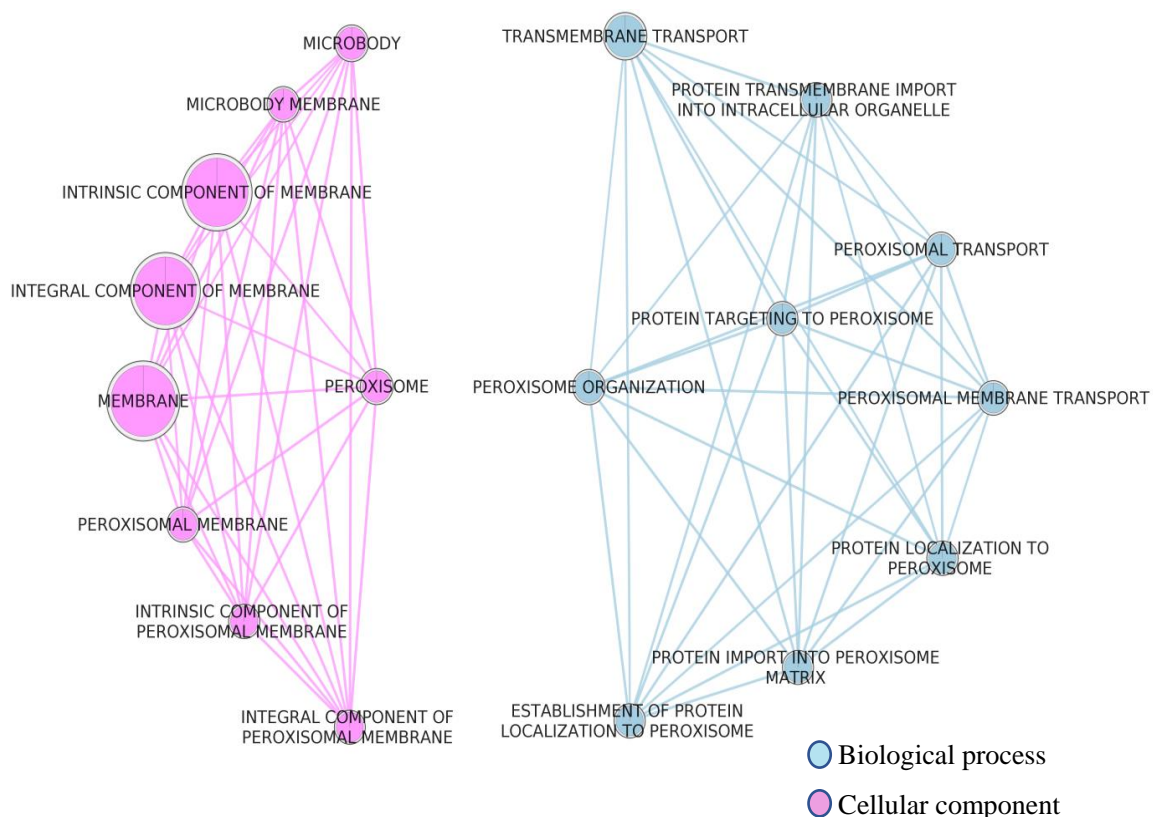


Figure 14. TA_Mycoparasite: GO Enrichment map of the Mycoparasite stage cluster genes from *T. atroviride* (TA)

During the Mycoparasite stage of interaction, AO showed GO enrichment of biological processes such as biological regulation, regulation of DNA-templated transcription, regulation of nucleobase-containing compound metabolic process, RNA biosynthetic process, regulation of nucleic acid-templated transcription, cell redox homeostasis, cellular homeostasis, regulation of cellular process, regulation of biological process, nucleic acid-templated transcription, regulation of RNA biosynthetic process, regulation of RNA

metabolic process, DNA-templated transcription, and nucleoside bisphosphate metabolic process, purine nucleoside bisphosphate metabolic process, ribonucleoside bisphosphate metabolic process and indole alkaloid metabolic process, indole alkaloid biosynthetic process, alkaloid metabolic process, alkaloid biosynthetic process and malate transport, malate transmembrane transport, C4-dicarboxylate transport, transmembrane transport, dicarboxylic acid transport and cellular response to chemical stimulus, response to chemical, cellular oxidant detoxification, detoxification, cellular detoxification, cellular response to toxic substance, response to toxic substance (Figure 15).

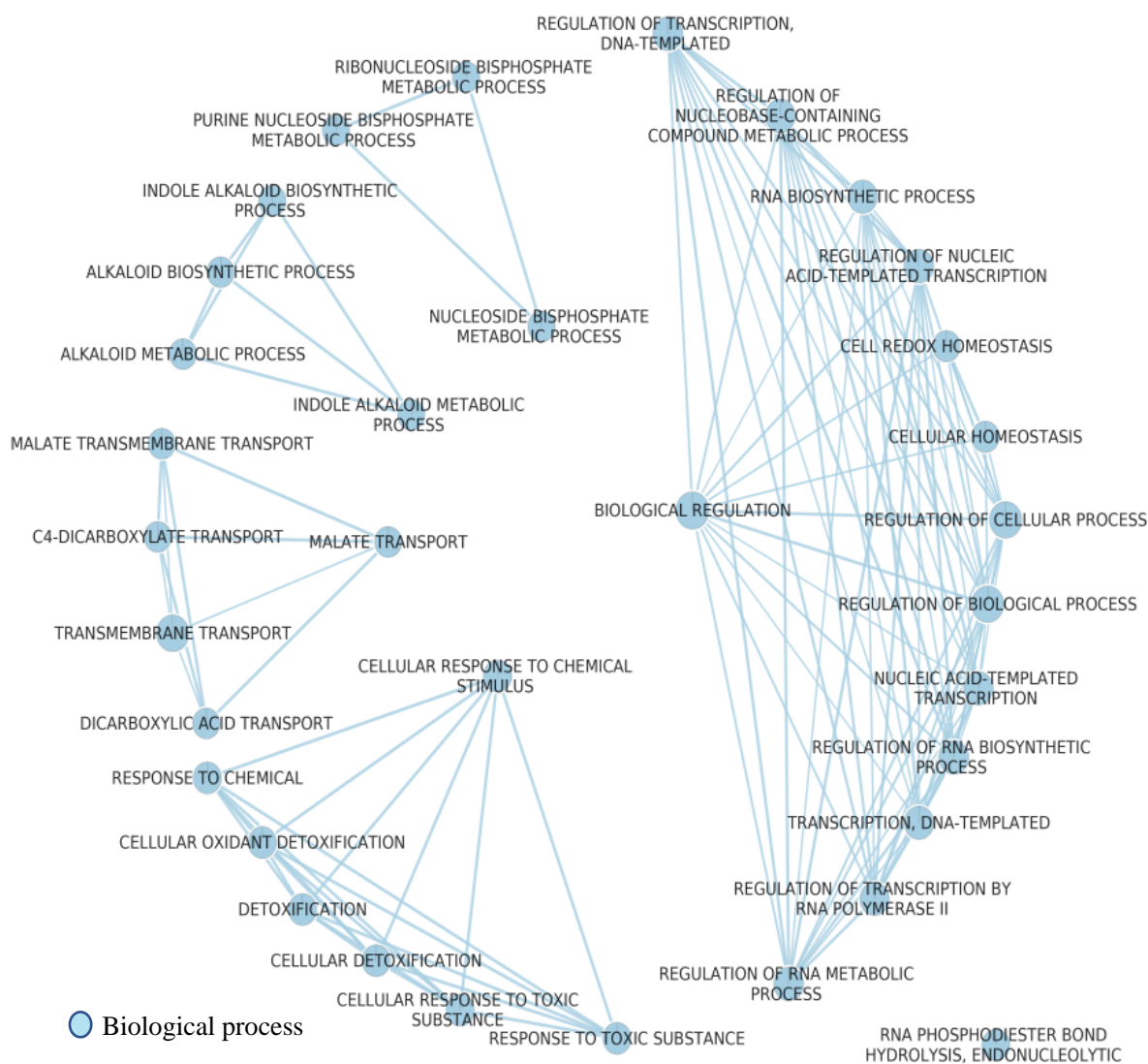


Figure 15. AO_Mycoparasite: GO Enrichment map of the Mycoparasite stage cluster genes from *A. ostoyae* (AO)

Apoptosis-related genes including ARMOST_18537, ARMOST_09700, ARMOST_18535, ARMOST_01402, ARMOST_12695, ARMOST_05616,

ARMOSt_09409, ARMOSt_09498 and ARMOSt_08960 were all upregulated at the Metabolite stage and all the nine genes including ARMOSt_18631 further reached a significantly higher expression in AO during the Mycoparasite stage of interaction with TA (Figure 16). These results were confirmed for the genes ARMOSt_18537, ARMOSt_18535, ARMOSt_05616 also by qPCR analysis (Figure 8).

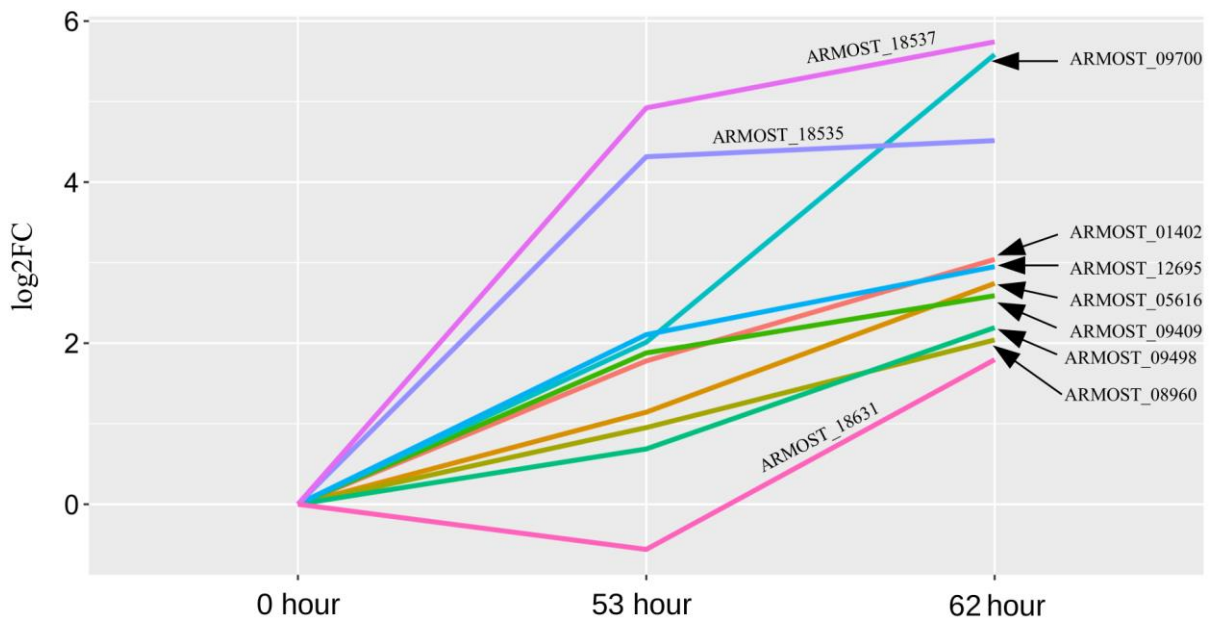


Figure 16. Apoptosis-related genes showing highest expression in *A. ostoyae* (AO) during the Mycoparasite stage

Our study on the transcriptional regulation of the secretory proteins revealed interesting differences between AO and TA at both stages of metabolic and mycoparasitic interaction. One of the most distinct differences between AO and TA was the percentage of small secretory proteins (SSPs) (classically secreted proteins < 300 amino acids). The percentage of SSPs in AO was 9.6% and 6.01% at the Metabolite stage and the Mycoparasite stage respectively, compared to TA where it was only 0.1% and 0.5% respectively. Majority of the secretory proteins in TA belonged to UPS with 9.6% and 11.6% at the two stages, respectively, while in AO, UPS secreted proteins only accounted for 4% and 4.6%. Secreted proteins reached higher level in AO during the Metabolite stage, especially the classically secreted proteins which accounted about 8.4% than 4.7% at the Mycoparasite stage (Figure 17).

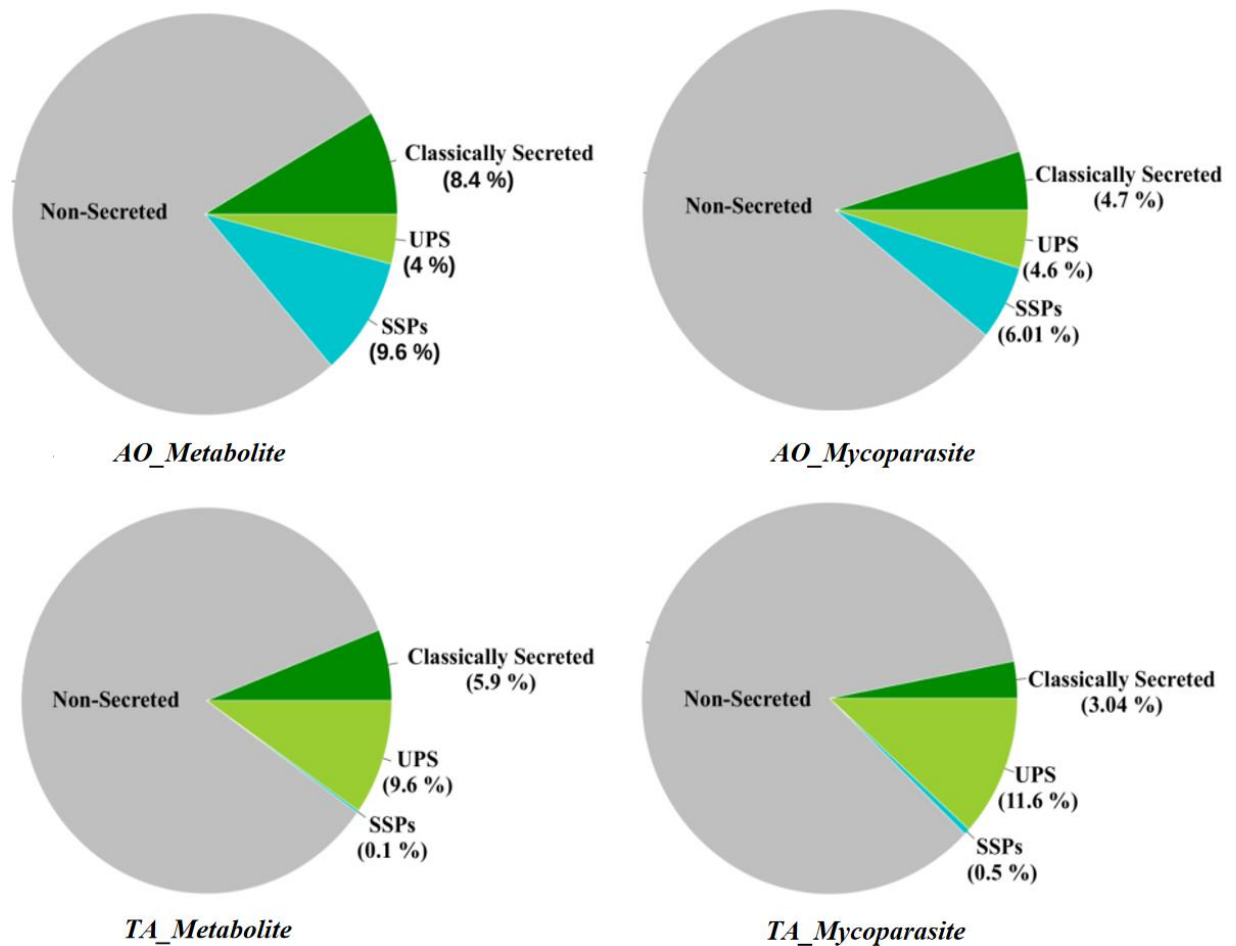


Figure 17. Upregulation of secretory proteins genes in the Metabolite and Mycoparasite stages of *A. ostoyae* (AO) and *T. atroviride* (TA)

An interesting phenomenon on the dynamics of CAZymes was observed in the transcriptomes of TA and AO during their non-physical and physical interactions; there was a significantly differential expression pattern of CAZymes when TA and AO were confronted with each other. For example, only genes encoding 6 enzymes of AA1 (peroxidase), AA3 (cellobiose dehydrogenase), AA7 (oligosaccharide oxidase), GH16 (xyloglucanase), GH18 (chitinase) and GH128 (β -1,3-glucanase) were upregulated in both TA and AO either at the Metabolite or at the Mycoparasite stage. However, the upregulation of genes for biosynthesis of AA11 (lytic polysaccharide monooxygenases), CBM13 (xylanase), CBM50 (chitin binding), CH3 (xylane esterase), GH2 (β -glucosidase), GH3 (α -glucosidase), GH17 (glucan endo-1,3- β -glucosidase), GH27 (α -galactosidase), GH54 (α -L-arabinofuranosidase), GH55 (β -1,3-glucanase), GH63 (α -glucosidase), GH65 (α,α -trehalase), GH71 (α -1,3-glucanase), GH72 (β -1,3-glucanosyltransglycosylase), GH92 (α -mannosidase) and GH105 (rhamnogalacturonyl hydrolase) were only observed in TA; while AO showed a specific increase in the enzyme level of AA2 (versatile peroxidase), CBM67 (α -L-rhamnosidase), CE4

(chitin deacetylase), CE8 (pectin methylesterase), GH6 (1,4- β -cellobiohydrolase), GH12 (endoglucanase), GH78 (α -L-rhamnosidase), GH79 (β -glucuronidase), GH152 (β -1,3-glucanase) and PL3 (pectate lyase) at either metabolite and mycoparasite stage. Overall, the majority of the genes upregulated in TA belonged to the family of glycoside hydrolases (GHs), whereas in case of AO it was auxiliary activities (AAs) (Figure 18).



Figure 18. Upregulation of secretory CAZyme genes at the Metabolite and Mycoparasite stages of the interaction between *A. ostoyae* (AO) and *T. atroviride* (TA)

At the Metabolite stage, genes related to serine peptidases (S08A, S08B, S09B, S09X, S12, S15, S33, S54) and metallo peptidases (M12A, M12B, M14A, M16A, M28E, M28X) were dominant in TA transcriptome; in contrast, AO showed lower number of peptidase-related genes including genes for two aspartic peptidases, four cysteine peptidases, one glutamic peptidase, one peptidase inhibitor, three metallo peptidases, two serine peptidases and one threonine peptidase. However, at the Mycoparasite stage, more types of peptidases were activated and the production of peptidases was dramatically increased in AO; genes related to serine peptidases (S01A, S08A, S09B, S09X, S10, S12, S15, S28, S33, S53), metallopeptidases (M12A, M16A, M16B, M19, M20A, M20D, M36, M76), peptidase inhibitors (I29, I51, I63), cysteine peptidases (C02A, C12, C14B, C19, C48, C56, C110) and aspartic peptidases (A01A, A11A) were significantly upregulated in AO (Figure 19). TA showed similar level but differentially compensatory expression pattern of peptidase-related genes at the Mycoparasite stage compared with the Metabolite stage.

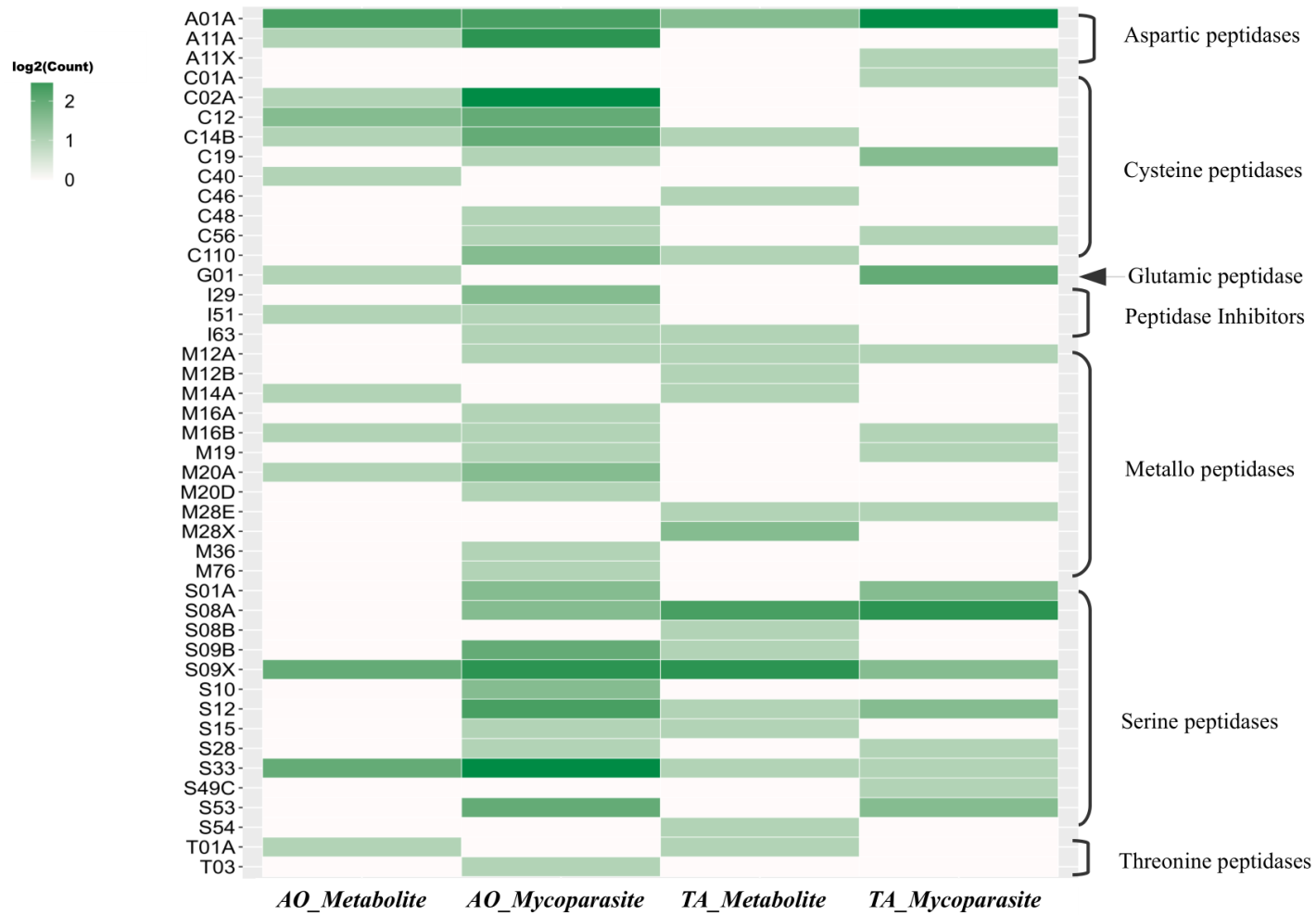


Figure 19. Upregulation of secretory peptidase genes during the Metabolite and Mycoparasite stages of the interaction between *A. ostoyae* (AO) and *T. atroviride* (TA)

4.3 Field experiment in a heavily *Armillaria*-damaged forest in the Keszthely Hills

Two *Trichoderma* isolates - *T. virens* SZMC 24205 and *T. atrobrunneum* SZMC 24206 – were selected for a field experiment. Both strains were isolated from a Keszthely soil sample associated with decaying *Armillaria* rhizomorphs, which have not revealed any *Armillaria* growth upon isolation attempts; furthermore, both exerted very good *in vitro* antagonistic abilities towards the tested *Armillaria* isolates and were able to produce hydroxamate-type siderophores and IAA. The isolates were applied to Turkey oak seedlings as a root treatment before planting in the form of a conidial suspension. The total survival rates calculated after 6 months for 120 treated and 115 control trees were 84.3% and 54.7%, respectively (Table 4), indicating that the applied treatment had a beneficial effect on the survival of oak seedlings planted into the soil of an *Armillaria*-infested forest area.

Table 4. Survival of *Trichoderma*-treated and control trees 6 months after planting into heavily *Armillaria*-infested soil

Parcel	Total No.	¹ Dead No.	² Growing No.	³ Survivor No.	⁴ FM No.	⁵ Corrected Total No.	Dead %	Growing %	Growing + Survivor %
1 (treated)	40	5	24	3	8	32	15.6	75.0	84.4
2 (treated)	40	5	27	5	3	37	13.5	73.0	86.5
3 (treated)	40	7	28	4	1	39	17.9	71.8	82.1
Total	120	17	79	12	12	108	15.7	73.1	84.3
4 (untreated)	40	23	5	2	10	30	76.7	16.7	23.3
5 (untreated)	39	13	19	2	5	34	38.2	55.9	61.8
6 (untreated)	36	7	24	0	5	31	22.6	77.4	77.4
Total	115	43	48	4	20	95	45.3	50.5	54.7

¹ already degraded/disappeared and dry seedlings; ² positive biomass production; ³ still alive but no biomass production; ⁴ failed measurement (size values after 6 month lower than the ones measured directly after planting); ⁵ Total—FM.

5 DISCUSSION

5.1 Different diversity pattern of *Armillaria* and *Trichoderma* species were discovered between the healthy spruce forest in Rosalia and the severely infected oak stand in Keszthely

Armillaria fruiting bodies, rhizomorphs, and soil samples were collected at previously established study sites from both spruce and oak stands; all of them with abundant rhizomorph and mushroom production. The conifer sampling sites selected in Rosalia represented a native environment for Norway spruce with single clones of *A. ostoyae* and *A. cepistipes* colonies appearing only around relatively freshly cut trunks. All identified genets appeared non-damaging and tolerable by the surrounding live trees. In contrast, the Turkey oak stand from Keszthely, Hungary was a heavily infested area with multiple *A. mellea* and *A. gallica* clones merged to form a continuous coverage of the whole stand. All remaining standing trees were showing symptoms of *Armillaria* infections. The coexisting species of *A. gallica* and *A. mellea* in the heavily *Armillaria*-damaged oak stand competed for rotten hardwood substrates and the dominating *A. mellea* seemed to be the most virulent contributing factor for the oak decline (Baumgartner and Rizzo, 2001b). A lot more isolates of *A. mellea* from the heavily *Armillaria* damaged oak stand were found, whereas *A. gallica* was observed to occur less frequently (Supplementary Table 1), in agreement with the severely damaged condition of oak forests in Keszthely Hill caused by infection of the more pathogenic *A. mellea*.

The exact, species-level molecular identification of isolated *Trichoderma* strains should be performed by the sequence analysis of a fragment of the *tef1a* gene fragment (Supplementary Table 1), as according to our recent knowledge about the taxonomy of the genus *Trichoderma*, ITS sequence analysis is not allowing an exact diagnosis in many cases (Overton *et al.*, 2006).

Bulk, rhizospheric and rhizomorph-associated soil samples were also subjected to *Trichoderma* isolation in a previous study (Jaklitsch, 2011). The reported diversity of *Trichoderma* had expanded to ~75 species in temperate Europe (Jaklitsch, 2009). Most of the *Trichoderma* species collected in this study from Keszthely and Rosalia (*T. tomentosum*, *T. paratroviride*, *T. hamatum*, *T. citrinoviride*, *T. atrobrunneum*, *T. simmonsii*, *T. atroviride*, *T. koningii*, *T. guizhouense*, *T. paraviridescens*, and *T. longipile*) had already been reported from Southern Europe (Jaklitsch and Voglmayr, 2015). Among them, the species *T. citrinoviride*, *T. atroviride*, *T. koningii*, *T. paraviridescens*, and *T. longipile* were also identified from Central

Europe (Blaszczyk *et al.*, 2016). The *T. harzianum* species complex (also known as *T. harzianum sensu lato*) from the *Harzianum* clade of the genus *Trichoderma* was supposed to comprise at least 14 species (Chaverri *et al.*, 2015), including the more recently described, biocontrol-relevant species of *T. atrobrunneum*, *T. guizhouense*, and *T. simmonsii* that were also found at both locations of our current investigation.

5.2 Several *Trichoderma* species showed strong antagonistic abilities against *Armillaria* species

The application of biocontrol agents as alternatives to chemical fungicides reduces the impacts and risks on human health as well as on the environment (Newitt and Prudence, 2019). *Trichoderma* species as effective biocontrol agents against diverse genera of pathogenic fungi can be used for plant disease management, especially in the case of soilborne diseases. Strains of *T. koningii*, *T. asperellum*, *T. atroviride*, *T. hamatum*, *T. virens*, the *T. harzianum* species complex and other *Trichoderma* taxa have been officially registered and commercialized as crop protection products and microbial fungicides throughout the world, including European countries (Woo *et al.*, 2014).

Antagonistic activity assessment *in vitro* by dual culture assay revealed in this study that strains of *T. virens* were the most excellent biocontrol candidates against *Armillaria* species, indicated by their highest BCI values. Besides *T. virens*, *T. atroviride*, *T. hamatum* and the members of the *T. harzianum* species complex (*T. simmonsii*, *T. atrobrunneum* and *T. guizhouense*), strains of *T. citrinoviride*, *T. paratroviride* and *T. tomentosum* also proved to be effective *in vitro* antagonists of *Armillaria* species with the potential to be used as biocontrol agents against *Armillaria* root rot.

In our study, a distinct geographical pattern was discovered from the distribution of *Trichoderma* species with different level of antagonistic abilities against *Armillaria*. Except for the two species of *T. simmonsii* and *T. atroviride* isolated from both locations of the oak stand in Keszhtely and the spruce forest in Rosalia and having relatively high antagonistic activities, the majority of species displaying good *in vitro* antagonistic abilities against *Armillaria* (such as *T. virens* and *T. atrobrunneum*) came from the heavily infested area of Keszthely Hills. It seems that native microorganisms isolated from soil, rhizosphere or directly from plant roots usually have a better adaptation and thus can display more efficient control of diseases than introduced exotic microorganisms (Weller, 1988). More antagonistic *Trichoderma* species dominated the severely *Armillaria*-infected soil, suggesting their great

potential to be selected as biocontrol agent providing guidance for the refinement of biocontrol approaches.

On the other hand, certain species and strains of *Trichoderma* showed weak antagonistic abilities against *Armillaria* strains, reflected by low BCI values. For example, all the tested isolates of *T. koningii* and *T. asperellum* had lower BCI values than the isolates of *T. virens*, *T. simmonsii*, *T. atrobrunneum*, *T. atroviride* and *T. hamatum*. Previously, *T. koningii* and *T. asperellum* showed excellent antagonistic activities during the application against other plant pathogens. For instance, *T. koningii* showed the highest growth inhibition of *Rhizoctonia solani* causing root rot in cotton, followed by *T. viride*, *T. harzianum* and *T. virens* (Gajera *et al.*, 2016). Similarly, *T. asperellum* was also frequently reported to be a strong necrotrophic mycoparasite parasitizing and feeding on a variety of fungal plant pathogens. For example, *T. asperellum* showed effective antagonistic activity against the white-rot fungus *Phellinus noxius*, the causal agent of an epidemic brown root rot disease of various coniferous and broad-leaved tree species (Chou *et al.*, 2019). In a study report, *T. longipile* suppressed mycelial growth of *Fusarium* species, as well as their mycotoxin production. However, in our study, the strain of *T. longipile* showed weak antagonistic ability against all tested *Armillaria* isolates, as indicated by its lowest BCI values (Błaszczuk *et al.*, 2017).

5.3 Extracellular enzyme secretion, siderophore production and IAA production are important parameters during the screening for biocontrol agents among *Trichoderma* strains

The *Trichoderma* isolates collected during this study were characterized for their abilities to produce polysaccharide-degrading enzymes of the cellulolytic (β -glucosidase and cellobiohydrolase) and xylanolytic (β -xylosidase) enzyme systems that are important for efficient competition in habitats rich of plant-derived polysaccharides, as well as acidic phosphatase playing a role in phosphorus mobilization. Interestingly, the isolates of species with the best *in vitro* antagonistic abilities against *Armillaria* (*T. virens*, *T. atrobrunneum*, *T. simmonsii* and *T. atroviride*) were among the worst producers of these extracellular enzymes and *vice versa*, suggesting that the main antagonistic mechanism of these *Trichoderma* species against *Armillaria* may be mycoparasitism of hyphae and rhizomorphs rather than competition for polysaccharides or increasing phosphorous availability to the tree roots. Certain *Trichoderma* species (*e.g.*, *T. reesei*) can be characterized with a predominantly saprophytic behavior, while others (*e.g.*, *T. virens*, *T. atroviride* and members of the Harzianum clade) are described as successful mycoparasitic species (Monfil and Casas-Flores,

2014). Extracellular hydrolytic enzymes are known as key players of both the saprophytic and the mycoparasitic behavior: the former is relying on the production of plant polysaccharide-degrading enzyme systems like cellulases or xylanases, whereas the latter is based on CWDEs targeting the cell wall of the fungal host (glucanases, chitinases, and proteases).

Characterization and detection of siderophore production may also be an important parameter to screen biocontrol candidates and understand their rhizosphere competence. The competition for iron may also contribute to the anti-*Armillaria* activity of the examined *Trichoderma* isolates, as the production of siderophores proved to be a general feature among them. Previous studies reported that certain strains of *T. asperellum*, *T. atrobrunneum*, *T. atroviride*, *T. gamsii*, *T. hamatum*, *T. harzianum*, *T. polysporum*, *T. reesei*, *T. virens*, *T. paratroviride*, *T. pyramidale*, *T. rufobrunneum*, *T. thermophilum*, *T. viridulum*, *T. guizhouense* and *T. simmonsii* were mainly used as biocontrol agents due to their siderophore-producing abilities (Anke *et al.*, 1991; Segarra *et al.*, 2010; Lehner *et al.*, 2013; Mukherjee *et al.*, 2018; Wang and Zhuang, 2019). Wang and Zhuang firstly reported the siderophore-producing ability of *T. guizhouense* and *T. simmonsii* (Wang and Zhuang, 2019). To the best of our knowledge, the production of siderophores by *T. citrinoviride*, *T. koningii*, *T. crassum*, *T. longipile* and *T. paraviridescens* strains is firstly demonstrated in the present study.

From the forest-derived *Trichoderma* isolates of our study, 40 were able to produce IAA with *T. hamatum* SZMC 24410, *T. citrinoviride* SZMC 26776 and *T. atrobrunneum* SZMC 24206 producing the highest quantities (18.49, 16.198, and 15.64 $\mu\text{g/mL}$, respectively). Data in the literature about the IAA-producing ability of *Trichoderma* strains is limited. Chagas *et al.* investigated the IAA production of *T. harzianum*, *T. pinnatum*, *T. longibrachiatum* and *T. asperelloides*, as well as two strains of *T. virens*, and recorded production values of 2.9–3.2 $\mu\text{g/mL}$ (Chagas *et al.*, 2016). In the present study, the detected values were in a wider concentration range (1.349–8.248 $\mu\text{g/mL}$). A previous study used a similar method to show that strains of *T. atrobrunneum*, *T. guizhouense*, *T. paratroviride* and *T. simmonsii* produce IAA at concentrations of 6.6, 10.3–21.8, 4.1–8.5, and 6.0–7.2 $\mu\text{g/mL}$ (Wang and Zhuang, 2019). In our study, the examined *T. guizhouense* and *T. paratroviride* isolates produced lower amounts of IAA. We also present the first data about the IAA production of *T. koningii*, *T. longipile*, *T. tomentosum*, *T. hamatum*, and *T. citrinoviride*.

A comparison of the data about the *in vitro* antagonism and the production of indole-3-acetic acid, siderophores as well as extracellular β -glucosidase, cellobiohydrolase,

β -xylosidase, and phosphatase enzymes among the *Trichoderma* isolates mostly revealed very similar values for isolates deriving from the same sample and belonging to the same species, suggesting that the respective isolates are clonal and represent the same strain, which is, in many cases, also supported by identical sequences of the *tef1 α* fragment used for species-level identification (Supplementary Table 1). Examples for probable clonality are the isolate groups *T. koningii* SZMC 24277/24278/24279, *T. atroviride* SZMC 24274/24275/24276 and SZMC 24413/24414, *T. simmonsii* SZMC 24435/26771/24436/24403/24404 and SZMC 26777/24412, or *T. atrobrunneum* SZMC 26772/24405. On the other hand, in certain cases, the differences in the physiological parameters or *tef1 α* sequences clearly revealed the presence of multiple strains from the same species in the same sample, e.g., *T. koningii* SZMC 2470/2471 vs. *T. koningii* SZMC 2472/2473, *T. simmonsii* SZMC 26770 vs. SZMC 24429/24430/24431/24433, *T. hamatum* SZMC 24409 vs. SZMC 24410, or *T. simmonsii* SZMC 26773 vs. SZMC 24408 – the difference of the latter two isolates is also supported by a series of single nucleotide polymorphisms in the analyzed *tef1 α* gene fragment (Supplementary Table 1).

5.4 Growth regression of *A. ostoyae* (AO) was reflected by its transcriptome patterns and defence reactions were induced in *A. ostoyae* by *T. atroviride* (TA)

T. atroviride was selected for our transcriptomic studies as it represents a well defined phylogenetic species (Dodd *et al.*, 2003) and showed good *in vitro* antagonistic activities against diverse haploid and diploid strains of *A. ostoyae* (Figure 5, Table 2). Although *T. harzianum sensu lato* is also a group of efficient biocontrol agents which were most commonly reported to be used in previous *Armillaria* biocontrol studies (Table 1), but it encompasses a complex of multiple cryptic species (Druzhinina *et al.*, 2010).

Biocontrol interaction between *Trichoderma* species and the target pathogen *Armillaria* were studied by dual culture assays (Pellegrini *et al.*, 2012), but little is known about their intricate molecular interplay during the mycoparasitic process. Our results suggested that AO sensed and responded to the presence of the neighboring invader TA and altered its performance and behavior accordingly. The most obvious negative effect caused by TA was the growth inhibition of AO (Figure 5). Complex responses reflected by a downtrend gene cluster with the confrontation time extended from 53 hours before physical contact to 62 hours during contact were found in AO. GO enrichment analysis of the downtrend cluster genes in AO showed enrichments of genes related to cell cycle control as well as the supramolecular

structures (Figure 9). It suggested that the growth regression of AO occurred even before physical contact with TA. It seems reasonable to infer that AO was mycoparasitically killed by TA at the post-mycoparasite stage based on the mapping result which did not show any transcripts for AO (Supplementary Figure 5). Moreover, consistent downregulation of both the cell cycle and DNA replication (Figure 9) and the upregulation of several apoptotic genes of AO (Figure 16) may indicate that AO cells likely underwent necrosis resulting in an intense degradation of RNA.

However, AO still struggled to survive and deployed several defence strategies against TA. At transcriptional level, the overall response of AO to TA revealed a defence reaction to an antagonistic biocontrol intruder, such as oxidation-reduction and defence processes and metabolism of toxic compounds. Specifically, the activation of genes implicated in oxidation-reduction and defence processes (high counts of genes responsible for glutathione peroxidase before contact, as well as DSBA-like thioredoxin domain and NADH:flavin oxidoreductase/NADH oxidase during physical contact were detected in AO), and transcriptional regulation (the transcriptional regulator NmrA-like domain protein was upregulated in AO at the Mycoparasite stage; it mediates the biotrophy to necrotrophy transition in *Phytophthora capsici* (Pham *et al.*, 2018)) indicated recognition and reaction of AO to the biocontrol agent (Figure 10).

Before physical contact, genes responsible for glutathione peroxidase expressed in AO (Figure 10) may be important for resistance to nitrosative and oxidative stress (Missall *et al.*, 2005), and could also be linked to the viability of AO. SnoaL-like domain and condensation domain for biosynthesis of polyketides and non-ribosomal peptides were dominated in AO transcriptome before contact (Figure 10). SnoaL belongs to a family of small polyketide cyclases responsible for the biosynthesis of polyketide antibiotics (Supplementary Figure 8) (Sultana *et al.*, 2004). Phenol hydroxylase hydroxylates phenol, a large group of plant secondary metabolites (Enroth *et al.*, 1998). The synthesis of phenolic compounds in cucumber enhanced by the treatment with *T. atroviride* seemed to be strongly associated with the induction of systemic defence responses contributing to the protection of cucumber from *R. solani* (Nawrocka *et al.*, 2018b). Genes for C-terminal dimerisation domain of phenol hydroxylase were abundant in AO (Figure 10), probably contributing to the virulence of AO. Furthermore, other genes possibly protecting AO from the biocontrol agent at the Mycoparasite stage were upregulated, such as a malic acid transport protein and voltage-dependent anion channel for the efficient production of malic acid (Figure 10), which was used as an antimicrobial agent inhibiting the growth of *Listeria monocytogenes*,

Salmonella enteritidis, *Escherichia coli* and *Rhizopus nigricans* (Raybaudi-Massilia *et al.*, 2009; El-Kadi, 2015; Cao *et al.*, 2020). Malic acid was found to be the most abundant organic acid in *A. mellea* fruiting bodies collected from nature (Kostić *et al.*, 2017). Indoleamine 2,3-dioxygenase (IDO) was highly expressed in AO at the Metabolite stage (Figure 10); it is a tryptophan-degrading enzyme supplying nicotinamide adenine dinucleotide (NAD(+)) via the kynurenine pathway in fungi (Yuasa and Ball, 2011, 2013). Correspondingly, upregulation of the kynurenine pathway in AO probably leads to the production of an intermediate, the quinolinic acid (QA) at the Metabolite stage (Figure 13). The antifungal properties of QA such as inhibition of fungal mycelia and fungal cell wall alterations were confirmed by testing on a hazardous fungal pathogen *Ceratocystis fimbriata* (Chen *et al.*, 2021). However, the antifungal activity of QA on *Trichoderma* species still needs further investigation.

5.5 Metabolite interactions were significantly induced

Transcriptional changes of genes associated with complex metabolic pathways occurred in TA in the presence of AO. Metabolic activations were highlighted by genes implicated in the upregulation of condensation domain, SDR and NAD-dependent epimerase/dehydratase (Figure 10), which are possibly involved in fundamental metabolic processes and the production of extracellular enzymes (Persson *et al.*, 2009; Islam *et al.*, 2019). The biological processes like cellular alcohol metabolic process and molecular functions such as catalytic activity category were enriched in TA at the Metabolite stage (Figure 11). Non-ribosomal peptides play an important role during the interaction process of biocontrol fungi with plant pathogens, insects and plants (Niu *et al.*, 2020). The genes predicted to be involved in secondary metabolite biosynthesis (NRPS, PKS-like, PKS, NRPS-PKS hybrid and NRPS-like) were highly expressed in TA at the Metabolite stage (Figure 12), suggesting that TA actively antagonized AO through the production of antimicrobial compounds, which was especially indicated by the significant expression of NRPS genes. These expression profiles indicated that the biocontrol processes were already activated by TA before physical contact with AO and AO consequently reacted by activating detoxification mechanisms and defence processes (Figure 10). On the other hand, the expression of genes encoding toxic secondary metabolites was underrepresented in AO as compared with TA at the Metabolite stage. Fungal ABC transporters (CDR ABC transporter and ABC-2 type transporter) which were well-characterized transmembrane proteins functioning in cellular detoxification were also detected to be expressed in the TA transcriptome during the Mycoparasite stage (Figure 10). In conclusion, genes encoding toxic secondary metabolites and ABC transporters possibly

implicated in the production of antifungal components and biocontrol molecules (Mukherjee *et al.*, 2012) were highly expressed in TA when its mycelia gradually reached and physically contacted with AO.

Peroxisome-related processes were activated in TA at the Mycoparasite stage (Figure 14). Peroxisomes are involved in lipid metabolism and implicated in a number of essential metabolic pathways and the homeostasis of reactive oxygen species (Peraza-Reyes and Berteaux-Lecellier, 2013). The peroxisome process also represents a type of defense systems that aims to protect the survival of the multicellular organism (Maruyama and Kitamoto, 2013). It seems that peroxisomes play an essential role in the TA survival and growth process at physical contact with AO (Figure 14), possibly through the ability to prevent excessive loss of cytoplasmic constituents upon hyphal lysis. However, apoptotic-like cell death seemed to occur in AO, reflected by the significant upregulation of apoptosis-related genes once the TA physically contacted with AO (Figure 16). In fungi, apoptosis can be induced by exposure to toxic metabolites or other stresses (Sharon *et al.*, 2009). To consistent with the apoptosis induction, biological processes such as cellular response to chemical stimulus, cellular oxidant detoxification, and cellular response to toxic substance were enriched in AO at the Mycoparasite stage (Figure 15).

5.6 CAZymes play an important role in the biocontrol process

CAZymes in *Trichoderma* species are responsible for degradation of plant residues as well as hydrolysis of fungal cell wall during mycoparasitism (Kubicek *et al.*, 2011). The different ecological behavior of the mycoparasites such as *T. virens*, *T. abtrobrunneum* and *T. atroviride*, compared to the industrially important cellulolytic *T. reesei* (with genome size of 34.1 Mbp), is reflected by their expansion of the genome size that enables them to maintain genes implicated in mycoparasitism (Kubicek *et al.*, 2011; Schmoll *et al.*, 2016). In the expanded genomes of the mycoparasites such as *T. atroviride* IMI206040 (36.1 Mbp) and *T. abtrobrunneum* ITEM 908 (39.2 Mbp), a higher number of CAZyme domains was found (Fanelli *et al.*, 2018). In our study, a focused investigation was performed on the CAZyme dynamics in the transcriptomes of AO and TA during the Metabolite and Myroparasite stages (Figure 18). In the transcriptomes of TA affected by AO, differential expression of CAZymes was found at both stages, including AAs of redox enzymes that act with CAZymes, carbohydrate esterases (CEs) that are responsible for the hydrolysis of carbohydrate esters, as well as GHs that are associated with the hydrolysis and/or rearrangement of glycosidic bonds. The family GHs containing the highest number of enzymes involved in fungal cell wall

degradation is strongly expressed in TA at the Metabolite stage, which may result in weakening AO. Among the different GHs-related families in TA, GH18 comprised chitinase proteins, which strongly bind to recalcitrant and insoluble substrates like chitin. High upregulation of such proteins increases the potential of TA to infect the cellular substrates of their host (Lienemann *et al.*, 2009). In the plant cell wall, the major constituents are hemicelluloses, cellulose and pectins, while the main carbohydrates in the fungal cell wall are glucan and chitin; therefore, the activation of genes encoding chitinolytic enzymes and glucanases probably plays an important role in the mycoparasitism on AO and is also an essential part of the synergistic action with antifungal secondary metabolites that leads to the death of the host (Harman *et al.*, 2004). However, as with extending incubation time, the expression of GHs in TA decreased significantly at the Mycoparasite stage, probably due to the saturation of these enzymes in the media. In the AO transcriptome, lower diversity and abundance of CAZymes were found before physical contact with TA; the expression of these CAZymes did not show significant change, except for the AAs of redox enzymes (AA1, AA2, AA3 and AA7) that were significantly up-regulated at the Mycoparasite stage, which might be essential for AO survival and substrate usage under the competitive stress of TA.

5.7 Peptidase dynamics is a crucial defence response of *A. ostoyae* (AO)

Since fungal cell walls contain proteins and lipids besides glucan and chitin, the involvement of peptidases and proteases in cell wall degradation seems to be necessary for *Trichoderma* mycoparasitism (Flores *et al.*, 1997). This may be reflected by more abundance and more variation of peptidases induced in TA than in AO during the initial interaction stage before mycelial contact (Figure 19). As the incubation time was prolonged, genes related to the peptidase activities still dominated in the transcriptome of TA for further mycoparasitic interaction. However, considerable variations were found in the set of peptidases in TA expressed between the Metabolite and Mycoparasite stages (Figure 19). This variation in TA seems to be induced by the defence reaction from AO. Not only the possible contribution of proteases to the degradation of fungal cell wall during *Trichoderma* mycoparasitism, but also their putative involvement in the interactions with different organisms triggered great interest for investigation. For example, PapA, as one of the extracellular aspartyl proteases from *T. asperellum* had 58% similarity to PapA in *T. harzianum* (Viterbo *et al.*, 2004). During challenging by the pathogen *R. solani* in plate confrontation tests, the encoding gene *papA* was found to be significantly upregulated (Viterbo *et al.*, 2004). Moreover, peptidases also act as proteolytic inactivators of virulence enzymes or other pathogenic factors from pathogens.

Certain metalloendopeptidases, serine proteases and aspartic proteases were induced to coexpress in *T. harzianum* during *in vitro* nematode egg-parasitism of *Caenorhabditis elegans*, and revealed a major biocontrol role of these proteases in this function (Szabó *et al.*, 2013). On the other hand, peptidase and protease function in the detoxification of toxic molecules was proven in the fungal plant pathogens *A. niger* and *R. solani* in response to bacterial biocontrol strains belonging to the genera *Serratia* and *Bacillus* (Benoit *et al.*, 2015; Gkarmiri *et al.*, 2015). The detoxification function of peptidases seems to be fully activated and put into effect in AO, as when the mycelia of TA extended towards interaction with AO, AO showed a dramatical reaction with a larger variety and more significant production of peptidases (Figure 19), suggesting that the biocontrol agent TA activates a typical defence process in AO.

5.8 Two selected biocontrol candidates showed promising biocontrol effect in a field experiment

Only limited information is available in the literature about field studies evaluating the applicability of *Trichoderma* strains against *Armillaria* root rot of trees. Otieno *et al.* screened *Trichoderma* isolates for antagonism to *Armillaria* in tea stem sections buried in the soil and selected a *T. harzianum* strain, the wheat bran culture of which significantly reduced the viability of *Armillaria* in woody blocks of inoculum (Otieno *et al.*, 2003b). The selected strain also exhibited high efficiency in the biocontrol of the destructive tree and bush pathogens from the genus *Armillaria* (Percival *et al.*, 2011). Schnabel *et al.* applied biannual drenches of *T. asperellum* and *T. gamsii*, formulated as Remedier WP, onto peach trees planted in spots where a tree had declined from *Armillaria* root rot during the previous season, but did not find any statistical significance in survival between the treated and control trees (Schnabel *et al.*, 2011). However, the surviving Remedier WP-treated trees were found to have significantly larger tree trunks compared to control trees three and four years after planting at one of the two replant sites involved in the study. In another study, spraying a combination of *T. harzianum* and *T. koningii* at concentrations of 2×10^7 CFU/mL and 3×10^7 CFU/mL, respectively, into holes made in an avocado orchard previously infested with *A. mellea* did not increase the survival rates of grafted peach (*Prunus persica*) saplings (Downer and Faber, 2019). The lack of *Trichoderma* effect on the survival of peach trees in the above studies may partly be due to the *Trichoderma* species applied: our study demonstrated that isolates of *T. asperellum* and *T. koningii* are not among the good *in vitro* antagonists of *Armillaria* species. Furthermore, the success of a tested control strategy may also rely on the thorough selection of the *Trichoderma* strains, which should also consider the origin of the isolates. The two

strains involved in the field test of our study were derived from a soil sample associated with *Armillaria* rhizomorphs which have not revealed any *Armillaria* growth, suggesting that the isolation of *Trichoderma* strains from naturally decaying *Armillaria* rhizomorphs and the soil surrounding them may increase the chances to find promising candidates for the successful biocontrol of *Armillaria* root rot. A similar strain isolation strategy from *Armillaria* rhizomorphs and soil samples around *Armillaria*-infected roots of cherry and almond trees revealed isolates of *T. virens* and *T. harzianum sensu lato* efficiently inhibiting both colony growth and rhizomorph formation of *A. mellea* (Asef *et al.*, 2008).

One of the limitations of *Trichoderma* application in forest stands is arising from the difficulties of delivery, as the regular treatment of large forest areas with a biocontrol product is not economically feasible. An obvious time point of intervention is the planting time of the seedlings, as their roots can be easily treated with microbial products by soaking. A further promising strategy could be the conditioning of the seedlings with microbial products before planting, which could be performed in nurseries under more controlled circumstances than the ones allowed by field conditions.

The interactions of introduced *Trichoderma* strains with other beneficial microorganisms such as mycorrhizal fungi need further investigations, as they may represent both advantages and disadvantages to the host plant (Szczałba *et al.*, 2019). *Trichoderma* may act negatively on mycorrhizal fungi via competition for the colonization sites and nutrients (Martínez-Medina *et al.*, 2009), or via direct mycoparasitic attack, which, however, may also increase the uptake of phosphorous by the mycorrhizal fungus as the result of stress reaction (De Jaeger *et al.*, 2011). Using beneficial fungi in forestry therefore requires the adjustment of *Trichoderma*–mycorrhizal fungus combinations to the host tree, as well as the optimization of the inoculation methods and the applied silvicultural practices.

SUMMARY

Armillaria species are among the economically most damaging soil-borne tree pathogens causing devastating root diseases world-wide. Bacterial and fungal biocontrol agents are promising environment-friendly alternatives to toxic chemicals to restrain and delimit the spread of harmful *Armillaria* activities in forest soils. Amongst the fungal biocontrol candidates, *Trichoderma* species, as mycoparasites, may efficiently employ diverse antagonistic mechanisms against fungal plant pathogens. In our current studies, a large-scale effort to screen, characterize and select *Trichoderma* strains with the potential to antagonize *Armillaria* species revealed promising candidates for direct field applications against advancing *Armillaria* infections. In addition, plate assays were used to perform dual confrontation tests between a haploid *A. ostoyae* isolate and our selected *T. atroviride* strain. Dual RNA-Seq based gene expression profiling was then used to evaluate the interactive activities between *Armillaria* and the mycoparasitic *Trichoderma* isolate.

In our initial field studies, *Armillaria* and *Trichoderma* isolates were collected from soil samples of damaged Hungarian oak and healthy Austrian spruce forests and identified to the species level. While *A. cepistipes* and *A. ostoyae* were found in the Austrian spruce forests, *A. mellea* and *A. gallica* clones dominated the Hungarian oak stands. A total of 64 *Trichoderma* isolates belonging to 14 species were also recovered. Different composition of *Trichoderma* communities was found between the two forest areas.

In vitro antagonism experiments were performed by dual culture assay to determine the potential of various *Trichoderma* strains in controlling pathogenic *Armillaria* isolates. Strains of *Trichoderma* that can be selected as excellent biocontrol candidates against *Armillaria* species were indicated by their high BCI values. Most of the *Trichoderma* strains isolated from the heavily *Armillaria*-infected areas proved to be effective *in vitro* antagonists of *Armillaria* species with the potential to be used as biocontrol agents against *Armillaria* root rot. On the other hand, certain species and strains of *Trichoderma* showed weak antagonistic abilities against *Armillaria* strains, reflected by low BCI values. Most of the weak antagonistic strains were isolated from the healthy forest areas.

The *Trichoderma* isolates collected during this study were characterized for their abilities to produce polysaccharide-degrading enzymes of the cellulolytic and xylanolytic enzyme systems as well as acidic phosphatase playing a role in phosphorus mobilization. However, the isolates of species with the best *in vitro* antagonistic abilities against *Armillaria* were among the worst producers of these extracellular enzymes and *vice versa*, suggesting that the main antagonistic mechanism of these *Trichoderma* species against *Armillaria* may be

mycoparasitism of hyphae and rhizomorphs rather than competition for polysaccharides or increasing phosphorous availability to the tree roots.

Characterization and detection of siderophore production was also an important parameter to screen biocontrol candidates and understand their rhizosphere competence. From the forest-derived *Trichoderma* isolates of our study, 40 were able to produce IAA. Most isolates of *Trichoderma* in our study showed siderophore-producing abilities. Several *Trichoderma* strains exhibited *in vitro* antagonistic abilities towards *Armillaria* species and produced siderophores and indole-3-acetic acid.

A. ostoyae is a facultative necrotroph and one of the most destructive forest pathogens from the genus *Armillaria*, causing root rot disease on woody plants worldwide. However, effective control measures are currently still under investigation to limit the population of this underground pathogen. The biocontrol attributes of *T. atroviride* relying on its markedly rich and powerful genome, proteome and secretome imply a great potential as environmentally sustainable alternatives to chemical fertilizers and pesticides for control of plant disease and forest protection. *T. atroviride* SZMC 24276 (TA) showed high antagonistic efficacy on the haploid *A. ostoyae* derivative SZMC 23093 (AO). The results from dual culture assay indicated that the haploid *A. ostoyae* derivative SZMC 23093 is highly susceptible to the mycelial invasion of *T. atroviride* SZMC 24276.

We analyzed the transcriptomes of AO and TA *in vitro* by dual culture assay for the investigation of their molecular interaction, using high-throughput next generation sequencing technology. During the pathogen–antagonist interaction on PDA media, different time points were captured for transcriptome analysis. We tried to reveal the dynamics of molecular interaction including the metabolite-level interaction before mycelia contact, mycoparasite-level interaction when TA mycelia physically contact with the colony of AO and post-mycoparasite interaction when TA overgrew on the surface of the colony of AO. We also intended to interpret the defence responses of AO at the transcriptional level triggered by the biocontrol invasion of TA, as well as the transcriptional responses of TA underpinning its biocontrol activities during the interaction with its host AO. Therefore, time course analysis, functional annotation, enriched pathways, analysis of differentially expressed genes including candidate biocontrol-related genes from TA and candidate defence-related genes from AO were operated.

The transcriptome analysis of the biocontrol agent and fungal pathogen *in vitro* by dual culture confrontation assay proved to be a useful approach to model the complex molecular dynamics of fungal interaction. To our knowledge, this study was the first transcriptome

analysis of *A. ostoyae* infected with a biocontrol fungus, and it could give insights to plant pathogen-biocontrol agent interaction mechanisms. The results indicated that TA deployed several biocontrol strategies when confronted with AO and multiple defense mechanisms of AO were initiated to protect against the serious negative effects caused by fungal attack.

The changes in the growing media environment caused by metabolites and other secreted from the confronted species and the challenges from physical mycelium invasion impact the transcriptome pattern of fungi. Multiple biocontrol mechanisms of TA were already activated even before physical contact. These included the production of hydrolytic enzymes and antibiotic secondary metabolites. On the other hand, the early transcriptional impact of TA before mycelial contact on the target pathogen AO induced multiple defence reactions such as production of QA. After contact, more defence strategies were deployed, such as the overexpression of peptidases probably involved in detoxification. However, significant growth regression still occurred in AO as TA grew to contact with the pathogen.

Overall, transcriptomic investigation of the fungal interaction revealed that the differential expression of defence genes enable AO to detect the metabolites or extracellular enzymes released from the biocontrol agent and somehow make an effort to defend from TA invasion. On the other hand, the transcriptomic reprogramming in TA induced by its host AO suggested a significant differential expression of the mycoparasitism-related genes which showed their great biocontrol potential to antagonize its host/prey AO.

A field experiment was carried out by applying two selected *Trichoderma* strains on two-year-old European Turkey oak seedlings planted in a forest area heavily overtaken by the rhizomorphs of numerous *Armillaria* colonies. Oak seedlings treated with *T. virens* and *T. atrobrunneum* displayed better survival under heavily *Armillaria*-infested soil conditions than the untreated controls. In conclusion, selected native *Trichoderma* strains, associated with *Armillaria* rhizomorphs, which may also have plant growth promoting properties, are potential antagonists of *Armillaria* spp., and such abilities can be exploited in the biological control of *Armillaria* root rot.

ÖSSZEFOGLALÁS

Az *Armillaria* fajok világszerte a fákat gazdaságilag leginkább károsító, talajban terjedő gombák közé tartoznak, melyek világszerte pusztító gyökérbetegségeket okoznak. A bakteriumokon és gombákon alapuló biokontroll ágensek a toxikus kémiai növényvédő szerek új, környezetbarát alternatívái a káros *Armillaria* fajok erdei talajban történő terjedésének megakadályozására. A biokontroll-jelölt gombák közül a *Trichoderma* fajok mikoparazitaként hatékonyan képesek lehetnek különféle antagonist mechanizmusokat alkalmazni a növénykárosító gombák ellen. Munkám során az *Armillaria* fajok antagonizálására potenciálisan alkalmas *Trichoderma* törzsek szűrésére, jellemzésére és szelektálására irányuló nagyszabású erőfeszítések az *Armillaria* fertőzések elleni közvetlen szabadföldi alkalmazásokra új, környezetbarát törzseket eredményeztek. Fentiekén túl táplémezeken kettős konfrontációs teszteket hajtottunk végre egy haploid *A. ostoyae* izolátum és egy kiválasztott *T. atroviride* törzs között, majd kettős RNS-Seq-alapú génexpressziós profilozást alkalmaztunk az *Armillaria* és a mikoparazita *Trichoderma* törzs közötti kölcsönhatásértékelésére.

Kezdeti terepmunkám során *Armillaria* és *Trichoderma* izolátumokat gyűjtöttünk károsított magyarországi tölgy-, illetve egészséges ausztriai fenyőerdők talajmintáiból, majd az izolátumokat fajszinten azonosítottuk. Még az ausztriai fenyvesben az *A. cepistipes* és *A. ostoyae* fajokat detektáltuk, addig a hazai tölgyállományban az *A. mellea* és az *A. gallica* klónok domináltak. A mintákból összesen 64 *Trichoderma* törzset is izoláltunk, melyek 14 fajt képviseltek. A két erdőterületen a *Trichoderma* közösségek eltérő összetételt mutattak.

Kettős tenyésztési tesztekkel *in vitro* antagonizmus-kísérleteket végeztünk a különböző *Trichoderma* törzsek patogén *Armillaria* izolátumok elleni védekezésre való potenciáljának meghatározására. Az *Armillaria* fajok ellen kiváló biokontroll jelöltként szelektált *Trichoderma* törzsek magas biokontroll index (BCI) értékeket mutattak. Az erősen *Armillaria*-fertőzött területekről izolált *Trichoderma* törzsek többsége az *Armillaria* fajok hatékony *in vitro* antagonistájaként bizonyult, így felhasználható lehet az *Armillaria* által okozott gyökérronthadás elleni biológiai védekezés céljaira. Másrészt viszont egyes *Trichoderma* fajok, illetve törzsek gyenge antagonist képességeket mutattak az *Armillaria* törzsekkel szemben, melyet alacsony BCI-értékeik tükröztek. A legtöbb gyenge antagonist képességekkel rendelkező izolátum az egészséges erdőterületekről származott.

A munka során összegyűjtött *Trichoderma* izolátumok jellemzése során megvizsgáltuk a törzsek cellulóz- és xilánbontó enzimrendszerekbe tartozó poliszacharidbontó enzimek,

valamint a foszfor mobilizációjában szerepet játszó savas foszfát termelésére való képességét. Az *Armillaria* elleni legjobb *in vitro* antagonista képességgel rendelkező fajok izolátumai ezen extracelluláris enzimek legrosszabb termelői közé tartoztak, és fordítva, ami arra utal, hogy ezeknek a *Trichoderma* fajoknak az *Armillaria* elleni fő antagonista mechanizmusa a hifák és rizomorfból mikoparazitizmusa lehet, nem pedig a poliszacharidokért folytatott kompetíció, vagy a gyökerek foszfor-hozzáféréseinek fokozása.

A sziderofórtermelés jellemzése és kimutatása szintén fontos paraméter a biokontroll-jelölt törzsek szűrése, illetve rizoszféra-kompetenciájuk megértésére szempontjából. Az erdei eredetű *Trichoderma* izolátumok közül 40 törzs volt képes indolecetsav (IAA) termelésére. A vizsgálatunkba vont *Trichoderma* izolátumok többsége sziderofórtermelő képességekkel is rendelkezett. Számos *Trichoderma* törzs az *Armillaria* fajokkal szembeni *in vitro* antagonista képessége mellett sziderofórokot és indol-3-ecetsavat is termelt.

A fakultatív nekrotrof *A. ostoyae* az *Armillaria* nemzetség egyik legpusztítóbb erdei kórokozója, mely világszerte gyökérotadási betegségeket okoz fászfűnvényeken. Jelenleg is folyik a hatékony védekezési intézkedések felmérése ezen földalatti kórokozó populációjának a korlátozása. A *T. atroviride* biokontroll tulajdonságai a faj genomjára, proteomjára és szekréciójára támaszkodva a műtrágyák és kémiai peszticidek környezetbarát alternatíváként komoly potenciált jelentenek a növénybetegségek elleni védekezés és az erdővédelem területén. A *T. atroviride* SZMC 24276 törzs (TA) jó antagonista képességgel rendelkezett a haploid *A. ostoyae* SZMC 23093 törzsszel (AO) szemben. A kettős tenyésztési vizsgálat eredményei alapján az haploid *A. ostoyae* SZMC 23093 törzs nagyfokú érzékenységet mutat a *T. atroviride* SZMC 24276 micéliuma általi invázióval szemben.

Az AO és a TA molekuláris kölcsönhatásainak vizsgálata céljából az *in vitro* kettős tenyésztésből kapott transzkriptomokat nagy teljesítményű, következő generációs szekvenálási technológia alkalmazásával elemeztük. A kórokozó-antagonista PDA táptalajon zajló kölcsönhatása során különböző időpontokat rögzítettünk a transzkriptomelemzés céljaira. Megpróbáltuk feltárni a molekuláris kölcsönhatás dinamikáját, beleértve a micéliumok egymással történő érintkezése előtti metabolit-szintű kölcsönhatást, a mikoparazita kölcsönhatást (amikor a TA micélium fizikailag érintkezik az AO telepével), valamint a poszt-mikoparazita kölcsönhatást (amikor a TA már ráövekedett az AO telepének felszínére). Szándékunk volt továbbá transzkripciós szinten értelmezni az AO esetben a TA biokontroll inváziója által kiváltott védekező válaszokat, valamint a TA biokontroll aktivitását

alátámasztó, az AO-val, mint gazdaszervezettel zajló kölcsönhatás során fellépő transzkripciós válaszait is. Ezért idősor-elemzést és funkcionális annotációt végeztünk, vizsgáltuk a dúsított útvonalakat, és elemeztük a differenciálisan expresszált géneket, beleértve a TA biokontrollal kapcsolatos, valamint az AO védekezéssel kapcsolatos génjelöltjeit.

A biokontroll ágens és a kórokozó *in vitro* kettős tenyészetben kivitelezett konfrontációs kísérletének transzkriptomelemzése hasznos megközelítésnek bizonyult a gombák kölcsönhatásának komplex molekuláris dinamikai modellezésére. Tudomásunk szerint ez az első transzkriptom-elemzési tanulmány biokontroll gomba által megtámadott *A. ostoyae* esetében, mely betekintést nyújthat a növényi kórokozó-biokontroll ágens kölcsönhatás mechanizmusába. Az eredmények alapján a TA számos biokontroll stratégiát alkalmazott az AO-val szembeni konfrontáció során, az AO esetében pedig számos védekezési mechanizmus indult be a gombatámadás okozta súlyos negatív hatások elleni védekezés érdekében.

A táptalaj környezetben az egymással konfrontált fajok metabolitjai és más szekrétumai hatására bekövetkezett változások, valamint a fizikai micéliuminvázió okozta kihívások befolyásolják a gombák transzkriptom-mintázatát. A TA számos biokontroll mechanizmusa már a fizikai érintkezés előtt aktiválódott. Ezek közé tartozik a hidrolitikus enzimek és az antibiotikus hatású másodlagos metabolitok termelése. Másrészt a TA korai, a micéliumok érintkezése előtt az AO kórokozóra gyakorolt transzkripciós hatása számos védekezési reakciót, például a kinolinsav (QA) termelését indukálta. Az érintkezés után további védekezési stratégiák indukálódtak, például megemelkedett a detoxifikációban feltételezhetően szerepet játszó peptidázok expressziója. Az AO-ban ennek ellenére azonban jelentős növekedésgátlás következett be az irányába növekedő TA hatására.

Összességében a gombák kölcsönhatásának transzkriptomikai vizsgálata alapján a védekező gének differenciális expressziója lehetővé teszi az AO számára a biokontroll ágens által kibocsátott metabolitok vagy extracelluláris enzimek érzékelését, illetve a TA inváziója elleni védekezés megkezdését. Másrészt a TA-nak a gazdaszervezet (AO) által indukált transzkriptomikai átprogramozása az AO, mint gazda/zsákmány antagonizálása szempontjából jelentős biokontroll potenciállal rendelkező, mikoparazitizmussal kapcsolatos gének differenciális expressziójához vezet.

Két kiválasztott *Trichoderma* törzs alkalmazásával szabadföldi kísérletet végeztünk két éves európai tölgyfalánokon, melyek egy, számos *Armillaria* telep rizomorfái által erősen fertőzött erdőterületre kerültek kiültetésre. A *T. virens* és *T. atrobrunneum* törzsekkel kezelt

tőgypalánták a kezeletlen kontrollokhoz képest jobb túlélést mutattak az *Armillaria* által erősen fertőzött talajban. Összefoglalva, az *Armillaria* rizomorfa törzseket kiválasztott natív *Trichoderma* törzsek, melyek növénynövekedést elősegítő tulajdonságokkal is rendelkezhetnek, az *Armillaria* fajok potenciális antagonistáinak bizonyultak, ami kihasználható lehet az *Armillaria* gyökérotadás elleni biológiai védekezésben.

(Fordította: Dr. Kredics László)

FINANCIAL SUPPORT

This research was funded by the Hungarian Government and the European Union within the frames of the Széchenyi 2020 Programme (GINOP-2.3.2-15-2016-00052). I thank for the grant from the Chinese CSC Scholarship Program, the Stipendium Hungaricum Scholarship Programme as well as the the Stipendium Hungaricum Dissertation Scholarship Programme.

ACKNOWLEDGEMENT

It is impossible to accomplish all of my work without support, guidance and collaboration from all kind of people, including my supervisors, my colleagues, collaborators, my friends, my families, etc. I would like to extend my deep appreciation and gratitude to Prof. Dr. Csaba Vágvölgyi, Dr. László Kredics, Dr. György Sipos, Dr. Martin Münsterkötter, Dr. Attila Szűcs, Simang Champramary, Dr. Gábor Nagy, Bettina Bóka, Orsolya Kedves, Viktor Dávid Nagy, Dr. Sándor Kocsubé Bernadett Pap, Dr. Gergely Maróti, Róbert Roszik, Dr. Zoltán Patocskai, Boris Indic, Dr. Lóránt Hatvani, Mónika Vörös, Dr. Tamás Marik, Dr. Chetna Tyagi, Rita Büchner, Henrietta Allaga, Dr. Aruna Vigneshwari, Adiyadolgor Turbat, Thu Huynh, Anuar Zhumakaev, etc.

I am so eager to express my sincere gratitude towards my supervisor Prof. Dr. Csaba Vágvölgyi, Head of the Department of Microbiology, Faculty of Science and Informatics, University of Szeged (Hungary). Prof. Dr. Csaba Vágvölgyi gave me the opportunity to work in an outstanding scientific environment in Szeged. I was so grateful and thankful to join this department as I had the chance to have conversations and interactions, through seminars or courses, with such a diverse group of outstanding scientific workers. He also facilitated a plenty of joint projects and lab visits. Our department formed a community of enthusiastic and industrious people, who provided assistances and suggestions during the entire time of my doctoral study, which I appreciated, and I am sure, it will remain a very important and special part of my life during my later scientific career. I am so thankful for all of these!

I would like to express my feeling of extreme thankfulness towards my PhD supervisor Dr. László Kredics for his broad knowledge, excellent guidance and constant support. I was also inspired by his kind and friendly personality. He helped me to become a person pursuing a lot positive characters such as independence, motivation and encouragement. His excellent scientific ideas and opinions benefit my research throughout the entire course of my doctoral study. I am so thankful to him for providing me such a good opportunity to work with many exceptional seniors and colleagues, for guiding me throughout the long journey of the interesting and meaningful project of biocontrol of *Armillaria* root rot disease, for giving me direction and freedom to express my own ideas and pursue critical thinking, for his timely response and help when I had difficulties during conducting experiments.

I am extremely thankful to Dr. György Sipos (University of Sopron), for his excellent suggestions and guidances to conduct experiments at each step so that I avoided a lot of mistakes and also saved me a lot of time and made each step of the experiments successfully. I always try to learn from him for his scientific inspiration and great insight toward the

Armillaria biocontrol research project. His willingness and patience during a large number of online discussions about the principle of research experiments will be remembered with strong and sincere gratitude. I relied on the enthusiasm and help of Dr. György Sipos – although we only met several times in person – a large number of emails we exchanged and the relevant technical expertise he provided brought success to our *Armillaria* biocontrol project. I am so thankful for all the help!

I am also thankful to Attila Szűcs from our department and Dr. Martin Münsterkötter, Simang Champramary (University of Sopron) for their support, suggestions and help. It is impossible to complete this work project without those great and motivated people who have plenty of complementary expertise and knowledge on bioinformatics. Therefore, I am so glad to have this opportunity to express my deep thankfulness to them for their inspiration and friendly nature and for spending a lot of time in helping me. They gave me tremendous help so that I can successfully complete my dissertation.

I am very happy to join in the Department of Microbiology where I started my doctoral research. It was a good opportunity to work with some hard working and exceptional seniors like Bettina Bóka, Dr. Lóránt Hatvani, Mónika Vörös, Tamás Marik, Chetna Tyagi, Aruna Vigneshwari, etc. Specially, Bettina Bóka taught me a lot since the first day I came, such as some basic experimental skills and the usage of every instrument and equipment in the lab, but what impressed me most was her stringent and careful attitude toward work. I am specifically thankful to Bettina Bóka for giving me a lot of practical help and always being available during working hours to give advises or discussions on solving labwork issues. I am also very thankful to other colleagues, such as Orsolya Kedves, Viktor Dávid Nagy, Adiyadolgor Turbat, Thu Huynh, Anuar Zhumakaev, Rita Büchner, Henrietta Allaga, etc. for providing tremendous support, help and creating a delightful and comfortable atmosphere and environment in the lab. Thanks to the help of all departmental colleagues, it was possible to progress the lab works rapidly with several different tasks in parallel; their self-forgetful help and support as well as their strong sense of responsibility during the lab's administration were fundamental to provide all 'ingredients' on time and get everything in the lab up-and-running.

I am truly thankful for the help of Bernadett Pap and Gergely Maróti from Hungarian Academy of Sciences, Biological Research Centre, Institute of Plant Biology, Szeged. Thanks Bernadett Pap for her large amount of practical help and Gergely Maróti for his multidisciplinary in bioinformatics that allowed our experiments to process efficiently and our collaboration with Gergely Maróti helped our project to develop. Bernadett Pap's constant motivation and innovations always provided solutions and always facilitated me to follow the

latest scientific information, such as methods and developments of Illumina technology. It was really a pleasure to work together.

I am so grateful for the help of Eszter Tóth, Csilla Szebenyi, Mónika Vörös, Ottó Bencsik (University of Szeged), and Jenő Fliszár (Bakonyerdő Ltd.) in the realization of the field experiment, the expert suggestions of László Szalay (University of Sopron) regarding the statistical evaluation of the results deriving from the field experiment.

I feel I am so lucky to be surrounded by so many friends from different nationalities. They helped me to get used to the unfamiliar but always friendly environment in the first year. I am so grateful for entertainment, the emotional support, the learning and the growth that my friends gave me. Having friends of different ethnic cultures and backgrounds never happened to me when I was in my own country. It was a precious experience and memory which gave me acceptance and promotion of the difference within religious and racial backgrounds and cultures, and also benefited me in many other ways.

I would like to thank my lovely families and friends in China for their understanding, encouragement, support and help throughout my PhD studies in Hungary.

I want to thank for the grant from the Chinese CSC Scholarship Program and Hungary Stipendium Hungaricum Tempus Public Foundation.

I will end by acknowledging for the constructive suggestions and comments for my thesis reviewers and committee.

LIST OF REFERENCES

- Adaskaveg, J.E., Forster, H., Wade, L., Thompson, D.F., Connell, J.H., 1999. Efficacy of sodium tetrathiocarbonate and propiconazole in managing *Armillaria* root rot of almond on peach rootstock. *Plant Disease* 83, 240-246.
- Aguín, O., Mansilla, J.P., Sainz, M.J., 2006. *In vitro* selection of an effective fungicide against *Armillaria mellea* and control of white root rot of grapevine in the field. *Pest Management Science* 62, 223-228.
- Aguín, O., Sainz, M.J., Pedro Mansilla, J., 2004. *Armillaria* species infesting vineyards in northwestern Spain. *European Journal of Plant Pathology* 110, 683-687.
- Amin, F., Razdan, V., Mohidin, F., Bhat, K., Sheikh, P., 2010. Effect of volatile metabolites of *Trichoderma* species against seven fungal plant pathogens *in-vitro*. *Journal of Phytological Research* 2, 34-37.
- Amiri, A., Bussey, K.E., Riley, M.B., Schnabel, G., 2008. Propiconazole inhibits *Armillaria tabescens* *in vitro* and translocates into peach roots following trunk infusion. *Plant Disease* 92, 1293-1298.
- Andrews S, F.K., A. Segonds-Pichon, L Biggins, C Krueger, S. Wingett, 2010. FASTQC. A quality control tool for high throughput sequence data. <https://www.bioinformatics.babraham.ac.uk/projects/fastqc/>.
- Anke, H., Kinn, J., Bergquist, K.-E., Sterner, O., 1991. Production of siderophores by strains of the genus *Trichoderma*. *Biology of Metals* 4, 176-180.
- Appel, D.N., Kurdyla, T., 1992. Intravascular injection with propiconazole in live oak for oak wilt control. *Plant Disease* 76, 1120-1124.
- Aramaki, T., Blanc-Mathieu, R., Endo, H., Ohkubo, K., Kanehisa, M., Goto, S., Ogata, H., 2020. KofamKOALA: KEGG Ortholog assignment based on profile HMM and adaptive score threshold. *Bioinformatics* 36, 2251-2252.
- Arhipova, N., Gaitnieks, T., Donis, J., Stenlid, J., Vasaitis, R., 2012. Heart-rot and associated fungi in *Alnus glutinosa* stands in Latvia. *Scandinavian Journal of Forest Research* 27, 327-336.
- Aro, N., Ilmá, M., Saloheimo, A., Penttilä M., 2003. ACEI of *Trichoderma reesei* is a repressor of cellulase and xylanase expression. *Applied and Environmental Microbiology* 69, 56-65.
- Aro, N., Saloheimo, A., Ilmá, M., Penttilä M., 2001. ACEII, a novel transcriptional activator involved in regulation of cellulase and xylanase genes of *Trichoderma reesei*. *Journal of Biological Chemistry* 276, 24309-24314.
- Asef, M.R., Goltapeh, E.M., Danesh, Y.R., 2008. Antagonistic effects of *Trichoderma* species in biocontrol of *Armillaria mellea* in fruit trees in Iran. *Journal of Plant Protection Research* 48, 213-222.
- Atanasova, L., Crom, S.L., Gruber, S., Couplier, F., Seidl-Seiboth, V., Kubicek, C.P., Druzhinina, I.S., 2013. Comparative transcriptomics reveals different strategies of *Trichoderma* mycoparasitism. *BMC Genomics* 14, 121.
- Baumgartner, K., 2004. Root collar excavation for postinfection control of *Armillaria* root disease of grapevine. *Plant Disease* 88, 1235-1240.
- Baumgartner, K., Coetzee, M.P., Hoffmeister, D., 2011. Secrets of the subterranean pathosystem of *Armillaria*. *Molecular Plant Pathology* 12, 515-534.

- Baumgartner, K., Rizzo, D., 2001a. Distribution of *Armillaria* species in California. *Mycologia* 93, 821-830.
- Baumgartner, K., Rizzo, D.M., 2001b. Ecology of *Armillaria* spp. in mixed-hardwood forests of California. *Plant Disease* 85, 947-951.
- Baumgartner, K., Rizzo, D.M., 2002. Spread of *Armillaria* root disease in a California vineyard. *American Journal of Enology and Viticulture* 53, 197.
- Baumgartner, K., Rizzo, D.M., 2006. Relative resistance of grapevine rootstocks to *Armillaria* root disease. *American Journal of Enology and Viticulture* 57, 408.
- Bendel, M., Kienast, F., Bugmann, H., Rigling, D., 2006. Incidence and distribution of *Heterobasidion* and *Armillaria* and their influence on canopy gap formation in unmanaged mountain pine forests in the Swiss Alps. *European Journal of Plant Pathology* 116, 85.
- Bendel, M., Rigling, D., 2008. Signs and symptoms associated with *Heterobasidion annosum* and *Armillaria ostoyae* infection in dead and dying mountain pine (*Pinus mugo* ssp. *uncinata*). *Forest Pathology* 38, 61-72.
- Benoit, I., van den Esker, M.H., Patyshakuliyeva, A., Mattern, D.J., Blei, F., Zhou, M., Dijksterhuis, J., Brakhage, A.A., Kuipers, O.P., de Vries, R.P., Kovács Á, T., 2015. *Bacillus subtilis* attachment to *Aspergillus niger* hyphae results in mutually altered metabolism. *Environmental Microbiology* 17, 2099-2113.
- Błaszczuk, L., Basińska-Barczak, A., Ćwiek-Kupczyńska, H., Gromadzka, K., Popiel, D., Stępień, Ł., 2017. Suppressive effect of *Trichoderma* spp. on toxigenic *Fusarium* species. *Polish Journal of Microbiology* 66, 85-100.
- Błaszczuk, L., Strakowska, J., Chelkowski, J., Gabka-Buszek, A., Kaczmarek, J., 2016. *Trichoderma* species occurring on wood with decay symptoms in mountain forests in Central Europe: genetic and enzymatic characterization. *Journal of Applied Genetics* 57, 397-407.
- Bolger, A.M., Lohse, M., Usadel, B., 2014. Trimmomatic: a flexible trimmer for Illumina sequence data. *Bioinformatics* 30, 2114-2120.
- Bononi, L., Chiamonte, J.B., Pansa, C.C., Moitinho, M.A., Melo, I.S., 2020. Phosphorus-solubilizing *Trichoderma* spp. from Amazon soils improve soybean plant growth. *Scientific Reports* 10, 2858.
- Braun, H., Woitsch, L., Hetzer, B., Geisen, R., Zange, B., Schmidt-Heydt, M., 2018. *Trichoderma harzianum*: Inhibition of mycotoxin producing fungi and toxin biosynthesis. *International Journal of Food Microbiology* 280, 10-16.
- Braze, N.J., Wick, R.L., Wargo, P.M., 2011. Effects of hydrolyzable tannins on *in vitro* growth of *Armillaria calvescens* and *A. gallica*. *Plant Disease* 95, 1255-1262.
- Bruhn, J.N., Wetteroff JR, J.J., Mihail, J.D., Kabrick, J.M., Pickens, J.B., 2008. Distribution of *Armillaria* species in upland Ozark Mountain forests with respect to site, overstory species composition and oak decline. *Forest Pathology* 30, 43-60.
- Cairney, J.W.G., Jennings, D.H., Ratcliffe, R.G., Southon, T.E., 1988. The physiology of basidiomycete linear organs II. Phosphate uptake by rhizomorphs of *Armillaria mellea*. *New Phytologist* 109, 327-333.
- Cao, W., Yan, L., Li, M., Liu, X., Xu, Y., Xie, Z., Liu, H., 2020. Identification and engineering a C4-dicarboxylate transporter for improvement of malic acid production in *Aspergillus niger*. *Applied Microbiology and Biotechnology* 104, 9773-9783.

- Cao, Y., Zheng, F., Wang, L., Zhao, G., Chen, G., Zhang, W., Liu, W., 2017. Rce1, a novel transcriptional repressor, regulates cellulase gene expression by antagonizing the transactivator Xyr1 in *Trichoderma reesei*. *Molecular Microbiology* 105, 65-83.
- Cha, J.Y., Igarashi, T., 1996. Biological species of *Armillaria* and their mycoparasitic associations with *Rhodophyllus abortivus* in Hokkaido. *Mycoscience* 37, 25.
- Chagas, L.F.B., De Castro, H.G., Colonia, B.S.O., De Carvalho Filho, M.R., Miller, L.D.O., Chagas, A.F.J., 2016. Efficiency of *Trichoderma* spp. as a growth promoter of cowpea (*Vigna unguiculata*) and analysis of phosphate solubilization and indole acetic acid synthesis. *Brazilian Journal of Botany* 39, 437-445.
- Chandelier, A., Gerarts, F., San Martin, G., Herman, M., Delahaye, L., 2016. Temporal evolution of collar lesions associated with ash dieback and the occurrence of *Armillaria* in Belgian forests. *Forest Pathology* 46, 289-297.
- Chapman, B., Xiao, G., 2000. Inoculation of stumps with *Hypholoma fasciculare* as a possible means to control *Armillaria* root disease. *Canadian Journal of Botany* 78, 129-134.
- Chapman, W., Schellenberg, B., Newsome, T., 2011. Assessment of *Armillaria* root disease infection in stands in south-central British Columbia with varying levels of overstory retention, with and without pushover logging. *Canadian Journal of Forest Research* 41, 1598-1605.
- Chaverri, P., Branco-Rocha, F., Jaklitsch, W., Gazis, R., Degenkolb, T., Samuels, G.J., 2015. Systematics of the *Trichoderma harzianum* species complex and the re-identification of commercial biocontrol strains. *Mycologia* 107, 558-590.
- Chen, L., Bóka, B., Kedves, O., Nagy, V., Champramary, S., Roszik, R., Patocskai, Z., Münsterkötter, M., Huynh, T., Indic, B., Vágvölgyi, C., Sipos, G., Kredics, L., 2019. Towards the biological control of devastating forest pathogens from the genus *Armillaria*. *Forests* 10, 1013.
- Chen, L., Shahab, D., Kedves, O., Champramary, S., Indic, B., Nagy, V.D., Vágvölgyi, C., Kredics L., Sipos G. Armillarioid root rot invasion: possibilities of silvicultural and chemical control. 9th Hardwood Proceedings: Part II pp. 90-97, 8 p. (2021)
- Chen, Y., Zhou, Y.D., Laborda, P., Wang, H.L., Wang, R., Chen, X., Liu, F.Q., Yang, D.J., Wang, S.Y., Shi, X.C., Laborda, P., 2021. Mode of action and efficacy of quinolinic acid for the control of *Ceratocystis fimbriata* on sweet potato Pest Management Science <https://doi.org/10.1002/ps.6495>.
- Chou, H., Xiao, Y.-T., Tsai, J.-N., Li, T.-T., Wu, H.-Y., Liu, L.-y.D., Tzeng, D.-S., Chung, C.-L., 2019. *In vitro* and in planta evaluation of *Trichoderma asperellum* TA as a biocontrol agent against *Phellinus noxius*, the cause of brown root rot disease of trees. *Plant Disease* 103, 2733-2741.
- Cleary, M., Burņeviča, N., Morrison, D., Thomsen, I., Sturrock, R., Vasaitis, R., Gaitnieks, T., Stenlid, J., 2013. Stump removal to control root disease in Canada and Scandinavia: A synthesis of results from long-term trials. *Forest Ecology and Management* 290, 5-14.
- Cleary, M., van der Kamp, B., Morrison, D., 2012a. Effects of wounding and fungal infection with *Armillaria ostoyae* in three conifer species. I. Host response to abiotic wounding in non-infected roots. *Forest Pathology* 42, 100-108.
- Cleary, M.R., van der Kamp, B.J., Morrison, D.J., 2012b. Pathogenicity and virulence of *Armillaria sinapina* and host response to infection in Douglas-fir, western hemlock and western redcedar in the southern interior of British Columbia. *Forest Pathology* 42, 481-491.

- Coetzee, M., Wingfield, B., Harrington, T., Steimel, J., Coutinho, T., Wingfield, M., 2001. The root fungus *Armillaria mellea* introduced into South Africa by early Dutch settlers. *Molecular Ecology* 10, 387-396.
- Collins, C., Keane, T.M., Turner, D.J., O'Keeffe, G., Fitzpatrick, D.A., Doyle, S., 2013. Genomic and proteomic dissection of the ubiquitous plant pathogen, *Armillaria mellea*: toward a new infection model system. *Journal of Proteome Research* 12, 2552-2570.
- Contreras-Cornejo, H.A., Macías-Rodríguez, L., Alfaro-Cuevas, R., López-Bucio, J., 2014. *Trichoderma* spp. improve growth of *Arabidopsis* seedlings under salt stress through enhanced root development, osmolite production, and Na⁺ elimination through root exudates. *Molecular Plant-Microbe Interactions* 27, 503-514.
- Cruikshank, M.G., Filipescu, C.N., 2012. Allometries of coarse tree, stem, and crown measures in Douglas-fir are altered by *Armillaria* root disease. *Botany* 90, 711-721.
- Cruz-Magalhães, V., Nieto-Jacobo, M.F., van Zijll de Jong, E., Rostás, M., Padilla-Arizmendi, F., Kandula, D., Kandula, J., Hampton, J., Herrera-Estrella, A., Steyaert, J.M., Stewart, A., Loguercio, L.L., Mendoza-Mendoza, A., 2019. The NADPH oxidases Nox1 and Nox2 differentially regulate volatile organic compounds, fungistatic activity, plant growth promotion and nutrient assimilation in *Trichoderma atroviride*. *Frontiers in Microbiology* 9, 3271.
- De Jaeger, N., de la Providencia, I.E., de Boulois, H.D., Declerck, S., 2011. *Trichoderma harzianum* might impact phosphorus transport by arbuscular mycorrhizal fungi. *FEMS Microbiology Ecology* 77, 558-567.
- Dean, J.F., Anderson, J.D., 1991. Ethylene biosynthesis-inducing xylanase : II. Purification and physical characterization of the enzyme produced by *Trichoderma viride*. *Plant Physiology* 95, 316-323.
- DeLong, R., Lewis, K., Simard, S., Gibson, S., 2011. Fluorescent pseudomonad population sizes baited from soils under pure birch, pure Douglas-fir, and mixed forest stands and their antagonism toward *Armillaria ostoyae* *in vitro*. *Canadian Journal of Forest Research* 32, 2146-2159.
- Ding, Y., Gardiner, D.M., Kazan, K., 2020. Transcriptome analysis reveals infection strategies employed by *Fusarium graminearum* as a root pathogen. *bioRxiv*, 2020.2005.2017.092288.
- Dodd, S.L., Lieckfeldt, E., Samuels, G.J., 2003. *Hypocrea atroviridis* sp. nov., the teleomorph of *Trichoderma atroviride*. *Mycologia* 95, 27-40.
- Downer, J., Faber, B., 2019. Non-chemical control of *Armillaria mellea* infection of *Prunus persica*. *Journal of Plant Science and Phytopathology* 3, 50-55.
- Druzhinina, I., Kopchinskiy, A., Komoń, M., Szakacs, G., Kubicek, C., 2005. An oligonucleotide barcode for species identification in *Trichoderma* and *Hypocrea*. *Fungal Genetis & Biology* 42, 813-828.
- Druzhinina, I.S., Kubicek, C.P., Komoń-Zelazowska, M., Mulaw, T.B., Bissett, J., 2010. The *Trichoderma harzianum* demon: complex speciation history resulting in coexistence of hypothetical biological species, recent agamospecies and numerous relict lineages. *BMC Evolutionary Biology* 10, 94.
- Dumas, M.T., 1992. Inhibition of *Armillaria* by bacteria isolated from soils of the boreal mixedwood forest of Ontario. *European Journal of Forest Pathology* 22, 11-18.
- Dutech, C., Labbe, F., Capdevielle, X., Lung-Escarmant, B., 2017. Genetic analysis reveals efficient sexual spore dispersal at a fine spatial scale in *Armillaria ostoyae*, the causal agent of root-rot disease in conifers. *Fungal Biology* 121, 550-560.

- El-Kadi, S., 2015. Effect of some organic acids on some fungal growth and their toxins production. *International Journal of Advances in Biology* 2, 1-11.
- Enroth, C., Neujahr, H., Schneider, G., Lindqvist, Y., 1998. The crystal structure of phenol hydroxylase in complex with FAD and phenol provides evidence for a concerted conformational change in the enzyme and its cofactor during catalysis. *Structure* 6, 605-617.
- Fanelli, F., Liuzzi, V.C., Logrieco, A.F., Altomare, C., 2018. Genomic characterization of *Trichoderma atrobrunneum* (*T. harzianum* species complex) ITEM 908: Insight into the genetic endowment of a multi-target biocontrol strain. *BMC Genomics* 19, 662-662.
- Fang, C., Chen, X., 2018. Potential biocontrol efficacy of *Trichoderma atroviride* with cellulase expression regulator ace1 gene knock-out. *3 Biotech* 8, 302-302.
- Filip, G., Roth, L., 1977. Stump injections with soil fumigants to eradicate *Armillaria mellea* from young-growth ponderosa pine killed by root rot. *Canadian Journal of Forest Research* 7, 226-231.
- Flores, A., Chet, I., Herrera-Estrella, A., 1997. Improved biocontrol activity of *Trichoderma harzianum* by over-expression of the proteinase-encoding gene prb1. *Current Genetics* 31, 30-37.
- Ford, K.L., Henricot, B., Baumgartner, K., Bailey, A.M., Foster, G.D., 2017. A faster inoculation assay for *Armillaria* using herbaceous plants. *Journal of Horticultural Science and Biotechnology* 92, 39-47.
- Fradj, N., de Montigny, N., M é rindol, N., Awwad, F., Boumghar, Y., Germain, H., 2020. A first insight into North American plant pathogenic fungi *Armillaria sinapina* transcriptome. *Biology* 9, 153.
- Gajera, H.P., Hirpara, D.G., Katakpara, Z.A., Patel, S.V., Golakiya, B.A., 2016. Molecular evolution and phylogenetic analysis of biocontrol genes acquired from SCoT polymorphism of mycoparasitic *Trichoderma koningii* inhibiting phytopathogen *Rhizoctonia solani* Kuhn. *Infection, Genetics and Evolution* 45, 383-392.
- Gajera, H.P., Vakharia, D.N., 2012. Production of lytic enzymes by *Trichoderma* isolates during *in vitro* antagonism with *Aspergillus niger*, the causal agent of collar rot of peanut. *Brazilian Journal of Microbiology* 43, 43-52.
- Geraldine, A.M., Lopes, F.A.C., Carvalho, D.D.C., Barbosa, E.T., Rodrigues, A.R., Brand ão, R.S., Ulhoa, C.J., Lobo Junior, M., 2013. Cell wall-degrading enzymes and parasitism of sclerotia are key factors on field biocontrol of white mold by *Trichoderma* spp. *Biological Control* 67, 308-316.
- Gkarmiri, K., Finlay, R.D., Alstr ö m, S., Thomas, E., Cubeta, M.A., H ö gberg, N., 2015. Transcriptomic changes in the plant pathogenic fungus *Rhizoctonia solani* AG-3 in response to the antagonistic bacteria *Serratia proteamaculans* and *Serratia plymuthica*. *BMC Genomics* 16, 630.
- Gonzalez, E., Ortega, A., Salazar-Badillo, F., Bautista, E., Douterlungne, D., Jimenez, J., 2018. The *Arabidopsis-Trichoderma* interaction reveals that the fungal growth medium is an important factor in plant growth induction. *Scientific Reports* 8, 16427.
- Gordon, S.A., Weber, R.P., 1951. Colorimetric estimation of indoleacetic acid. *Plant Physiology* 26, 192-195.
- Guillaumin, J., Mohammed, C., Anselmi, N., Courtecuisse, R., Gregory, S., Holdenrieder, O., Intini, M., Lung, B., Marxm ü ller, H., Morrison, D., Rishbeth, J., Termorshuizen, A., Tirro, B., Van Dam, B., 1993. Geographical distribution and ecology of the *Armillaria* species in Western Europe. *European Journal of Forest Pathology* 23, 341.

- Guo, T., Wang, H.C., Xue, W.Q., Zhao, J., Yang, Z.L., 2016. Phylogenetic analyses of *Armillaria* reveal at least 15 phylogenetic lineages in China, seven of which are associated with cultivated *Gastrodia elata*. PLoS One 11, e0154794-e0154794.
- Guo, R., Wang, Z., Zhou, C., Liu, Z., Zhang, P., Fan, H., 2020. Transcriptomic analysis reveals biocontrol mechanisms of *Trichoderma harzianum* ACCC30371 under eight culture conditions. Journal of Forestry Research 31, 1863-1873.
- Gutter, W.D., Baumgartner, K., Browne, G.T., Eskalen, A., Latham, S.R., Petit, E., Bayramian, L.A., 2004. Root diseases of grapevines in California and their control. Australasian Plant Pathology 33, 157-165.
- Halifu, S., Deng, X., Song, X., Song, R., Liang, X., 2020. Inhibitory mechanism of *Trichoderma virens* ZT05 on *Rhizoctonia solani*. Plants 9, 912.
- Harman, G.E., Howell, C.R., Viterbo, A., Chet, I., Lorito, M., 2004. *Trichoderma* species — opportunistic, avirulent plant symbionts. Nature Reviews Microbiology 2, 43-56.
- Heinzelmann, R., Prospero, S., Rigling, D., 2017. Virulence and stump colonization ability of *Armillaria borealis* on Norway spruce seedlings in comparison to sympatric *Armillaria* species. Plant Disease 101, 470-479.
- Heinzelmann, R., Prospero, S., Rigling, D., 2018. Frequent diploidisation of haploid *Armillaria ostoyae* strains in an outdoor inoculation experiment. Fungal Biology 122, 147-155.
- Heinzelmann, R., Rigling, D., 2016. Mycelial fan formation of three sympatric *Armillaria* species on excised stem segments of *Picea abies*. Forest Pathology 46, 187-199.
- Hood, I., 2012. Fungi decaying fallen stems of rimu (*Dacrydium cupressinum*, Podocarpaceae) in southern Westland, New Zealand. New Zealand Journal of Botany 50, 59-69.
- Hood, I., Horner, I., Gardner, J., Sandberg, C., 2002. *Armillaria* root disease of *Pinus radiata* in New Zealand. 1: Basidiospore dispersal. New Zealand Journal of Forestry Science 32, 94-102.
- Hood, I., Oliva, J., Kimberley, M., Burņeviĉa, N., Bakys, R., 2015. *Armillaria novae-zelandiae* and other basidiomycete wood decay fungi in New Zealand *Pinus radiata* thinning stumps. Forest Pathology 45, 298-310.
- Hood, I., Petrini, L., Gardner, J., 2008. Colonisation of woody material in *Pinus radiata* plantations by *Armillaria novae-zelandiae* basidiospores. Australasian Plant Pathology 37, 347-352.
- Inbar, J., Chet, I., 1996. The role of lectins in recognition and adhesion of the mycoparasitic fungus *Trichoderma* spp. to its host. Advances in Experimental Medicine Biology 408, 229-231.
- Islam, R., Brown, S., Taheri, A., Dumenyo, C.K., 2019. The gene encoding NAD-dependent epimerase/dehydratase, wcaG, affects cell surface properties, virulence, and extracellular enzyme production in the soft rot phytopathogen, *Pectobacterium carotovorum*. Microorganisms 7, 172.
- Iturralde, E.T., Stocco, M.C., Faura, A., Monaco, C.I., Cordo, C., Perez-Gimenez, J., Lodeiro, A.R., 2020. Coinoculation of soybean plants with *Bradyrhizobium japonicum* and *Trichoderma harzianum*: Coexistence of both microbes and relief of nitrate inhibition of nodulation. Biotechnology Reports 26, e00461.
- Jacobs, K., Berg, L., 2000. Inhibition of fungal pathogens of woody plants by the plant growth regulator paclobutrazol. Pest Management Science 56, 407-412.

- Jaklitsch W.M., 2009. European species of *Hypocrea*. Part I. The green-spored species. *Studies in Mycology* 63, 1–91.
- Jaklitsch, W.M., 2011. European species of *Hypocrea* part II: species with hyaline ascospores. *Fungal Diversity* 48, 1-250.
- Jaklitsch, W.M., Voglmayr, H., 2015. Biodiversity of *Trichoderma* (*Hypocreaceae*) in southern Europe and Macaronesia. *Studies in Mycology* 80, 1-87.
- Jones, E.E., Rabeendran, N., Stewart, A., 2014a. Biocontrol of *Sclerotinia sclerotiorum* infection of cabbage by *Coniothyrium minitans* and *Trichoderma* spp. *Biocontrol Science and Technology* 24, 1363-1382.
- Jones, P., Binns, D., Chang, H.Y., Fraser, M., Li, W., McAnulla, C., McWilliam, H., Maslen, J., Mitchell, A., Nuka, G., Pesseat, S., Quinn, A.F., Sangrador-Vegas, A., Scheremetjew, M., Yong, S.Y., Lopez, R., Hunter, S., 2014b. InterProScan 5: genome-scale protein function classification. *Bioinformatics* 30, 1236-1240.
- Keča, N., Karadžić, D., Woodward, S., 2009. Ecology of *Armillaria* species in managed forests and plantations in Serbia. *Forest Pathology* 39, 217-231.
- Kedves, O., Shahab, D., Champramary, S., Chen, L., Indic, B., Bóka, B., Nagy, V.D., Vágvölgyi, C., Kredics, L., Sipos, G., 2021. Epidemiology, biotic interactions and biological control of Armillarioids in the Northern hemisphere. *Pathogens* 10, 76.
- Khan, R.A.A., Najeeb, S., Hussain, S., Xie, B., Li, Y., 2020. Bioactive secondary metabolites from *Trichoderma* spp. against phytopathogenic fungi. *Microorganisms* 8, 817.
- Kim, M.S., Hanna, J.W., Klopfenstein, N.B., 2010. First report of an *Armillaria* root disease pathogen, *Armillaria gallica*, associated with several new hosts in Hawaii. *Plant Disease* 94, 1503.
- Kimberley, M., Hood, I., Gardner, J., 2002. *Armillaria* root disease of *Pinus radiata* in New Zealand. 6: Growth loss. *New Zealand Journal of Forestry Science* 32, 148-162.
- King, A.D.J., Hocking, A.D., Pitt, J.I., 1979. Dichloran-rose bengal medium for enumeration and isolation of molds from foods. *Applied and Environmental Microbiology* 37, 959-964.
- Klein-Gebbinck, H., Blenis, P., Hiratsuka, Y., 1993. Fireweed (*Epilobium angustifolium*) as a possible inoculum reservoir for root-rotting *Armillaria* species. *Plant Pathology* 42, 132-136.
- Klopfenstein, N.B., Lundquist, J.E., Hanna, J.W., Kim, M.S., McDonald, G.I., 2009. First report of *Armillaria sinapina*, a cause of *Armillaria* root disease, associated with a variety of forest tree hosts on sites with diverse climates in Alaska. *Plant Disease* 93, 111.
- Knudsen, G.R., Dandurand, L.-M.C., 2014. Ecological complexity and the success of fungal biological control agents. *Advances in Agriculture* 2014, 542703.
- Kopchinskiy, A., Komon, M., Kubicek, C.P., Druzhinina, I.S., 2005. TrichoBLAST: a multilocus database for *Trichoderma* and *Hypocrea* identifications. *Mycological Research* 109, 658-660.
- Kostić, M., Smiljković, M., Petrović, J., Glamočlija, J., Barros, L., Ferreira, I.C.F.R., Ćirić, A., Soković, M., 2017. Chemical, nutritive composition and a wide range of bioactive properties of honey mushroom *Armillaria mellea* (Vahl: Fr.) Kummer. *Food & Function* 8, 3239-3249.
- Kubicek, C.P., Baker, S., Gamauf, C., Kenerley, C.M., Druzhinina, I.S., 2008. Purifying selection and birth-and-death evolution in the class II hydrophobin gene families of the ascomycete *Trichoderma/Hypocrea*. *BMC Evolutionary Biology* 8, 4.

- Kubicek, C.P., Herrera-Estrella, A., Seidl-Seiboth, V., Martinez, D.A., Druzhinina, I.S., Thon, M., Zeilinger, S., Casas-Flores, S., Horwitz, B.A., Mukherjee, P.K., Mukherjee, M., Kredics, L., Alcaraz, L.D., Aerts, A., Antal, Z., Atanasova, L., Cervantes-Badillo, M.G., Challacombe, J., Chertkov, O., McCluskey, K., Couplier, F., Deshpande, N., von Döhren, H., Ebbole, D.J., Esquivel-Naranjo, E.U., Fekete, E., Flipphi, M., Glaser, F., Gómez-Rodríguez, E.Y., Gruber, S., Han, C., Henrissat, B., Hermosa, R., Hernández-Oñate, M., Karaffa, L., Kosti, I., Le Crom, S., Lindquist, E., Lucas, S., Lübeck, M., Lübeck, P.S., Margeot, A., Metz, B., Misra, M., Nevalainen, H., Omann, M., Packer, N., Perrone, G., Uresti-Rivera, E.E., Salamov, A., Schmoll, M., Seiboth, B., Shapiro, H., Sukno, S., Tamayo-Ramos, J.A., Tisch, D., Wiest, A., Wilkinson, H.H., Zhang, M., Coutinho, P.M., Kenerley, C.M., Monte, E., Baker, S.E., Grigoriev, I.V., 2011. Comparative genome sequence analysis underscores mycoparasitism as the ancestral life style of *Trichoderma*. *Genome Biology* 12, R40.
- Kubicek, C.P., Steindorff, A.S., Chenthamara, K., Manganiello, G., Henrissat, B., Zhang, J., Cai, F., Kopchinskiy, A.G., Kubicek, E.M., Kuo, A., Baroncelli, R., Sarrocco, S., Noronha, E.F., Vannacci, G., Shen, Q., Grigoriev, I.V., Druzhinina, I.S., 2019. Evolution and comparative genomics of the most common *Trichoderma* species. *BMC Genomics* 20, 485.
- Kumar, K., Manigundan, K., Amaresan, N., 2017. Influence of salt tolerant *Trichoderma* spp. on growth of maize (*Zea mays*) under different salinity conditions. *Journal of Basic Microbiology* 57, 141-150.
- Labbé F., Marcais, B., Dupouey, J.-L., Bédouard, T., Capdevielle, X., Piou, D., Robin, C., Dutech, C., 2015. Pre-existing forests as sources of pathogens? The emergence of *Armillaria ostoyae* in a recently planted pine forest. *Forest Ecology and Management* 357, 248-258.
- Lawn, P.A., 2005. An assessment of the valuation methods used to calculate the index of sustainable economic welfare (ISEW), genuine progress indicator (GPI), and sustainable net benefit index (SNBI). *Environment, Development and Sustainability* 7, 185-208.
- Lee, C., Dey, D., Muzika, R.-M., 2016a. Oak stump-sprout vigor and *Armillaria* infection after clearcutting in southeastern Missouri, USA. *Forest Ecology and Management* 374, 211-219.
- Lee, S., Hung, R., Yap, M., Bennett, J., 2015. Age matters: the effects of volatile organic compounds emitted by *Trichoderma atroviride* on plant growth. *Archives of Microbiology* 197, 723-727.
- Lee, S., Yap, M., Behringer, G., Hung, R., Bennett, J.W., 2016b. Volatile organic compounds emitted by *Trichoderma* species mediate plant growth. *Fungal Biology and Biotechnology* 3, 7.
- Legrand, P., Ghahari, S., Guillaumin, J.J., 1996. Occurrence of genets of *Armillaria* spp. in four mountain forests in Central France: the colonization strategy of *Armillaria ostoyae*. *The New Phytologist* 133, 321-332.
- Lehner, S.M., Atanasova, L., Neumann, N.K., Krska, R., Lemmens, M., Druzhinina, I.S., Schuhmacher, R., 2013. Isotope-assisted screening for iron-containing metabolites reveals a high degree of diversity among known and unknown siderophores produced by *Trichoderma* spp. *Applied and Environmental Microbiology* 79, 18-31.
- Lehtijärvi, A., Doğmuş -Lehtijärvi, H.T., Aday, A.G., 2012. *Armillaria ostoyae* associated with dying 60-year-old Scots pines in northern Turkey. *Forest Pathology* 42, 267-269.
- Li, N., Alfiky, A., Wang, W., Islam, M., Nourollahi, K., Liu, X., Kang, S., 2018. Volatile compound-mediated recognition and inhibition between *Trichoderma* biocontrol agents and *Fusarium oxysporum*. *Frontiers in Microbiology* 9, 2614.
- Li, Y., Hood, I., 1992. A preliminary study into the biological control of *Armillaria novae-zelandiae* and *A. limonea*. *Australasian Plant Pathology* 21, 24-28.
- Li, M.F., Li, G.H., Zhang, K.Q., 2019. Non-volatile metabolites from *Trichoderma* spp. *Metabolites* 9.

- Lienemann, M., Boer, H., Paananen, A., Cottaz, S., Koivula, A., 2009. Toward understanding of carbohydrate binding and substrate specificity of a glycosyl hydrolase 18 family (GH-18) chitinase from *Trichoderma harzianum*. *Glycobiology* 19, 1116-1126.
- Livak, K.J., Schmittgen, T.D., 2001. Analysis of relative gene expression data using real-time quantitative PCR and the 2(-Delta Delta C(T)) Method. *Methods* 25, 402-408.
- Loc, N.H., Huy, N.D., Quang, H.T., Lan, T.T., Thu Ha, T.T., 2019. Characterisation and antifungal activity of extracellular chitinase from a biocontrol fungus, *Trichoderma asperellum* PQ34. *Mycology* 11, 38-48.
- Longa, C., Savazzini, F., Tosi, S., Elad, Y., Pertot, I., 2009. Evaluating the survival and environmental fate of the biocontrol agent *Trichoderma atroviride* SC1 in vineyards in northern Italy. *Journal of Applied Microbiology* 106, 1549-1557.
- López, A.C., Alvarenga, A.E., Zapata, P.D., Luna, M.F., Villalba, L.L., 2019. *Trichoderma* spp. from Misiones, Argentina: Effective fungi to promote plant growth of the regional crop *Ilex paraguariensis* St. Hil. *Mycology* 10, 210-221.
- Lu, Z., Tombolini, R., Woo, S., Zeilinger, S., Lorito, M., Jansson, J.K., 2004. In vivo study of *Trichoderma*-pathogen-plant interactions, using constitutive and inducible green fluorescent protein reporter systems. *Applied and Environmental Microbiology* 70, 3073.
- Luisi, N., Lerario, P., 1996. Observations on *Armillaria* occurrence in declining oak woods of southern Italy. *Annales des Sciences Forestières* 53, 389-394.
- Lundquist, J., 2000. A method of estimating direct and indirect effects of *Armillaria* root disease and other small-scale forest disturbances on canopy gap size. *Forest Science* 46, 356-362.
- Lundquist, J.E., 1993. Spatial and temporal characteristics of canopy gaps caused by *Armillaria* root disease and their management implications in lowveld forests of South Africa. *European Journal of Forest Pathology* 23, 362-371.
- Lung-Escarmant, B., Guyon, D., 2004. Temporal and spatial dynamics of primary and secondary infection by *Armillaria ostoyae* in a *Pinus pinaster* plantation. *Phytopathology* 94, 125-131.
- Lushaj, B., Woodward, S., Keca, N., Intini, M., 2010. Distribution, ecology and host range of *Armillaria* species in Albania. *Forest Pathology* 40, 485-499.
- Lygis, V., Vasiliauskas, R., Larsson, K.-H., Stenlid, J., 2005. Wood-inhabiting fungi in stems of *Fraxinus excelsior* in declining ash stands of northern Lithuania, with particular reference to *Armillaria cepistipes*. *Scandinavian Journal of Forest Research* 20, 337-346.
- Maere, S., Heymans, K., Kuiper, M., 2005. BiNGO: a Cytoscape plugin to assess overrepresentation of gene ontology categories in biological networks. *Bioinformatics* 21, 3448-3449.
- Mallett, K., Volney, W.J.A., 1998. The effect of *Armillaria* root disease on lodgepole pine tree growth. *Canadian Journal of Forest Research* 29, 252-259.
- Marçais, B., Bréda, N., 2006. Role of an opportunistic pathogen in the decline of stressed oak trees. *Journal of Ecology* 94, 1214-1223.
- Marçais, B., Caď, O., 2006. Spatial pattern of the density of *Armillaria* epiphytic rhizomorphs on tree collar in an oak stand. *Forest Pathology* 36, 32-40.

- Mart ínez-Medina, A., Rold án, A., Pascual, J., 2009. Performance of a *Trichoderma harzianum* bentonite-vermiculite formulation against *Fusarium wilt* in seedling nursery melon plants. HortScience 44, 2025-2027.
- Maruyama, J., Kitamoto, K., 2013. Expanding functional repertoires of fungal peroxisomes: contribution to growth and survival processes. Frontiers in Physiology 4, 177.
- Meena, M., Swapnil, P., Zehra, A., Dubey, M.K., Upadhyay, R.S., 2017. Antagonistic assessment of *Trichoderma* spp. by producing volatile and non-volatile compounds against different fungal pathogens. Archives of Phytopathology and Plant Protection 50, 629-648.
- Merico, D., Isserlin, R., Stueker, O., Emili, A., Bader, G.D., 2010. Enrichment map: a network-based method for gene-set enrichment visualization and interpretation. PLoS One 5, e13984.
- Mesanza, N., Iturrutxa, E., Patten, C.L., 2016. Native rhizobacteria as biocontrol agents of *Heterobasidion annosum* s.s. and *Armillaria mellea* infection of *Pinus radiata*. Biological Control 101, 8-16.
- Metaliaj, R., Sicoli, G., Luisi, N., 2006. Pathogenicity of *Armillaria* isolates inoculated on five *Quercus* species at different watering regimes. Phytopathologia Mediterranea 45, 3-9.
- Mihail, J.D., Bruhn, J.N., 2005. Foraging behaviour of *Armillaria* rhizomorph systems. Mycological Research 109, 1195-1207.
- Mihail, J., Bruhn, J., Leininger, T., 2002. The effects of moisture and oxygen availability on rhizomorph generation by *Armillaria tabescens* in comparison with *A. gallica* and *A. mellea*. Mycological Research 106, 697-704.
- Milagres, A.M., Machuca, A., Napoleao, D., 1999. Detection of siderophore production from several fungi and bacteria by a modification of chrome azurol S (CAS) agar plate assay. Journal of Microbiological Methods 37, 1-6.
- Missall, T.A., Cherry-Harris, J.F., Lodge, J.K., 2005. Two glutathione peroxidases in the fungal pathogen *Cryptococcus neoformans* are expressed in the presence of specific substrates. Microbiology 151, 2573-2581.
- Monfil, V.O., Casas-Flores, S., 2014. Chapter 32 - Molecular mechanisms of biocontrol in *Trichoderma* spp. and their applications in agriculture. In: Gupta, V.K., Schmoll, M., Herrera-Estrella, A., Upadhyay, R.S., Druzhinina, I., Tuohy, M.G. (Eds.), Biotechnology and Biology of *Trichoderma*. Elsevier, Amsterdam, pp. 429-453.
- Moraes Bazioli, J., Belinato, J.R., Costa, J.H., Akiyama, D.Y., Pontes, J.G.M., 2019. Biological control of citrus postharvest phytopathogens. Toxins 11, 460.
- Morrison, D., 2009. Epidemiology of *Armillaria* root disease in Douglas-fir plantations in the cedar-hemlock zone of the southern interior of British Columbia. Forest Pathology 41, 31-40.
- Morrison, D.J., 2004. Rhizomorph growth habit, saprophytic ability and virulence of 15 *Armillaria* species. Forest Pathology 34, 15-26.
- Morrison, D., Pellow, K., Nemeč, A., Norris, D., Semenov, P., 2001. Effects of selective cutting on the epidemiology of *Armillaria* root disease in the southern interior of British Columbia. Canadian Journal of Forest Research 31, 59-70.
- Mukherjee, P.K., Horwitz, B.A., Kenerley, C.M., 2012. Secondary metabolism in *Trichoderma*-a genomic perspective. Microbiology (Reading) 158, 35-45.

- Mukherjee, P.K., Hurley, J.F., Taylor, J.T., Puckhaber, L., Lehner, S., Druzhinina, I., Schumacher, R., Kenerley, C.M., 2018. Ferricrocin, the intracellular siderophore of *Trichoderma virens*, is involved in growth, conidiation, gliotoxin biosynthesis and induction of systemic resistance in maize. *Biochemical and Biophysical Research Communications* 505, 606-611.
- Munnecke, D.E., Kolbezen, M.J., Wilbur, W.D., Ohr, H.D., 1981. Interactions involved in controlling *Armillaria mellea* Plant Disease 65, 6.
- Nagamani, P., Someshwar, B., Mohan Kumar, B., Kumaran, V., 2017. Effect of volatile and non volatile compounds of *Trichoderma* spp. against soil borne diseases of chickpea. *International Journal of Current Microbiology and Applied Sciences* 6, 1486-1491.
- Nawrocka, J., Małolepsza, U., Szymczak, K., Szczech, M., 2018a. Involvement of metabolic components, volatile compounds, PR proteins, and mechanical strengthening in multilayer protection of cucumber plants against *Rhizoctonia solani* activated by *Trichoderma atroviride* TRS25. *Protoplasma* 255, 359-373.
- Nawrocka, J., Szczech, M., Małolepsza, U., 2018b. *Trichoderma atroviride* enhances phenolic synthesis and cucumber protection against *Rhizoctonia solani*. *Plant Protection Science* 54, 17-23.
- Nelson, E.E., Pearce, M.H., Malajczuk, N., 1995. Effects of *Trichoderma* spp. and ammonium sulphamate on establishment of *Armillaria luteobubalina* on stumps of *Eucalyptus diversicolor*. *Mycological Research* 99, 957-962.
- Newitt, J.T., Prudence, S.M.M., 2019. Biocontrol of cereal crop diseases using *Streptomyces*. *Pathogens* 8, 78.
- Nieto-Jacobo, M.F., Steyaert, J.M., Salazar-Badillo, F.B., Nguyen, D.V., Rostás, M., Braithwaite, M., De Souza, J.T., Jimenez-Bremont, J.F., Ohkura, M., Stewart, A., Mendoza-Mendoza, A., 2017. Environmental growth conditions of *Trichoderma* spp. affects indole acetic acid derivatives, volatile organic compounds, and plant growth promotion. *Frontiers in Plant Science* 8, 102-102.
- Niu, X., Thaochan, N., Hu, Q., 2020. Diversity of linear non-ribosomal peptide in biocontrol fungi. *Journal of Fungi* 6, 61.
- Ohashi, K., Kawai, S., Murata, K., 2013. Secretion of quinolinic acid, an intermediate in the kynurenine pathway, for utilization in NAD⁺ biosynthesis in the yeast *Saccharomyces cerevisiae*. *Eukaryotic Cell* 12, 648-653.
- Olanrewaju, O.S., Glick, B.R., Babalola, O.O., 2017. Mechanisms of action of plant growth promoting bacteria. *World Journal of Microbiology & Biotechnology* 33, 197.
- Oliva, J., Suz, L., Colinas, C., 2008. Ecology of *Armillaria* species on silver fir (*Abies alba*) in the Spanish Pyrenees. *Annals of Forest Science* 66, 603.
- Omdal, D., 1995. Variation in pathogenicity and virulence of isolates of *Armillaria ostoyae* on eight tree species. *Plant Disease* 79, 939.
- Onsando, J., Waudu, S.W., 1994. Interaction between *Trichoderma* species and *Armillaria* root rot fungus of tea in Kenya. *International Journal of Pest Management* 40, 69-74.
- Oskiera, M., Szczech, M., Bartoszewski, G., 2015. Molecular identification of *Trichoderma* strains collected to develop plant growth-promoting and biocontrol agents. *Journal of Horticultural Research* 23, 75-86.
- Otieno, W., Jeger, M.J., Termorshuizen, A.J., 2003a. Effect of infesting soil with *Trichoderma harzianum* and amendment with coffee pulp on survival of *Armillaria*. *Biological Control* 26, 293-301.

- Otieno, W., Termorshuizen, A., Jeger, M., Othieno, C.O., 2003b. Efficacy of soil solarization, *Trichoderma harzianum*, and coffee pulp amendment against *Armillaria* sp. *Crop Protection* 22, 325-331.
- Overton B.E., Stewart E.L., Geiser D.M., 2006. Systematics of *Hypocrea citrina* and related taxa. *Studies in Mycology* 56, 1–38.
- Pareek, M., Allaway, W.G., Ashford, A.E., 2006. *Armillaria luteobubalina* mycelium develops air pores that conduct oxygen to rhizomorph clusters. *Mycological Research* 110, 38-50.
- Pareek, M., Cole, L., Ashford, A.E., 2001. Variations in structure of aerial and submerged rhizomorphs of *Armillaria luteobubalina* indicate that they may be organs of absorption. *Mycological Research* 105, 1377-1387.
- Park, Y.-H., Chandra Mishra, R., Yoon, S., Kim, H., Park, C., Seo, S.-T., Bae, H., 2019. Endophytic *Trichoderma citrinoviride* isolated from mountain-cultivated ginseng (*Panax ginseng*) has great potential as a biocontrol agent against ginseng pathogens. *Journal of Ginseng Research* 43, 408-420.
- Patro, R., Duggal, G., Love, M.I., Irizarry, R.A., Kingsford, C., 2017. Salmon provides fast and bias-aware quantification of transcript expression. *Nature Methods* 14, 417-419.
- Pearce, M., Malajczuk, N., 1990. Inoculation of *Eucalyptus diversicolor* thinning stumps with wood decay fungi for control of *Armillaria luteobubalina*. *Mycological Research* 94, 32-37.
- Pearce, M., Nelson, E., Malajczuk, N., 1995. Effects of the cord-forming saprotrophs *Hypholoma australe* and *Phanerochaete filamentosa* and of ammonium sulphamate on establishment of *Armillaria luteobubalina* on stumps of *Eucalyptus diversicolor*. *Mycological Research* 99, 951-956.
- Pellegrini, A., Corneo, P.E., Camin, F., Ziller, L., Tosi, S., Pertot, I., 2012. Studying trophic interactions between a plant pathogen and two different antagonistic microorganisms using a ¹³C-labeled compound and isotope ratio mass spectrometry. *Rapid Communications in Mass Spectrometry* 26, 510-516.
- Pellegrini, A., Corneo, P.E., Camin, F., Ziller, L., Tosi, S., Pertot, I., 2013. Isotope ratio mass spectrometry identifies soil microbial biocontrol agents having trophic relations with the plant pathogen *Armillaria mellea*. *Applied Soil Ecology* 64, 142-151.
- Pellegrini, A., Prodorutti, D., Pertot, I., 2014. Use of bark mulch pre-inoculated with *Trichoderma atroviride* to control *Armillaria* root rot. *Crop Protection* 64, 104-109.
- Peraza-Reyes, L., Berteaux-Lecellier, V., 2013. Peroxisomes and sexual development in fungi. *Frontiers in Physiology* 4, 244-244.
- Perazzolli, M., Herrero, N., Sterck, L., Lenzi, L., Pellegrini, A., Puopolo, G., Van de Peer, Y., Pertot, I., 2016. Transcriptomic responses of a simplified soil microcosm to a plant pathogen and its biocontrol agent reveal a complex reaction to harsh habitat. *BMC Genomics* 17, 838.
- Percival, G.C., Smiley, E.T., Fox, R.T.V., 2011. Root collar excavation with *Trichoderma* inoculations as a potential management strategy for honey fungus (*Armillaria mellea*). *Arboricultural Journal* 33, 267-280.
- Persson, B., Kallberg, Y., Bray, J.E., Bruford, E., Dellaporta, S.L., Favia, A.D., Duarte, R.G., Jörnvall, H., Kavanagh, K.L., Kedishvili, N., Kisiela, M., Maser, E., Mindnich, R., Orchard, S., Penning, T.M., Thornton, J.M., Adamski, J., Oppermann, U., 2009. The SDR (short-chain dehydrogenase/reductase and related enzymes) nomenclature initiative. *Chemico-Biological Interactions* 178, 94-98.

- Pham, J., Stam, R., Heredia, V.M., Csukai, M., Huitema, E., 2018. An NMRA-like protein regulates gene expression in *Phytophthora capsici* to drive the infection cycle on tomato. *Molecular Plant-Microbe Interactions* 31, 665-677.
- Pittner, E., Marek, J., Bortuli, D., Santos, L., Knob, A., Cacilda, M.D.R.F., 2019. Defense responses of wheat plants (*Triticum aestivum* L.) against brown spot as a result of possible elicitors application. *Arquivos do Instituto Biol ógico* 86, 1-16.
- Prospero, S., Holdenrieder, O., Rigling, D., 2004. Comparison of the virulence of *Armillaria cepistipes* and *Armillaria ostoyae* on four Norway spruce provenances. *Forest Pathology* 34, 1-14.
- Prospero, S., Holdenrieder, O., Rigling, D., 2006. Rhizomorph production and stump colonization by co-occurring *Armillaria cepistipes* and *Armillaria ostoyae*: An experimental study. *Forest Pathology* 36, 21-31.
- Qualhato, T.F., Lopes, F.A.C., Steindorff, A.S., Brand ão, R.S., Jesuino, R.S.A., Ulhoa, C.J., 2013. Mycoparasitism studies of *Trichoderma* species against three phytopathogenic fungi: evaluation of antagonism and hydrolytic enzyme production. *Biotechnology Letters* 35, 1461-1468.
- Rawlings, N.D., Waller, M., Barrett, A.J., Bateman, A., 2014. MEROPS: the database of proteolytic enzymes, their substrates and inhibitors. *Nucleic Acids Research* 42, D503-509.
- Raybaudi-Massilia, R.M., Mosqueda-Melgar, J., Mart ín-Belloso, O., 2009. Antimicrobial activity of malic acid against *Listeria monocytogenes*, *Salmonella enteritidis* and *Escherichia coli* O157:H7 in apple, pear and melon juices. *Food Control* 20, 105-112.
- Raziq, F., Fox, R., 2005. Combinations of fungal antagonists for biological control of *Armillaria* root rot of strawberry plants. *Biological Agriculture & Horticulture* 23, 45 - 57.
- Raziq, F., Fox, R.T.V., 2004. The effect of carrier substrate, dose rate and time of application on biocontrol efficacy of fungal antagonists against *Armillaria* root rot of strawberry plants. *Biological Agriculture & Horticulture* 22, 157-172.
- Reaves, J., Shaw, C., Roth, L., 1993. Infection of Ponderosa pine trees by *Armillaria ostoyae*: residual inoculum versus contagion. *Northwest Science* 67, 156-162.
- Reaves, J.L., Shaw, C.G., Mayfield, J.E., 1990. The effects of *Trichoderma* spp. isolated from burned and non-burned forest soils on the growth and development of *Armillaria ostoyae* in culture. *Northwest Science* 64, 39-44.
- Redfern, D.B., 1973. Growth and behaviour of *Armillaria mellea* rhizomorphs in soil. *Transactions of the British Mycological Society* 61, 569-581.
- Rizzo, D., Blanchette, R., May, G., 1995. Distribution of *Armillaria ostoyae* genets in a *Pinus resinosa*-*Pinus banksiana* forest. *Canadian Journal of Botany* 73, 776-787.
- Rizzo, D.M., Slaughter, G.W., 2001. Root disease and canopy gaps in developed areas of Yosemite Valley, California. *Forest Ecology and Management* 146, 159-167.
- Robinson, R., Morrison, D., 2001. Lesion formation and host response to infection by *Armillaria ostoyae* in the roots of western larch and Douglas-fir. *Forest Pathology* 31, 371-385.
- Robinson, R., Smith, R., 2001. Fumigation of karri regrowth stumps with metham-sodium to control *Armillaria luteobubalina*. *Australian Forestry* 64, 209-215.
- Ross-Davis, A.L., Stewart, J.E., Hanna, J.W., Kim, M.S., Knaus, B.J., Cronn, R., Rai, H., Richardson, B.A., McDonald, G.I., Klopfenstein, N.B., 2013. Transcriptome of an *Armillaria* root disease pathogen

reveals candidate genes involved in host substrate utilization at the host–pathogen interface. *Forest Pathology* 43, 468-477.

Roth, L.F., Rolph, L., Cooley, S., 1980. Identifying infected Ponderosa pine stumps to reduce costs of controlling *Armillaria* root rot. *Journal of Forestry* 78, 145-151.

Ryder, L.S., Harris, B.D., Soanes, D.M., Kershaw, M.J., Talbot, N.J., Thornton, C.R., 2012. Saprotrophic competitiveness and biocontrol fitness of a genetically modified strain of the plant-growth-promoting fungus *Trichoderma hamatum* GD12. *Microbiology (Reading)* 158, 84-97.

Saier, M.H., Reddy, V.S., Moreno-Hagelsieb, G., Hendargo, K.J., Zhang, Y., Iddamsetty, V., Lam, K.J.K., Tian, N., Russum, S., Wang, J., Medrano-Soto, A., 2021. The transporter classification database (TCDB): 2021 update. *Nucleic Acids Research* 49, D461-d467.

Sarrocchio, S., Matarese, F., Baroncelli, R., Vannacci, G., Seidl-Seiboth, V., Kubicek, C.P., Vergara, M., 2017. The constitutive endopolygalacturonase TvPG2 regulates the induction of plant systemic resistance by *Trichoderma virens*. *Phytopathology* 107, 537-544.

Savazzini, F., Longa, C., Pertot, I., 2009. Impact of the biocontrol agent *Trichoderma atroviride* SC1 on soil microbial communities of a vineyard in northern Italy. *Soil Biology and Biochemistry* 41, 1457-1465.

Scarselletti, R., Faull, J.L., 1994. *In vitro* activity of 6-pentyl- α -pyrone, a metabolite of *Trichoderma harzianum*, in the inhibition of *Rhizoctonia solani* and *Fusarium oxysporum* f. sp. lycopersici. *Mycological Research* 98, 1207-1209.

Schmoll, M., Dattenböck, C., Carreras-Villaseñor, N., Mendoza-Mendoza, A., Tisch, D., Alemán, M.I., Baker, S.E., Brown, C., Cervantes-Badillo, M.G., Cetz-Chel, J., Cristobal-Mondragon, G.R., Delaye, L., Esquivel-Naranjo, E.U., Frischmann, A., Gallardo-Negrete, J.d.J., García-Esquivel, M., Gomez-Rodriguez, E.Y., Greenwood, D.R., Hernández-Oñate, M., Kruszewska, J.S., Lawry, R., Mora-Montes, H.M., Muñoz-Centeno, T., Nieto-Jacobo, M.F., Nogueira Lopez, G., Olmedo-Monfil, V., Osorio-Concepcion, M., Piłsyk, S., Pomraning, K.R., Rodriguez-Iglesias, A., Rosales-Saavedra, M.T., Sánchez-Arreguín, J.A., Seidl-Seiboth, V., Stewart, A., Uresti-Rivera, E.E., Wang, C.-L., Wang, T.-F., Zeilinger, S., Casas-Flores, S., Herrera-Estrella, A., 2016. The genomes of three uneven siblings: Footprints of the lifestyles of three *Trichoderma* species. *Microbiology and Molecular Biology Reviews* 80, 205-327.

Schnabel, G., Agudelo, P., Henderson, G.W., Rollins, P.A., 2012. Aboveground root collar excavation of peach trees for *Armillaria* root rot management. *Plant Disease* 96, 681-686.

Schnabel, G., Rollins, A.P., Henderson, G.W., 2011. Field evaluation of *Trichoderma* spp. for control of *Armillaria* root rot of peach. *Plant Health Progress* 12, 3.

Schwyn, B., Neilands, J.B., 1987. Universal chemical assay for the detection and determination of siderophores. *Analytical Biochemistry* 160, 47-56.

Segarra, G., Casanova, E., Avilés, M., Trillas, I., 2010. *Trichoderma asperellum* strain T34 controls *Fusarium* wilt disease in tomato plants in soilless culture through competition for iron. *Microbial Ecology* 59, 141-149.

Shannon, P., Markiel, A., Ozier, O., Baliga, N.S., Wang, J.T., Ramage, D., Amin, N., Schwikowski, B., Ideker, T., 2003. Cytoscape: a software environment for integrated models of biomolecular interaction networks. *Genome Research* 13, 2498-2504.

Sharma, V., Salwan, R., Sharma, P.N., 2003. Differential response of extracellular proteases of *Trichoderma harzianum* against fungal phytopathogens. *Current Microbiology* 73, 419-425.

- Sharon, A., Finkelstein, A., Shlezinger, N., Hatam, I., 2009. Fungal apoptosis: function, genes and gene function. *FEMS Microbiology Reviews* 33, 833-854.
- Shaw, C.G.I., 1980. Characteristics of *Armillaria mellea* on pine (*Pinus ponderosa*) root systems in expanding centers of root rot. *Northwest Science* 54, 137-145.
- Shaw, C.G.I., Roth, L.F., 1976. Persistence and distribution of a clone of *Armillaria mellea* in a ponderosa pine forest. *Phytopathology* 66, 1210-1213.
- Shaw, S., Le Cocq, K., Paszkiewicz, K., Moore, K., Winsbury, R., de Torres Zabala, M., Studholme, D.J., Salmon, D., Thornton, C.R., Grant, M.R., 2016. Transcriptional reprogramming underpins enhanced plant growth promotion by the biocontrol fungus *Trichoderma hamatum* GD12 during antagonistic interactions with *Sclerotinia sclerotiorum* in soil. *Molecular Plant Pathology* 17, 1425-1441.
- Shearer, B., Crane, C., Fairman, R., Grant, M., 1998. Susceptibility of plant species in coastal dune vegetation of south-western Australia to killing by *Armillaria luteobubalina*. *Australian Journal of Botany* 46, 321-334.
- Sicoli, G., Annese, V., Gioia, T., de Luisi, N., 2003. *Armillaria* pathogenicity tests on oaks in Southern Italy [Quercus - Apulia]. *Journal of Plant Pathology (Italy)* 84, 107-111.
- Sipos, G., Anderson, J.B., Nagy, L.G., 2018. *Armillaria*. *Current Biology* 28, 297-298.
- Sipos, G., Prasanna, A.N., Walter, M.C., O'Connor, E., Bálint, B., Krizsán, K., Kiss, B., Hess, J., Varga, T., Slot, J., Riley, R., Břka, B., Rigling, D., Barry, K., Lee, J., Mihaltcheva, S., LaButti, K., Lipzen, A., Waldron, R., Moloney, N.M., Sperisen, C., Kredics, L., Vágvölgyi, C., Patrignani, A., Fitzpatrick, D., Nagy, I., Doyle, S., Anderson, J.B., Grigoriev, I.V., Guldener, U., Münsterkötter, M., Nagy, L.G., 2017. Genome expansion and lineage-specific genetic innovations in the forest pathogenic fungi *Armillaria*. *Nature Ecology & Evolution* 1, 1931-1941.
- Skovsgaard, J.P., Thomsen, I., Skovsgaard, I., Martinussen, T., 2009. Associations among symptoms of dieback in even-aged stands of ash (*Fraxinus excelsior* L.). *Forest Pathology* 40, 7-18.
- Smith, M.L., Bruhn, J.N., Anderson, J.B., 1992. The fungus *Armillaria bulbosa* is among the largest and oldest living organisms. *Nature* 356, 428-431.
- Smith, M.L., Bruhn, J.N., Anderson, J.B., 1994. Relatedness and distribution of *Armillaria* genets infecting red pine seedlings. *Phytopathology* 84, 822-829.
- Solla, A., Aguín, O., Cubera, E., Sampedro, L., Mansilla, J.P., Zas, R., 2011. Survival time analysis of *Pinus pinaster* inoculated with *Armillaria ostoyae*: genetic variation and relevance of seed and root traits. *European Journal of Plant Pathology* 130, 477-488.
- Solla, A., Tomlinson, F., Woodward, S., 2002. Penetration of *Picea sitchensis* root bark by *Armillaria mellea*, *Armillaria ostoyae* and *Heterobasidion annosum*. *Forest Pathology* 32, 55-70.
- Sood, M., Kapoor, D., Kumar, V., Sheteiwiy, M.S., Ramakrishnan, M., Landi, M., Araniti, F., Sharma, A., 2020. *Trichoderma*: The "secrets" of a multitasking biocontrol agent. *Plants* 9, 762.
- Speckbacher, V., Ruzsanyi, V., 2020. The *Trichoderma atroviride* strains P1 and IMI 206040 differ in their light-response and VOC production. *Molecules* 25, 208-214.
- Stoppacher, N., Kluger, B., Zeilinger, S., Krska, R., Schuhmacher, R., 2010. Identification and profiling of volatile metabolites of the biocontrol fungus *Trichoderma atroviride* by HS-SPME-GC-MS. *Journal of Microbiological Methods* 81, 187-193.

- Sturrock, R.N., 2000. Management of root diseases by stumping and push-falling. Canada.Natural Resources Canada. Canadian Forest Service. Technology transfer noteNo. 16, 8.
- Sultana, A., Kallio, P., Jansson, A., Wang, J.-S., Niemi, J., Mänttä P., Schneider, G., 2004. Structure of the polyketide cyclase *SnoaL* reveals a novel mechanism for enzymatic aldol condensation. *The EMBO Journal* 23, 1911-1921.
- Syed Ab Rahman, S.F., Singh, E., Pieterse, C.M.J., Schenk, P.M., 2018. Emerging microbial biocontrol strategies for plant pathogens. *Plant Science* 267, 102-111.
- Szabó M., Urbán, P., Virányi, F., Kredics, L., Fekete, C., 2013. Comparative gene expression profiles of *Trichoderma harzianum* proteases during *in vitro* nematode egg-parasitism. *Biological Control* 67, 337-343.
- Szczałba, M., Kopta, T., Gaśtoł, M., Sękara, A., 2019. Comprehensive insight into arbuscular mycorrhizal fungi, *Trichoderma* spp. and plant multilevel interactions with emphasis on biostimulation of horticultural crops. *Journal of Applied Microbiology* 127, 630-647.
- Szekeres, A., Leitgeb, B., Kredics, L., Manczinger, L., Vágölygi, C., 2006. A novel, image analysis-based method for the evaluation of *in vitro* antagonism. *Journal of Microbiological Methods* 65, 619-622.
- Tarus, P.K., Lang'at-Thoruwa, C.C., Wanyonyi, A.W., Chhabra, S.C., 2003. Bioactive metabolites from *Trichoderma harzianum* and *Trichoderma longibrachiatum*. *Bulletin of the Chemical Society of Ethiopia* 17, 185-190.
- Tchameni, S.N., Cotârlet, M., Ghinea, I.O., Bedine, M.A.B., Sameza, M.L., Borda, D., Bahrim, G., Dinică, R.M., 2020. Involvement of lytic enzymes and secondary metabolites produced by *Trichoderma* spp. in the biological control of *Pythium myriotylum*. *International Microbiology* 23, 179-188.
- Thomidis, T., Exadaktylou, E., 2012. Effectiveness of cyproconazole to control *Armillaria* root rot of apple, walnut and kiwifruit. *Crop Protection* 36, 49–51.
- Törönen, P., Medlar, A., Holm, L., 2018. PANNZER2: a rapid functional annotation web server. *Nucleic Acids Research* 46, W84-W88.
- Travadon, R., Smith, M.E., Fujiyoshi, P., Douhan, G.W., Rizzo, D.M., Baumgartner, K., 2012. Inferring dispersal patterns of the generalist root fungus *Armillaria mellea*. *New Phytologist* 193, 959-969.
- Tsykun, T., Rigling, D., Nikolaychuk, V., Prospero, S., 2012. Diversity and ecology of *Armillaria* species in virgin forests in the Ukrainian Carpathians. *Mycological Progress* 11, 403-414.
- Turner, J.A., Fox, R.T.V., 1977. Prospects for the chemical control of *Armillaria* species. *Proceedings of the 1977 British Crop Protection Conference-Pests and Diseases* 1, 235-240.
- Vasaitis, R., Stenlid, J., Thomsen, I., Barklund, P., Dahlberg, A., 2008. Stump removal to control root rot in forest stands. A literature study. *Silva Fennica* 42, 457-483.
- Vasconcellos, R., Cardoso, E., 2009. Rhizospheric *Streptomyces* as potential biocontrol agents of *Fusarium* and *Armillaria* pine rot and as PGPR for *Pinus taeda*. *BioControl* 54, 807-816.
- Vinale, F., Ghisalberti, E.L., Sivasithamparam, K., Marra, R., Ritieni, A., Ferracane, R., Woo, S., Lorito, M., 2009. Factors affecting the production of *Trichoderma harzianum* secondary metabolites during the interaction with different plant pathogens. *Letters in Applied Microbiology* 48, 705-711.
- Viterbo, A., Harel, M., Chet, I., 2004. Isolation of two aspartyl proteases from *Trichoderma asperellum* expressed during colonization of cucumber roots. *FEMS Microbiology Letters* 238, 151-158.

- Wang, C., Zhuang, W., 2019. Evaluating effective *Trichoderma* isolates for biocontrol of *Rhizoctonia solani* causing root rot of *Vigna unguiculata*. *Journal of Integrative Agriculture* 18, 2072-2079.
- Wang, L., Lv, X., Cao, Y., Zheng, F., Meng, X., Shen, Y., Chen, G., Liu, W., Zhang, W., 2019a. A novel transcriptional regulator RXE1 modulates the essential transactivator XYR1 and cellulase gene expression in *Trichoderma reesei*. *Applied Microbiology and Biotechnology* 103, 4511-4523.
- Wang, L., Yang, R., Cao, Y., Zheng, F., Meng, X., Zhong, Y., Chen, G., Zhang, W., Liu, W., 2019b. CLP1, a novel plant homeo domain protein, participates in regulating cellulase gene expression in the filamentous fungus *Trichoderma reesei*. *Frontiers in Microbiology* 10, 1700.
- Weller, D.M., 1988. Biological control of soilborne plant pathogens in the rhizosphere with bacteria. *Annual Review of Phytopathology* 26, 379-407.
- West, J., Fox, R., 2002. Stimulation of *Armillaria mellea* by phenolic fungicides. *Annals of Applied Biology* 140, 291-295.
- West, J., Hughes, C., Fox, R.T.V., 2000. *Armillaria mellea* can infect the perennial weed, *Rumex obtusifolius*, in the UK. *Plant Pathology* 49, 808.
- Westwood, A., Conciatori, F., Tardif, J., Knowles, K., 2012. Effects of *Armillaria* root disease on the growth of *Picea mariana* trees in the boreal plains of central Canada. *Forest Ecology and Management* 266, 1-10.
- White, T., Bruns, T., Lee, S., Taylor, J., Innis, M., Gelfand, D., Sninsky, J., 1990. Amplification and direct sequencing of fungal ribosomal RNA genes for phylogenetics. In: *PCR Protocols Academic Press*, pp. 315-322.
- Wickham, H., 2016. *ggplot2: Elegant graphics for data analysis*. Springer-Verlag New York. ISBN 978-3-319-24277-4, <https://ggplot2.tidyverse.org>.
- Wingfield, B.D., Ambler, J.M., Coetzee, M.P., de Beer, Z.W., Duong, T.A., Joubert, F., Hammerbacher, A., McTaggart, A.R., Naidoo, K., Nguyen, H.D., Ponomareva, E., Santana, Q.S., Seifert, K.A., Steenkamp, E.T., Trollip, C., van der Nest, M.A., Visagie, C.M., Wilken, P.M., Wingfield, M.J., Yilmaz, N., 2016. IMA Genome-F 6: Draft genome sequences of *Armillaria fuscipes*, *Ceratocystiopsis minuta*, *Ceratocystis adiposa*, *Endoconidiophora laricicola*, *E. polonica* and *Penicillium freii* DAOMC 242723. *IMA Fungus* 7, 217-227.
- Wolf, T., Shelest, V., Nath, N., Shelest, E., 2016. CASSIS and SMIPS: Promoter-based prediction of secondary metabolite gene clusters in eukaryotic genomes. *Bioinformatics* 32, 1138-1143.
- Woo, S., Ruocco, M., Vinale, F., Nigro, M., Marra, R., Lombardi, N., Pascale, A., Lanzuise, S., Manganiello, G., Lorito, M., 2014. *Trichoderma*-based products and their widespread use in agriculture. *The Open Mycology Journal* 8, 71-126.
- Wu, M, Gu, L., 2020. TCseq: Time course sequencing data analysis. R package version 1.15.0.
- Wu, Q., Sun, R., Ni, M., Yu, J., Li, Y., Yu, C., Dou, K., Ren, J., Chen, J., 2017. Identification of a novel fungus, *Trichoderma asperellum* GDFS1009, and comprehensive evaluation of its biocontrol efficacy. *PLoS One* 12, e0179957.
- Yafetto, L., Davis, D.J., Money, N.P., 2009. Biomechanics of invasive growth by *Armillaria* rhizomorphs. *Fungal Genetics & Biology* 46, 688-694.
- Yu, G., Wang, L.G., Han, Y., He, Q.Y., 2012. clusterProfiler: an R package for comparing biological themes among gene clusters. *OMICS* 16, 284-287.

- Yuasa, H.J., Ball, H.J., 2011. Molecular evolution and characterization of fungal indoleamine 2,3-dioxygenases. *Journal of Molecular Evolution* 72, 160-168.
- Yuasa, H.J., Ball, H.J., 2013. Indoleamine 2,3-dioxygenases with very low catalytic activity are well conserved across kingdoms: IDOs of Basidiomycota. *Fungal Genetics & Biology* 56, 98-106.
- Zagryadskaya, Y.A., Lysak, L.V., Chernov, I.Y., 2015. Bacterial communities in the fruit bodies of ground basidiomycetes. *Eurasian Soil Science* 48, 620-626.
- Zhan, M., Tian, M., Wang, W., Li, G., Lu, X., Cai, G., Yang, H., Du, G., Huang, L., 2020. Draft genomic sequence of *Armillaria gallica* 012m: insights into its symbiotic relationship with *Gastrodia elata*. *Brazilian Journal of Microbiology* 51, 1539-1552.
- Zhang, H., Yohe, T., Huang, L., Entwistle, S., Wu, P., Yang, Z., Busk, P.K., Xu, Y., Yin, Y., 2018. dbCAN2: a meta server for automated carbohydrate-active enzyme annotation. *Nucleic Acids Research* 46, W95-w101.
- Zhang, J., Chen, Y., Wu, C., Liu, P., Wang, W., Wei, D., 2019a. The transcription factor ACE3 controls cellulase activities and lactose metabolism via two additional regulators in the fungus *Trichoderma reesei*. *Journal of Biological Chemistry* 294, 18435-18450.
- Zhang, S., Gan, Y., Xu, B., 2019b. Mechanisms of the IAA and ACC-deaminase producing strain of *Trichoderma longibrachiatum* T6 in enhancing wheat seedling tolerance to NaCl stress. *BMC Plant Biology* 19, 22.
- Zhao, L., Wang, Y., 2020. Effects of *Trichoderma asperellum* and its siderophores on endogenous auxin in *Arabidopsis thaliana* under iron-deficiency stress. *International Microbiology* 23, 501-509.

LIST OF PUBLICATIONS

MTMT Author ID: 10057722

JOURNAL ARTICLES USED FOR ATTAINING THE PHD DEGREE

Kedves O, Shahab D, Champramary S, **Chen L**, Indic B, Bóka B, Nagy VD, Vágvölgyi C, Kredics L, Sipos G. Epidemiology, biotic interactions and biological control of Armillarioids in the Northern Hemisphere. *PATHOGENS*, 2021, 10(1):76. <https://doi.org/10.3390/pathogens10010076> (IF2021: 3.492)

Chen L, Bóka B, Kedves O, Nagy VD, Szűcs A, Champramary S, Roszik R, Patocska Z, Münsterkötter M, Huynh T, Indic B, Vágvölgyi C, Sipos G, Kredics L. Towards the biological control of devastating forest pathogens from the genus *Armillaria*. *FORESTS*, 2019; 10(11):1013. <https://doi.org/10.3390/f10111013> (IF2019: 2.221)

Cumulative impact factor of the publications directly related to the thesis: 5.713

FURTHER PUBLICATIONS RELATED WITH THE TOPIC OF THE DISSERTATION

Conference paper:

Chen L, Shahab D, Kedves O, Champramary S, Indic B, Nagy VD, Vágvölgyi C, Kredics L, Sipos G. Armillarioid root rot invasion: possibilities of silvicultural and chemical control. 9TH HARDWOOD PROCEEDINGS: PART II pp. 90-97, 8 p. (2021)

Conference abstracts:

Vágvölgyi C, Sipos G, **Chen L**, Kedves O, Kredics L. Biology and control of *Armillaria* species, emerging pathogenic fungi of forests. In: Kende, Zoltán (szerk.) Abstract book of the 19th Alps-Adria Scientific Workshop 26th April - 1st May 2020, Wisła, Poland Gödöllő, Magyarország : Szent István Egyetemi Kiadó Nonprofit Kft. (2020) 100 p. p. 60.

Kedves O, **Chen L**, Bóka B, Kedves A, Kónya Z, Vágvölgyi C, Sipos G, Kredics L. A gyökérotthadást okozó *Armillaria* (tuskógomba) fajok elleni biológiai védekezés. In: Barna, Boglárka Johanna; Kovács, Petra; Molnár, Dóra; Pató, Viktória Lilla (szerk.) XXIII. Tavaszi Szőlő Konferencia (2020). Absztraktkötet: MI és a tudomány jövője. Budapest, Magyarország: Doktoranduszok Országos Szövetsége (DOSZ) (2020) pp. 43-44.

Bencsik-Bóka B, Sahu N, Huynh T, Kedves O, Merényi Z, Kovács G, **Chen L**, Champramary S, Patocskai Z, Münsterkötter M, Vágvölgyi C, Nagy GL, Sipos G, Kredics L. Classical and 'OMICS' approaches towards the biological control of devastating forest pathogens from the genus *Armillaria*. In: A Magyar Mikrobiológiai Társaság 2018. évi Nagygyűlése és a XIII. Fermentációs Kollokvium: Absztraktfüzet (2018) p. 6.

Kredics L, Sahu N, Huynh T, Kedves O, Merényi Z, Kovács G, **Chen L**, Bóka B, Patocskai Z, Münsterkötter M, Vágvölgyi C, Nagy LG, Sipos G. Devastating forest pathogens from the genus *Armillaria*: from genomics to biocontrol. In: Grenni P, Fernández-López M, Mercado-Blanco J. (eds.) Soil biodiversity and European woody agroecosystem. Rome, Olaszország: Water Research Institute, National Research Council of Italy (2018) pp. 48-49.

Kredics L, Körmöczy P, Bóka B, Racic G, Kedves O, Nagy VD, **Chen L**, Hatvani L, Szekeres A, Sipos G, Pankovic D, Vágvölgyi C. Development of biocontrol strategies based on antagonistic *Trichoderma* strains. In: Monostori T. (ed.) 16th Wellmann International Scientific Conference: Book of Abstracts. Hódmezővásárhely, Hungary: Szegedi Tudományegyetem Mezőgazdasági Kar (2018) pp. 11-12.

Kredics L, **Chen L**, Kedves O, Büchner R, Hatvani L, Allaga H, Nagy VD, Racic G, Pankovic D, Skrbic B, Vágvölgyi C. Monitoring biocontrol microorganisms in agricultural environments: *Trichoderma* in the spotlight. In: Cotoraci C, Ardelean A. (eds.) 20th Danube-Kris-Mures-Tisa (DKMT) Euroregion Conference on Environment and Health - Book of Abstracts. Arad, Romania: "Vasile Goldis" University Press, (2018) pp. 48-49.

Bóka B, Sipos G, Marik T, Jakab J, Imre V, **Chen L**, Kedves O, Nagy VD, Allaga H, Kredics L, Vágvölgyi C. Rhizomorph-associated microbiome as a potential source of biocontrol agents against *Armillaria* root rot. In: Kriiska K, Rosenvald K, Meitern A, Ostonen I. (eds.) Woody Root 7 : 7th International Symposium on Physiological Processes in Roots of Woody Plants. Tartu, Estonia: University of Tartu (2017) p. 86.

Kedves O, Bóka B, **Chen L**, Imre V, Kredics L, Sipos G, Vágvölgyi C. *Armillaria* elleni védekezésben alkalmazható potenciális biokontrollágensek foszformobilizáló, valamint siderofór- és indol-3-ecetsav-termelő képessége - Phosphor mobilization and the production of siderophores and indol-3-acetic acid by potential microbial biocontrol agents of *Armillaria* root rot. MIKOLÓGIAI KÖZLEMÉNYEK-CLUSIANA 56: 107-108. (2017)

Kredics L, Bóka B, **Chen L**, Kedves O, Imre V, Sipos G, Vágvölgyi C. Fitopatogén *Armillaria* fajok ellen potenciálisan alkalmazható biokontrollágensek izolálása és azonosítása - Isolation and identification of potential biological control agents of phytopathogenic *Armillaria* species. MIKOLÓGIAI KÖZLEMÉNYEK-CLUSIANA 56: 78-80. (2017)

Kredics L, Bóka B, **Chen L**, Kedves O, Imre V, Sipos G, Vágvölgyi C. Isolation, identification and characterization of potential microbial biocontrol agents of *Armillaria* species damaging tree crops. ACTA MICROBIOLOGICA ET IMMUNOLOGICA HUNGARICA 64(S1): p. 139. (2017)

Sipos G, Bóka B, Kedves O, **Chen L**, Patocskai Z, Münsterkötter M, Vágvölgyi C, Kredics L. A pusztító erdészeti kártevő *Armillaria* (tuskógomba) fajok genetikai vizsgálata és a biológiai védekezés lehetőségei. In: Bidló A, Facskó F. (eds.) Soproni Egyetem Erdőmérnöki Kar VI. Kari Tudományos Konferencia: a konferencia előadásainak és poszttereinek kivonatai. Sopron, Hungary: Soproni Egyetem Kiadó, (2017) pp. 16-17.

Vágvölgyi C, Bóka B, Sipos G, Jakab J, Imre V, Marik T, Kedves O, **Chen L**, Allaga H, Nagy VD, Khaled JM, Alharbi NS, Kredics L. Screening of rhizomorph-associated soil samples for potential biocontrol agents against forest-damaging *Armillaria* species. In: 19th DKMT Euroregional Conference on Environment and Health: Program and abstracts. Szeged, Hungary: University of Szeged, Faculty of Medicine (2017) p. 55

OTHER PUBLICATIONS

Kredics L, **Chen L**, Kedves O, Büchner R, Hatvani L, Allaga H, Nagy VD, Khaled JM, Alharbi NS, Vágvölgyi C. Molecular tools for monitoring *Trichoderma* in agricultural environments. FRONTIERS IN MICROBIOLOGY 2018, 9:1599. doi:10.3389/fmicb.2018.01599 (IF2018: 4.019)

Zhu X, Zhou T, **Chen L**, Zheng S, Chen S, Zhang D, Li G, Wang Z. Arf6 controls endocytosis and polarity during asexual development of *Magnaporthe oryzae*. FEMS MICROBIOLOGY LETTERS 2016 Nov; 363(22):fnw248. doi: 10.1093/femsle/fnw248. (IF2016: 1.765)

Zhong Z, Norvinyeku J, Yu J, Chen M, Cai R, Hong Y, **Chen L**, Zhang D, Wang B, Zhou J, Lu G, Chen X, Wang Z. Two different subcellular-localized Acetoacetyl-CoA acetyltransferases differentiate diverse functions in *Magnaporthe oryzae*. FUNGAL GENETICS AND BIOLOGY 2015 Oct; 83: 58-67. doi: 10.1016/j.fgb.2015.08.008. (IF2015: 2.933)

Zhong Z, Norvinyeku J, Chen M, Bao J, Lin L, **Chen L**, Lin Y, Wu X, Cai Z, Zhang Q, Lin X, Hong Y, Huang J, Xu L, Zhang H, Chen L, Tang W, Zheng H, Chen X, Wang Y, Lian B, Zhang L, Tang H, Lu G, Ebbola DJ, Wang B, Wang Z. Directional selection from host plants is a major force driving host specificity in *Magnaporthe* species. SCIENTIFIC REPORTS 2016 May 6; 6: 25591. doi: 10.1038/srep25591. (IF2016: 4.259)

Zhou T, Dagdas YF, Zhu X, Zheng S, **Chen L**, Cartwright Z, Talbot NJ, Wang Z. The glycogen synthase kinase MoGsk1, regulated by Mps1 MAP kinase, is required for fungal development and pathogenicity in *Magnaporthe oryzae*. SCIENTIFIC REPORTS 2017 Apr 19; 7(1):945. doi: 10.1038/s41598-017-01006-w. (IF2017: 4.122)

Cumulative impact factor of publications not directly related to the thesis: 17.098

Total impact factor: 22.811

Scientific journal articles: 7

Conference paper: 1

Conference abstracts: 12

SUPPLEMENTARY MATERIAL

Supplementary Table 1. *Armillaria* and *Trichoderma* isolates collected during the study

Location	GPS-N	GPS-E	Collection date	Sample	Isolate identifier	Diagnosis	ITS (GenBank)	<i>tef1α</i> (GenBank)
<i>Armillaria</i> isolates								
Rosalia, Austria	47° 41.649	16° 17.940	28.10.2016.	fruiting body	SZMC 24125	<i>Armillaria cepistipes</i>	-	MN580140
	47° 41.640	16° 17.937	28.10.2016.	fruiting body	SZMC 24126	<i>Armillaria cepistipes</i>	-	MN580151
	47° 41.628	16° 17.929	28.10.2016.	rhizomorph	SZMC 24128	<i>Armillaria ostoyae</i>	-	MN580144
	47° 41.629	16° 17.964	28.10.2016.	fruiting body	SZMC 24129	<i>Armillaria ostoyae</i>	-	MN580139
	47° 41.621	16° 17.948	28.10.2016.	fruiting body	SZMC 24130	<i>Armillaria ostoyae</i>	-	MN580142
Keszthely, Hungary	46° 48.728	17° 16.992	20.07.2016	bulk soil	SZMC 24095	<i>Armillaria gallica</i>	-	MN580162
	46° 48.712	17° 16.994	20.07.2016	bulk soil	SZMC 24098	<i>Armillaria gallica</i>	-	MN580163
	46° 48.702	17° 16.987	29.10.2016.	bulk soil	SZMC 24099	<i>Armillaria gallica</i>	-	MN580160
	46° 48.657	17° 16.954	29.10.2016.	fruiting body	SZMC 24131	<i>Armillaria mellea</i>	MN585779	MN580137
	46° 48.671	17° 16.959	29.10.2016.	fruiting body	SZMC 24132	<i>Armillaria mellea</i>	MN585780	MN580159
	46° 48.706	17° 16.949	29.10.2016.	fruiting body	SZMC 24133	<i>Armillaria mellea</i>	MN585781	MN580138
	46° 48.723	17° 16.974	29.10.2016.	fruiting body	SZMC 24134	<i>Armillaria mellea</i>	MN585777	MN580152
	46° 48.712	17° 16.978	29.10.2016.	fruiting body	SZMC 24135	<i>Armillaria mellea</i>	-	MN580145
	46° 48.736	17° 16.992	29.10.2016.	fruiting body	SZMC 24651	<i>Armillaria mellea</i>	-	MN580153
	46° 48.772	17° 16.992	29.10.2016.	fruiting body	SZMC 24136	<i>Armillaria mellea</i>	MN585778	MN580155
	46° 48.760	17° 16.982	29.10.2016.	fruiting body	SZMC 24137	<i>Armillaria mellea</i>	MN585776	MN580154
	46° 48.749	17° 16.936	29.10.2016.	fruiting body	SZMC 24139	<i>Armillaria mellea</i>	MN585782	MN580158

Supplementary Table 1 Cont.

Location	GPS-N	GPS-E	Collection date	Sample	Isolate identifier	Diagnosis	ITS (GenBank)	<i>tef1α</i> (GenBank)
	46° 48.720	17° 17.009	29.10.2016.	fruiting body	SZMC 24140	<i>Armillaria mellea</i>	MN585783	MN580146
	46°48.736	17°16.992	03.11.2016.	fruiting body	SZMC 24141	<i>Armillaria mellea</i>	-	MN580150
	46°48.665	17°16.993	03.11.2016.	fruiting body	SZMC 24142	<i>Armillaria mellea</i>	-	MN580143
	46°48.738	17°16.956	03.11.2016.	fruiting body	SZMC 24143	<i>Armillaria gallica</i>	-	MN580141
	46°48.877	17°17.143	03.11.2016.	fruiting body	SZMC 24144	<i>Armillaria mellea</i>	-	MN580148
	46°48.883	17°17.153	03.11.2016.	fruiting body	SZMC 24145	<i>Armillaria mellea</i>	-	MN580149
	46°48.917	17°17.062	03.11.2016.	fruiting body	SZMC 24146	<i>Armillaria mellea</i>	-	MN580161
	46°48.892	17°16.941	03.11.2016.	fruiting body	SZMC 24147	<i>Armillaria mellea</i>	-	MN580157
	46°48.883	17°16.937	03.11.2016.	fruiting body	SZMC 24148	<i>Armillaria mellea</i>	-	MN580156
	46°47.935	17°16.958	03.11.2016.	fruiting body	SZMC 24149	<i>Armillaria mellea</i>	-	MN580147
<i>Trichoderma</i> isolates								
Rosalia, Austria	47° 41.649	16° 17.940	28.10.2016.	bulk soil	SZMC 24270	<i>Trichoderma koningii</i>	MN516459	MN520036
					SZMC 24271	<i>Trichoderma koningii</i>	MN516460	MN520038
					SZMC 24272	<i>Trichoderma koningii</i>	MN516461	MN520042
					SZMC 24273	<i>Trichoderma koningii</i>	MN516462	MN520041
	47° 41.640	16° 17.937	28.10.2016.	bulk soil	SZMC 24274	<i>Trichoderma atroviride</i>	MN516463	MN520048
					SZMC 24275	<i>Trichoderma atroviride</i>	MN516464	MN520049
					SZMC 24276	<i>Trichoderma atroviride</i>	MN516465	MN520050
	47° 41.618	16° 17.873	28.10.2016.	bulk soil	SZMC 24277	<i>Trichoderma koningii</i>	MN516466	MN520033
					SZMC 24278	<i>Trichoderma koningii</i>	MN516467	MN520040

Supplementary Table 1 Cont.

Location	GPS-N	GPS-E	Collection date	Sample	Isolate identifier	Diagnosis	ITS (GenBank)	<i>tef1α</i> (GenBank)
					SZMC 24279	<i>Trichoderma koningii</i>	MN516468	MN520039
					SZMC 24280	<i>Trichoderma asperellum</i>	MN516469	MN520031
	47° 41.629	16° 17.964	28.10.2016.	bulk soil	SZMC 24285	<i>Trichoderma koningii</i>	MN516474	MN520034
					SZMC 24286	<i>Trichoderma koningii</i>	MN516475	MN520037
					SZMC 24287	<i>Trichoderma koningii</i>	MN516476	MN520035
					SZMC 24288	<i>Trichoderma asperellum</i>	MN516477	MN520032
	47° 41.621	16° 17.948	28.10.2016.	bulk soil	SZMC 24289	<i>Trichoderma asperellum</i>	MN516478	MN520030
					SZMC 24290	<i>Trichoderma koningii</i>	MN516479	MN520043
	47° 40.896	16° 17.211	28.10.2016.	bulk soil	SZMC 24291	<i>Trichoderma longipile</i>	MN516480	MN520056
	47° 41.628	16° 17.929	28.10.2016.	rhizomorph	SZMC 24281	<i>Trichoderma guizhouense</i>	MN516470	MN520084
					SZMC 24282	<i>Trichoderma paraviridescens</i>	MN516471	MN520044
					SZMC 24283	<i>Trichoderma simmonsii</i>	MN516472	MN520079
					SZMC 24284	<i>Trichoderma simmonsii</i>	MN516473	MN520078
Keszthely, Hungary	46° 48.657	17° 16.954	29.10.2016.	bulk soil	SZMC 24429	<i>Trichoderma simmonsii</i>	-	MN520069
					SZMC 24430	<i>Trichoderma simmonsii</i>	-	MN520071
					SZMC 24431	<i>Trichoderma simmonsii</i>	-	MN520077
					SZMC 26770	<i>Trichoderma simmonsii</i>	-	MN520072
					SZMC 24433	<i>Trichoderma simmonsii</i>	-	MN520081
	46° 48.671	17° 16.959	29.10.2016.	bulk soil	SZMC 24434	<i>Trichoderma tomentosum</i>	-	MN520066
	46° 48.706	17° 16.949	29.10.2016.	bulk soil	SZMC 24435	<i>Trichoderma simmonsii</i>	-	MN520075

Supplementary Table 1 Cont.

Location	GPS-N	GPS-E	Collection date	Sample	Isolate identifier	Diagnosis	ITS (GenBank)	<i>tef1α</i> (GenBank)
					SZMC 26771	<i>Trichoderma simmonsii</i>	-	MN520080
					SZMC 24436	<i>Trichoderma simmonsii</i>	-	MN520068
					SZMC 24403	<i>Trichoderma simmonsii</i>	-	MN520076
					SZMC 24404	<i>Trichoderma simmonsii</i>	-	MN520082
	46° 48.723	17° 16.974	29.10.2016.	bulk soil	SZMC 26772	<i>Trichoderma atrobrunneum</i>	-	MN520090
					SZMC 24405	<i>Trichoderma atrobrunneum</i>	-	MN520091
	46° 48.712	17° 16.978	29.10.2016.	bulk soil	SZMC 26773	<i>Trichoderma simmonsii</i>	-	MN520083
					SZMC 26774	<i>Trichoderma virens</i>	-	MN520058
					SZMC 24408	<i>Trichoderma simmonsii</i>	-	MN520067
	46° 48.736	17° 16.992	29.10.2016.	bulk soil	SZMC 24409	<i>Trichoderma hamatum</i>	-	MN520028
					SZMC 24410	<i>Trichoderma hamatum</i>	-	MN520029
	46°48.772	17°16.992	29.10.2016.	rhizosphere	SZMC 26778	<i>Trichoderma atroviride</i>	MN516444	MN520052
					SZMC 26779	<i>Trichoderma atroviride</i>	MN516445	MN520051
					SZMC 26780	<i>Trichoderma atroviride</i>	MN516446	MN520053
	46° 48.769	17° 16.961	29.10.2016.	bulk soil	SZMC 24411	<i>Trichoderma paratroviride</i>	-	MN520045
					SZMC 26775	<i>Trichoderma citrinoviride</i>	-	MN520054
					SZMC 26776	<i>Trichoderma citrinoviride</i>	-	MN520055
					SZMC 26777	<i>Trichoderma simmonsii</i>	-	MN520070
					SZMC 24412	<i>Trichoderma simmonsii</i>	-	MN520074
	46° 48.749	17° 16.936	29.10.2016.	rhizosphere	SZMC 24413	<i>Trichoderma atroviride</i>		MN520047

Supplementary Table 1 Cont.

Location	GPS-N	GPS-E	Collection date	Sample	Isolate identifier	Diagnosis	ITS (GenBank)	<i>tef1α</i> (GenBank)
					SZMC 24414	<i>Trichoderma atroviride</i>		MN520046
	46° 48.738	17° 16.956	20.07.2016.	rhizomorph	SZMC 24292	<i>Trichoderma virens</i>	MN516447	MN520059
					SZMC 24293	<i>Trichoderma virens</i>	MN516448	MN520061
					SZMC 24294	<i>Trichoderma virens</i>	MN516449	MN520062
					SZMC 24295	<i>Trichoderma virens</i>	MN516450	MN520060
					SZMC 24296	<i>Trichoderma virens</i>	MN516451	MN520064
	46° 48.758	17° 16.959	20.07.2016	rhizomorph	SZMC 24297	<i>Trichoderma atrobrunneum</i>	MN516452	MN520087
					SZMC 24298	<i>Trichoderma simmonsii</i>	MN516453	MN520073
					SZMC 24299	<i>Trichoderma atrobrunneum</i>	MN516454	MN520086
					SZMC 24300	<i>Trichoderma crassum</i>	MN516455	MN520057
					SZMC 24301	<i>Trichoderma atrobrunneum</i>	MN516456	MN520088
					SZMC 24302	<i>Trichoderma atrobrunneum</i>	MN516457	MN520089
					SZMC 24303	<i>Trichoderma virens</i>	MN516458	MN520063
	46° 48.722	17° 16.993	20.07.2016	rhizomorph	SZMC 24205	<i>Trichoderma virens</i>	-	MN520065
					SZMC 24206	<i>Trichoderma atrobrunneum</i>	MN516443	MN520085

Supplementary Table 2. *In vitro* antagonistic abilities of *Trichoderma* isolates towards *Armillaria* isolates

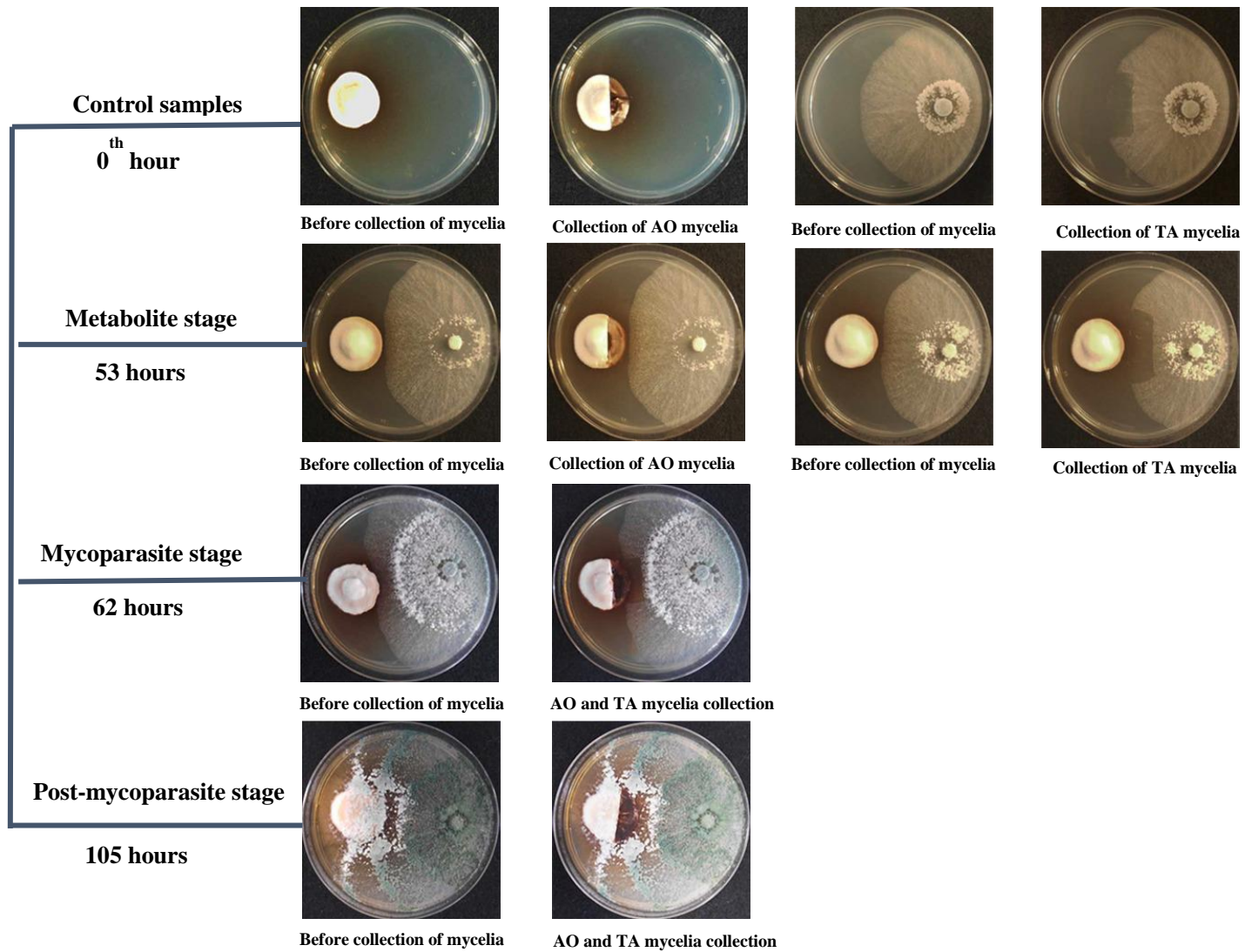
Species	Isolate	number of tested <i>Armillaria</i> isolates	BCI values ≥80	Percentage of BCI≥80 (%)
<i>T. tomentosum</i>	SZMC 24434	25	15	60.00
<i>T. paratroviride</i>	SZMC 24411	25	19	76.00
<i>T. crassum</i>	SZMC 24300	25	13	52.00
<i>T. hamatum</i>	SZMC 24409	25	9	36.00
<i>T. hamatum</i>	SZMC 24410	25	16	64.00
<i>T. citrinoviride</i>	SZMC 26775	25	12	48.00
<i>T. citrinoviride</i>	SZMC 26776	25	13	52.00
<i>T. virens</i>	SZMC 26774	25	24	96.00
<i>T. virens</i>	SZMC 24205	25	17	68.00
<i>T. virens</i>	SZMC 24292	25	22	88.00
<i>T. virens</i>	SZMC 24293	25	22	88.00
<i>T. virens</i>	SZMC 24294	25	23	92.00
<i>T. virens</i>	SZMC 24295	25	22	88.00
<i>T. virens</i>	SZMC 24296	25	22	88.00
<i>T. virens</i>	SZMC 24303	25	24	96.00
<i>T. atrobrunneum</i>	SZMC 26772	25	19	76.00
<i>T. atrobrunneum</i>	SZMC 24405	25	15	60.00
<i>T. atrobrunneum</i>	SZMC 24206	25	6	24.00
<i>T. atrobrunneum</i>	SZMC 24297	25	10	40.00
<i>T. atrobrunneum</i>	SZMC 24299	25	6	24.00
<i>T. atrobrunneum</i>	SZMC 24301	25	11	44.00
<i>T. atrobrunneum</i>	SZMC 24302	25	10	40.00
<i>T. simmonsii</i>	SZMC 24430	25	15	60.00
<i>T. simmonsii</i>	SZMC 24431	25	17	68.00
<i>T. simmonsii</i>	SZMC 26770	25	21	84.00
<i>T. simmonsii</i>	SZMC 24433	25	16	64.00
<i>T. simmonsii</i>	SZMC 24435	25	19	76.00
<i>T. simmonsii</i>	SZMC 24436	25	18	72.00
<i>T. simmonsii</i>	SZMC 24403	25	17	68.00
<i>T. simmonsii</i>	SZMC 24404	25	18	72.00
<i>T. simmonsii</i>	SZMC 26773	25	19	76.00
<i>T. simmonsii</i>	SZMC 24408	25	10	40.00
<i>T. simmonsii</i>	SZMC 26777	25	17	68.00
<i>T. simmonsii</i>	SZMC 24412	25	16	64.00
<i>T. simmonsii</i>	SZMC 24298	25	13	52.00
<i>T. simmonsii</i>	SZMC 24283	25	18	72.00
<i>T. simmonsii</i>	SZMC 24284	25	16	64.00
<i>T. atroviride</i>	SZMC 26778	25	12	48.00
<i>T. atroviride</i>	SZMC 26779	25	8	32.00

Supplementary Table 2 Cont.

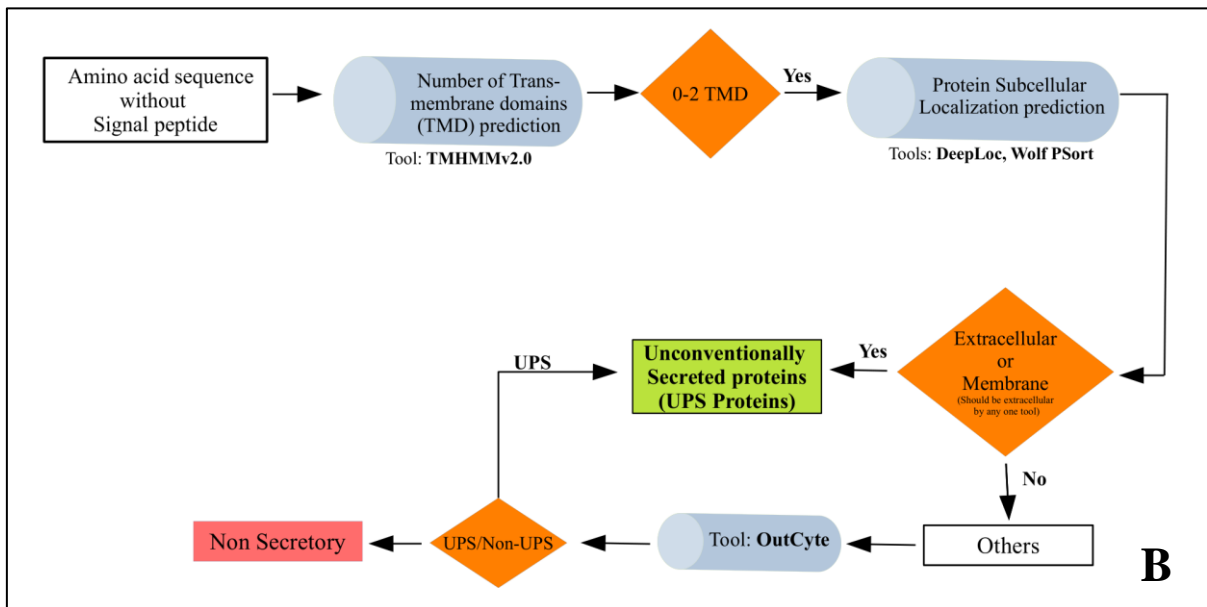
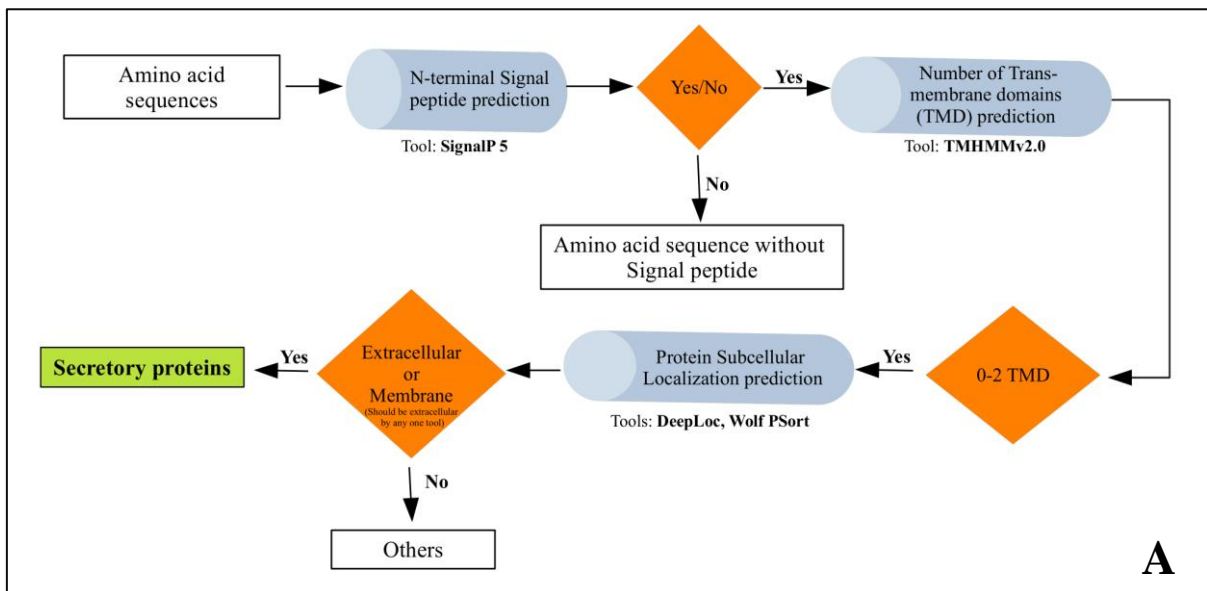
Species	Isolate	number of tested <i>Armillaria</i> isolates	BCI values ≥80	Percentage of BCI≥80 (%)
<i>T. atroviride</i>	SZMC 26780	25	10	40.00
<i>T. atroviride</i>	SZMC 24413	25	16	64.00
<i>T. atroviride</i>	SZMC 24414	25	14	56.00
<i>T. atroviride</i>	SZMC 24274	25	14	56.00
<i>T. atroviride</i>	SZMC 24275	25	12	48.00
<i>T. atroviride</i>	SZMC 24276	25	10	40.00
<i>T. koningii</i>	SZMC 24270	25	9	36.00
<i>T. koningii</i>	SZMC 24271	25	9	36.00
<i>T. koningii</i>	SZMC 24272	25	9	36.00
<i>T. koningii</i>	SZMC 24273	25	7	28.00
<i>T. koningii</i>	SZMC 24277	25	9	36.00
<i>T. koningii</i>	SZMC 24278	25	7	28.00
<i>T. koningii</i>	SZMC 24279	25	10	40.00
<i>T. koningii</i>	SZMC 24285	25	7	28.00
<i>T. koningii</i>	SZMC 24286	25	8	32.00
<i>T. koningii</i>	SZMC 24287	25	7	28.00
<i>T. koningii</i>	SZMC 24290	25	10	40.00
<i>T. asperellum</i>	SZMC 24280	25	9	36.00
<i>T. asperellum</i>	SZMC 24288	25	7	28.00
<i>T. asperellum</i>	SZMC 24289	25	8	32.00
<i>T. guizhouense</i>	SZMC 24281	25	16	64.00
<i>T. paraviridescens</i>	SZMC 24282	25	6	24.00
<i>T. longipile</i>	SZMC 24291	25	6	24.00

Supplementary Table 3. Primers used in the present study

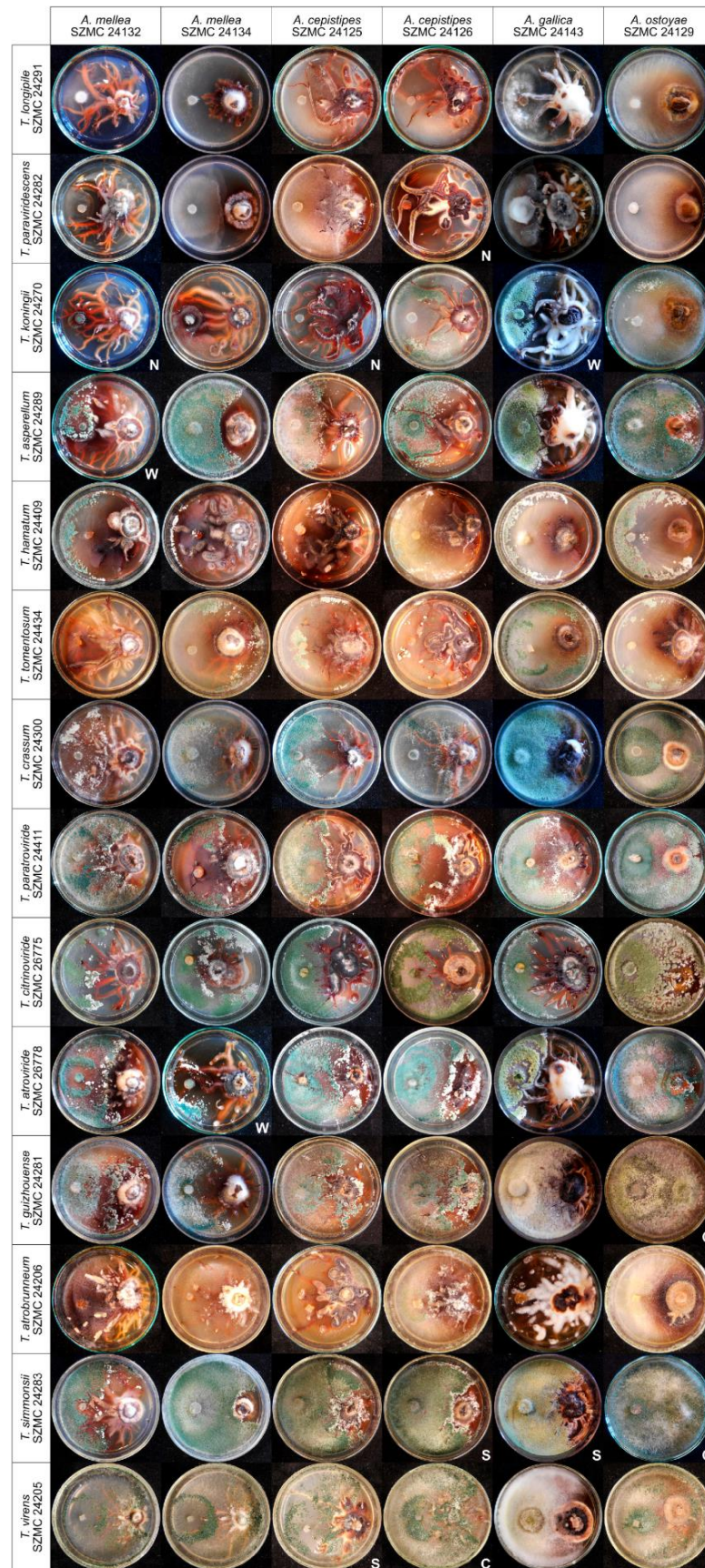
Primers	Sequence 5'-3'	Function of genes
<i>Primers for species identification</i>		
ITS4	TCCTCCGCTTATTGATATGC	ITS
ITS5	GGAAGTAAAAGTCGTAACAAGG	
TEF-LLErev	AACTTGCAGGCAATGTGG	<i>tef1α</i>
EF1-728F	CATCGAGAAGTTCGAGAAGG	
<i>Primers for qRT-PCR experiments</i>		
<i>Armillaria</i>		
ARMOST_13362 Fw	GACAACCTTCGCAGTCAG	Quinolinic acid pathway
ARMOST_13362 Rev	CACCACGCAACTCCATAC	
ARMOST_03616 Fw	ACGCCACGGCTAAGAAGAGG	Quinolinic acid pathway
ARMOST_03616 Rev	CCCAAGCGAAGCGACAACAG	
ARMOST_04226 Fw	CATAAATCCCGCACAACAGC	Quinolinic acid Pathway
ARMOST_04226 Rev	ATGATCTGCAACGCCTCTAC	
ARMOST_05856 Fw	AAGACGGCAACCAAGAAC	SnoaL
ARMOST_05856 Rev	TTCGCCAAGGATTACCAC	
ARMOST_05857 Fw	ACTGCTAACGTCGCTGTTAC	SnoaL
ARMOST_05857 Rev	CGAAATTCGCCAAGGATTGC	
ARMOST_05616 Fw	GACCGACGATAGCACCAATCC	Apoptosis-related
ARMOST_05616 Rev	TCGTTIGTCCGCCATGTCC	
ARMOST_18535 Fw	GATCATGCACCGTCGAAGAAG	Apoptosis-related
ARMOST_18535 Rev	ACCGAGAACCGTCTCAATACC	
ARMOST_18537 Fw	TGTCACCGTCGTCAGTAG	Apoptosis-related
ARMOST_18537 Rev	TCAGCCTTCTCGTCCTTC	
ARMOST_03733 Fw2	TCCAAAGGTGAACAGGCAGAAG	Actin
ARMOST_03733 Rev2	TATCAAGTCGCCGTGTCAGATG	
ARMOST_14637 Fw	CAAGGCGGGCATTCAACTCAAC	<i>gpd</i>
ARMOST_14637 Rev	AGCGAACACCAAGAGGTCACAG	
<i>Trichoderma</i>		
XM_014093434.1 Fw	TCTGGTCGCTGCATTTCC	SnoaL
XM_014093434.1 Rev	GGAACTCGCCTTGATGAGTG	
XM_014092940.1 Fw	CTGGAGCAATGAGTGAAGTG	SnoaL
XM_014092940.1 Rev	TGAGTCTGCTAGACCTCAAG	
eIF-4F	GTCCAACACTACGATGAGACTGTC	<i>tef1α</i>
eIF-4R	TCGTGGCCCTTGATAACAG	



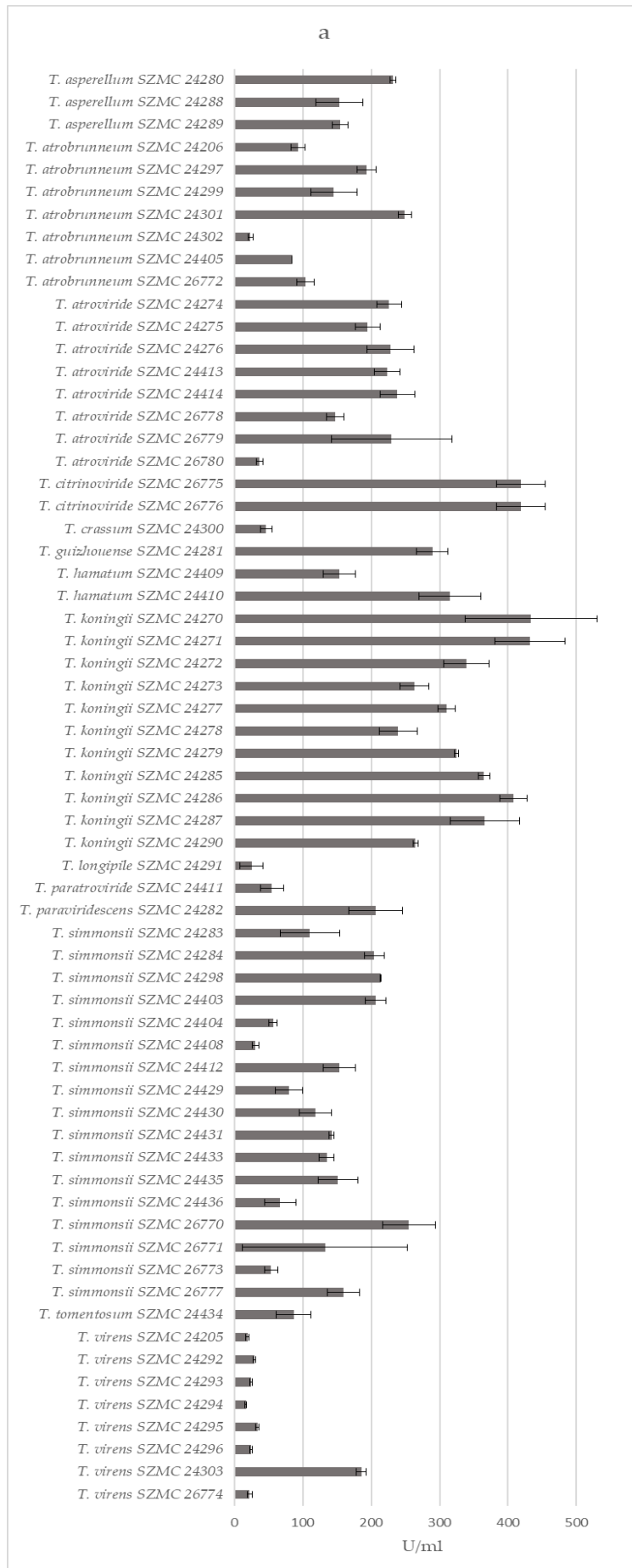
Supplementary Figure 1. Experimental design and practical details of mycelia sample collection for RNA extraction



Supplementary Figure 2. Secretory protein prediction pipeline for AO and TA: (A) shows the pipeline and tools used to predict classically secreted proteins. SignalPv5 is initially used to predict the N-terminal signal and cleavage site followed by TMHMMv2.0 to predict the number of transmembrane domains (TMDs) and DeepLoc v1.0 and Wolf PSort to predict the subcellular localization signals present in the amino acid sequences. (B) outlines the pipeline followed for predicting proteins that are sorted to extracellular region but are without signal peptide at the N-terminal region, i.e. proteins secreted by unconventional pathway (UPS proteins). Besides Wolf PSort and DeepLoc, we also used Outcyte to predict UPS proteins.



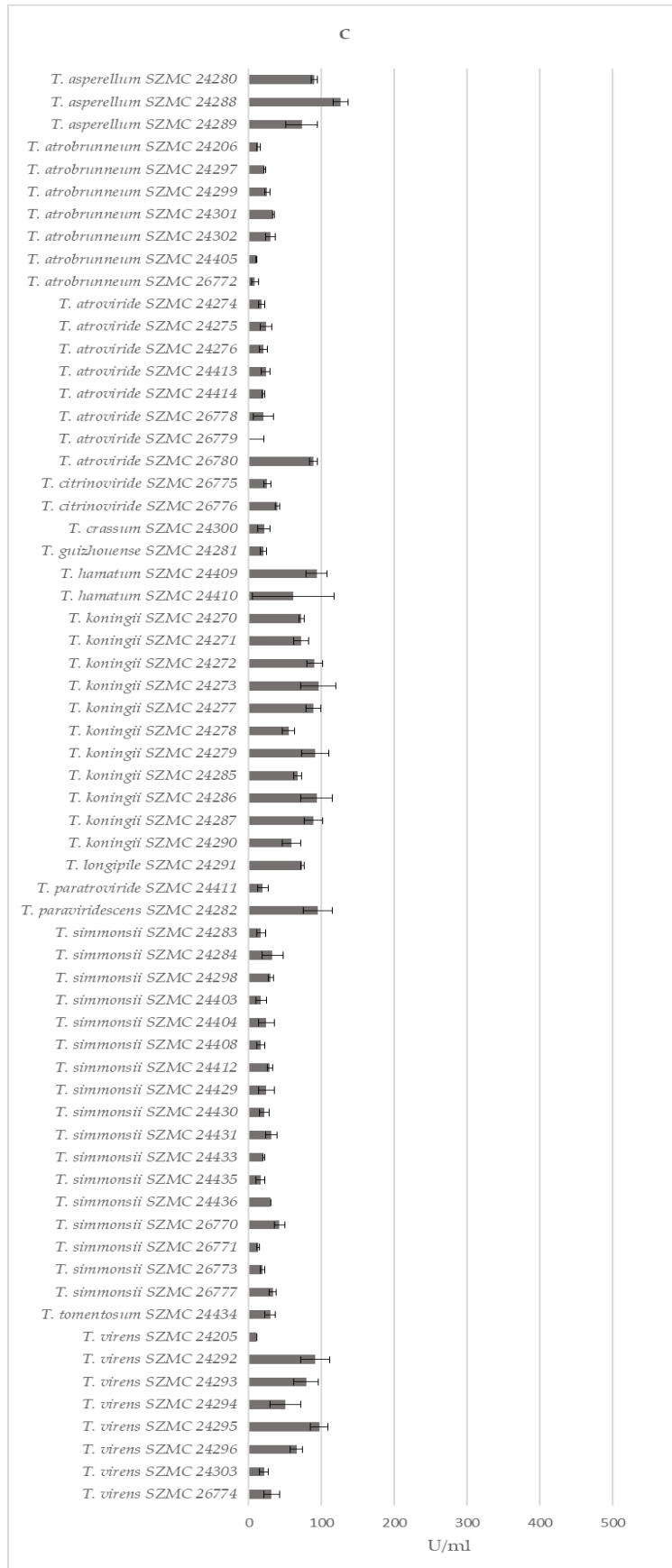
Supplementary Figure 3. *In vitro* antagonism of *Trichoderma* strains from different species against *Armillaria mellea*, *A. cepistipes*, *A. gallica* and *A. ostoyae*. Example plates are marked with N: no inhibition; W: weak inhibition; S: strong inhibition; C: complete overgrowth of *Armillaria* by *Trichoderma*.



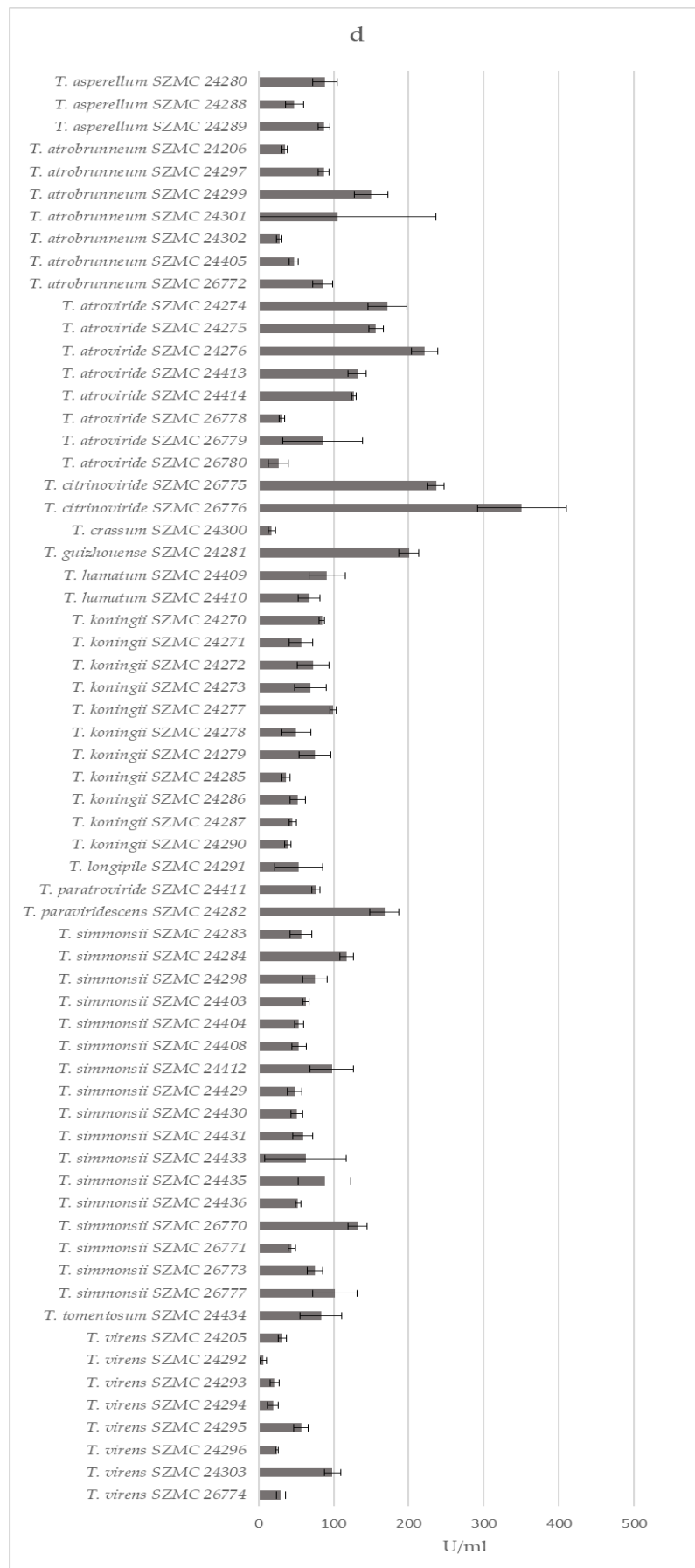
Supplementary Figure 4 Cont.



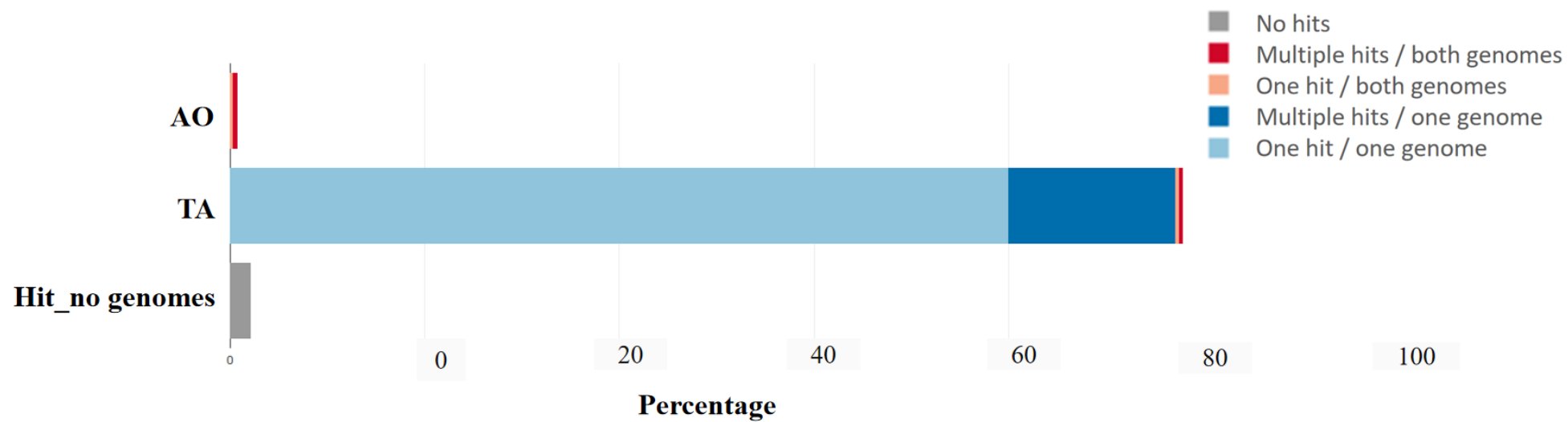
Supplementary Figure 4 Cont.



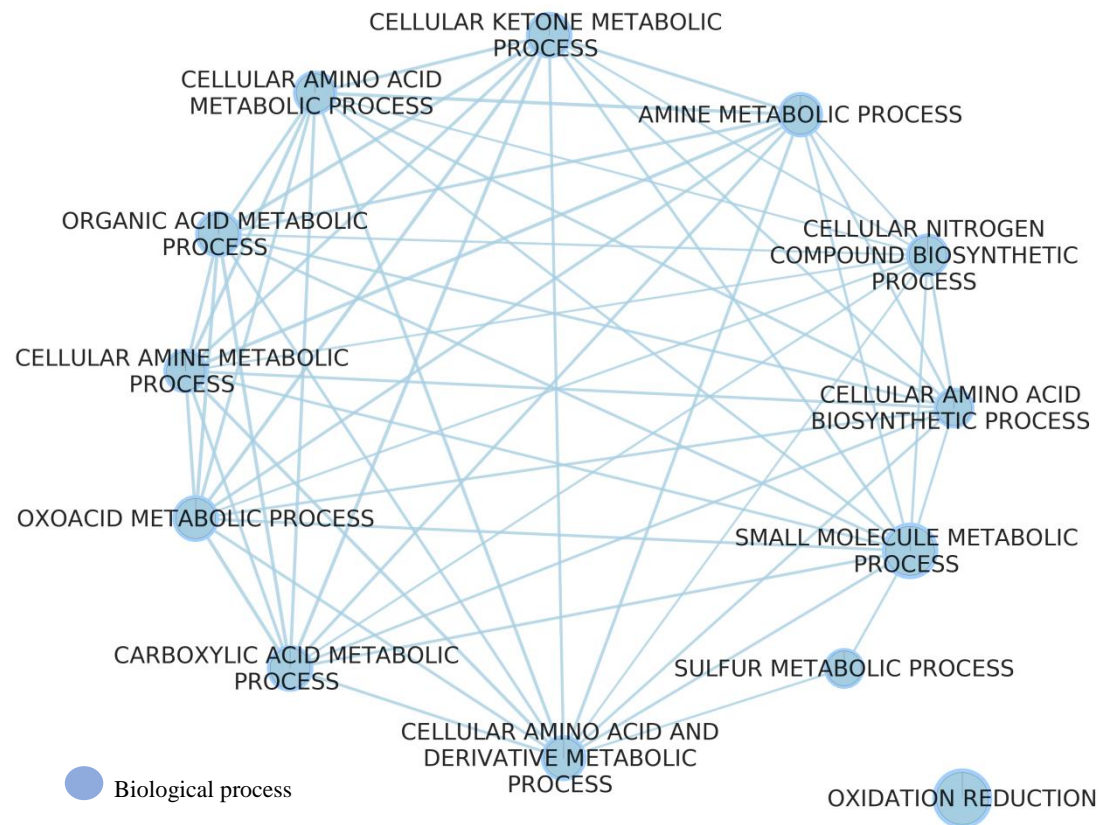
Supplementary Figure 4 Cont.



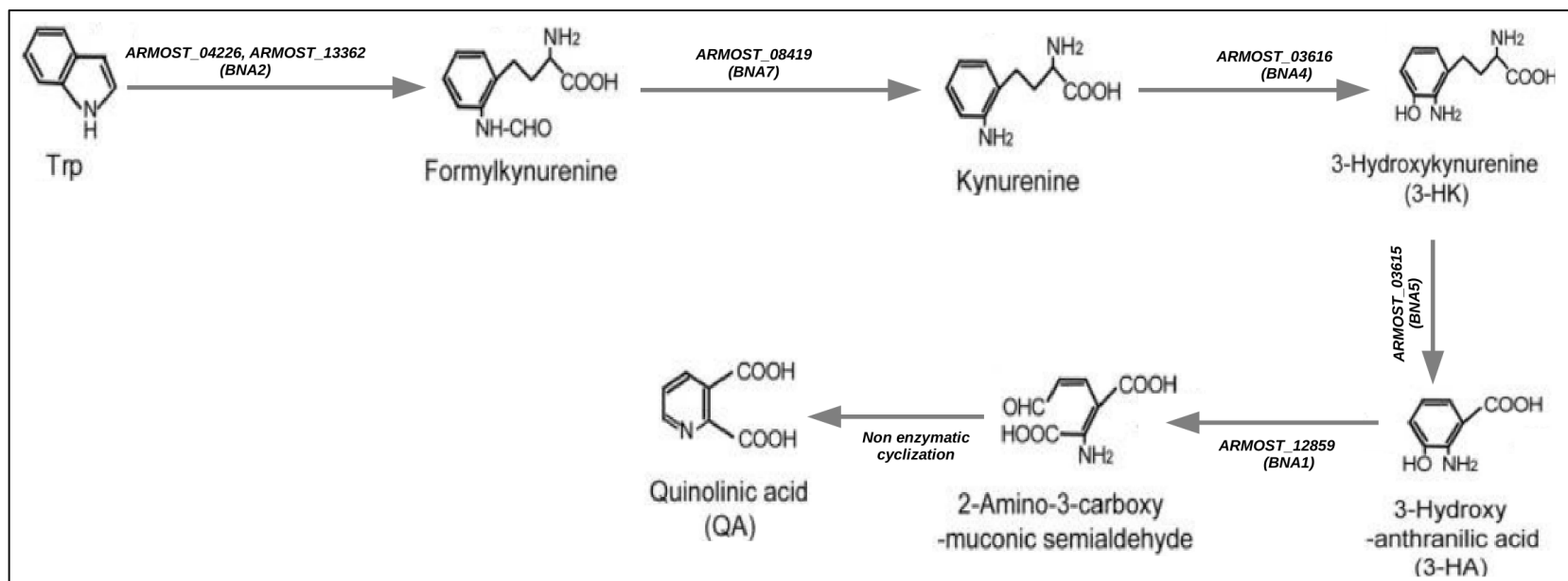
Supplementary Figure 4. Extracellular enzyme activities of *Trichoderma* isolates derived from forest soil samples: (a) β -glucosidase, (b) cellobiohydrolase, (c) β -xylosidase, and (d) phosphatase.



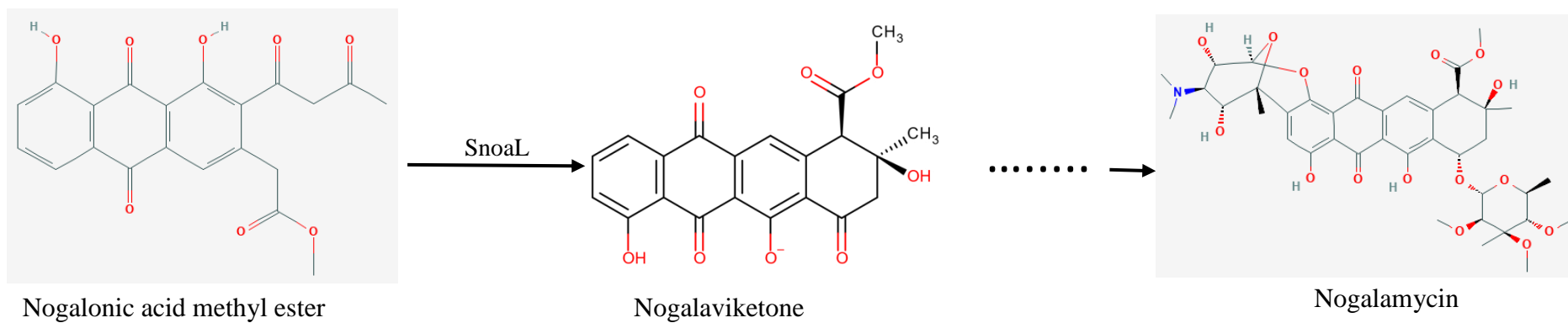
Supplementary Figure 5. Mapping result at the post-mycoparasite stage (105 hrs): One hit means probably single copy gene; Multiple hits means probably multicopy gene; One genome means present in *T. atroviride* (TA) or *A. ostoyae* (AO) only; Multiple genomes means orthologous gene present in both TA and AO genome.



Supplementary Figure 6. GO molecular function enrichment map created based on the Downtrend cluster genes of *T. atroviride* (TA)



Supplementary Figure 7. Quinolinic acid synthesis pathway in yeast adapted from (Ohashi *et al.*, 2013). *A. ostoyae* (AO) genes homologous to BNA genes involved in different steps of quinolinic acid synthesis are shown in the figure.



Supplementary Figure 8. Involvement of SnoaL in nogalamycin biosynthesis pathway adapted from (Sultana *et al.*, 2004)